US Army Corps
of Engineers

AD-A215 209

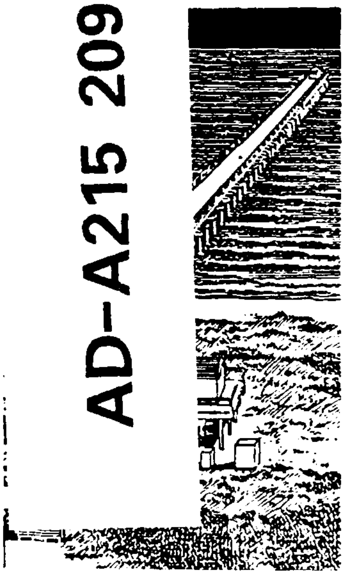

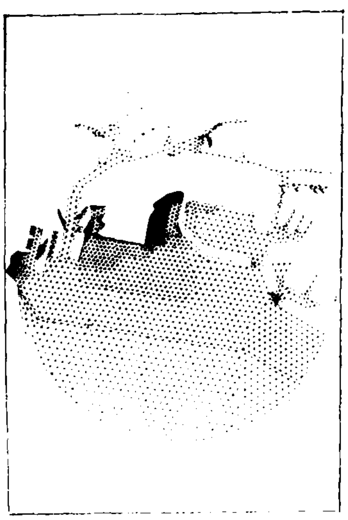

2

TECHNICAL REPORT CERC-89-16

LOS ANGELES - LONG BEACH HARBOR COMPLEX 2020 PLAN HARBOR RESONANCE ANALYSIS

Numerical Model Investigation

by

Francis E. Sargent

Coastal Engineering Research Center

DEPARTMENT OF THE ARMY
Waterways Experiment Station, Corps of Engineers
3909 Halls Ferry Road, Vicksburg, Mississippi 39180-6199

US ARMY ENGINEER WATERWAYS EXPERIMENT STATION

November 1989

Final Report

Approved For Public Release. Distribution Unlimited

Prepared for US Army Engineer District, Los Angeles
Los Angeles, California 90053-2325

COASTAL ENGINEERING RESEARCH CENTER

Unclassified

SECURITY CLASSIFICATION OF THIS PAGE

REPORT DOCUMENTATION PAGE

Form Approved OMB No. 0704-0188

1a. REPORT SECURITY CLASSIFICATION Unclassified	1b. RESTRICTIVE MARKINGS
2a. SECURITY CLASSIFICATION AUTHORITY 2b. DECLASSIFICATION / DOWNGRADING SCHEDULE	3. DISTRIBUTION / AVAILABILITY OF REPORT Approved for public release; distribution unlimited
4. PERFORMING ORGANIZATION REPORT NUMBER(S) Technical Report CERC-89-16	5. MONITORING ORGANIZATION REPORT NUMBER(S)
6a. NAME OF PERFORMING ORGANIZATION USAEWES, Coastal Engineering Research Center 6b. OFFICE SYMBOL (If applicable)	7a. NAME OF MONITORING ORGANIZATION
6c. ADDRESS (City, State, and ZIP Code) 3909 Halls Ferry Road Vicksburg, MS 39180-6199	7b. ADDRESS (City, State, and ZIP Code)
8a. NAME OF FUNDING / SPONSORING ORGANIZATION USAED, Los Angeles 8b. OFFICE SYMBOL (If applicable)	9. PROCUREMENT INSTRUMENT IDENTIFICATION NUMBER
8c. ADDRESS (City, State, and ZIP Code) Los Angeles, CA 90053-2325	10. SOURCE OF FUNDING NUMBERS PROGRAM ELEMENT NO. / PROJECT NO. / TASK NO. / WORK UNIT ACCESSION NO.

11. TITLE (Include Security Classification)
Los Angeles - Long Beach Harbor Complex 2020 Plan Harbor Resonance Analysis; Numerical Model Investigation

12. PERSONAL AUTHOR(S)
Sargent, Francis E.

13a. TYPE OF REPORT	13b. TIME COVERED	14. DATE OF REPORT (Year, Month, Day)	15. PAGE COUNT
Final report	FROM Mar 88 TO Oct 88	November 1989	98

16. SUPPLEMENTARY NOTATION
Available from National Technical Information Service, 5285 Port Royal Road, Springfield, VA 22161.

17. COSATI CODES			18. SUBJECT TERMS (Continue on reverse if necessary and identify by block number)
FIELD	GROUP	SUB-GROUP	See reverse.

19. ABSTRACT (Continue on reverse if necessary and identify by block number)

A numerical harbor resonance model of the Los Angeles - Long Beach Harbor Complex was used to study harbor oscillations in the [illegible]- to 400-sec period range. Four finite element grids were digitized representing existing conditions and two Phase 2 and one Phase 1 layout from the 2020 Plan. The hybrid finite element numerical model HARBD, which includes terms for bottom friction and boundary absorption, was used in this study. Mean boundary amplification response factors were obtained for 30 basins representing existing and proposed areas of interest. It was concluded that the Phase 2 Scheme A layout had the lowest response, followed by the Phase 2 Scheme B response, and that Phase 1 Scheme B had the highest response. Neither of the Phase 2 layouts was considered to have response factors significantly above the other to consider excluding either plan based solely on [illegible] response. For the Port of Los Angeles, both Phase 2 plans produced nearly identical responses. The areas producing the highest responses were East Channel and 2020 Southern Slip for Los Angeles, and the Pier [illegible] Extension and 2020 Slip for Long Beach.

20. DISTRIBUTION / AVAILABILITY OF ABSTRACT ☒ UNCLASSIFIED/UNLIMITED ☐ SAME AS RPT. ☐ DTIC USERS	21. ABSTRACT SECURITY CLASSIFICATION Unclassified
22a. NAME OF RESPONSIBLE INDIVIDUAL	22b. TELEPHONE (Include Area Code) / 22c. OFFICE SYMBOL

DD Form 1473, JUN 86 — Previous editions are obsolete. — SECURITY CLASSIFICATION OF THIS PAGE

Unclassified

18. SUBJECT TERMS (Continued).

Harbor resonance
Harbors--Hydrodynamics (LC)
Harbors--California (LC)
Los Angeles (Calif.)--Harbor (LC)
Long Beach (Calif.)--Harbor (LC)
Numerical models
Ship motion
2020 Master Plan (WES)

Accession For	
NTIS GRA&I	☑
DTIC TAB	☐
Unannounced	☐
Justification	
By	
Distribution/	
Availability Codes	
Dist	Avail and/or Special
A-1	

PREFACE

A numerical harbor resonance model investigation of the Los Angeles - Long Beach Harbor Complex was authorized by the US Army Engineer District, Los Angeles (SPL), on 1 March 1988. The model investigation was sponsored by SPL, and funding was provided by the Ports of Los Angeles (POLA) and Long Beach (POLB) under a study agreement with SPL.

The numerical study was conducted at the Coastal Engineering Research Center (CERC) of the US Army Engineer Waterways Experiment Station (WES) from March to October 1988 in the Wave Processes Branch (WPB), Wave Dynamics Division (WDD), CERC, under the direction of Dr. James R. Houston, Chief, CERC; Mr. Charles C. Calhoun, Jr., Assistant Chief, CERC; Mr. Claude E. Chatham, Jr., Chief, WDD; and Mr. Douglas G. Outlaw, Chief, WPB. The numerical model investigation was conducted by Mr. Francis E. Sargent, Hydraulic Engineer, WPB, and Ms. Robin Hoban, Contract Student, who provided assistance in grid preparation. This report was edited by Ms. Shirley A. J. Hanshaw, Information Technology Laboratory, WES.

During the course of the investigation, liaison between POLA and POLB was maintained by means of conferences, telephone communications, presentation of preliminary results, and monthly progress reports. Messrs. Vern Hall and John Jarwar were the points of contact (POC) for POLA, and Messrs. Dan Allen, Rich Weeks, and Mike Burke were POC's for POLB.

Project management for SPL was administered by Mr. Angel P. Fuertes under the general direction of Mr. Stephen S. Fine, Chief, Coastal Branch and Mr. Alan Alcorn, Chief, Waterways and Harbors Section, North Coast, in the Planning Division. COL Tadahiko Ono was District Engineer of SPL during the course of this study.

COL Larry B. Fulton, EN, was Commander and Director of WES during report publication. Dr. Robert W. Whalin was Technical Director.

CONTENTS

Page

PREFACE 1

CONVERSION FACTORS, NON-SI TO SI (METRIC)
UNITS OF MEASUREMENT 3

PART I: INTRODUCTION 4

The Prototype 4
Purpose of Study 6

PART II: NUMERICAL MODEL 10

PART III: APPLICATION OF NUMERICAL MODEL 12

Numerical Data Analysis 13
Grid and Boundary Conditions 14

PART IV: RESULTS 15

Long Beach 15
Los Angeles 17
Los Angeles-Long Beach Complex and 2020 Landfill 19

PART V: CONCLUSIONS 20

REFERENCES 22

BIBLIOGRAPHY 23

TABLE 1

PLATES 1-68

CONVERSION FACTORS, NON-SI TO SI (METRIC) UNITS OF MEASUREMENT

Non-SI units of measurement used in this report can be converted to SI (metric) units as follows:

Multiply	By	To Obtain
acres	4,046.856	square metres
feet	0.3048	metres
tons (2,000 pounds, mass)	0.907194	metric tons

LOS ANGELES - LONG BEACH HARBOR COMPLEX

2020 PLAN HARBOR RESONANCE ANALYSIS

Numerical Model Investigation

PART I: INTRODUCTION

The Prototype

1. The Los Angeles - Long Beach Harbor Complex is situated in San Pedro Bay (Figure 1) on the south California coastline (118°15' W, 33°45' N). The Ports are protected from incident wave energies by three rubble-mound breakwaters (Bottin 1988). Breakwater construction began with the San Pedro Breakwater during 1900-12, continued with the Middle Breakwater during 1932-37 and 1940-42, and finished with the Long Beach Breakwater during 1941-43 and 1946-49. The breakwaters provide sufficient protection for short-period waves but are considered to be highly permeable to low amplitude-low frequency waves (Houston 1976). The present day bathymetry and harbor geometry has evolved from continued growth and development by the Ports and Federal interests.

2. Future growth of the harbors is expected during the next few decades as shown in the Operations, Facilities, and Infrastructure Study (Vickerman Zachary Miller, Inc. 1988). Cargo throughput by the year 2020 is projected to be 221,800,000 tons,* while the maximum historical throughput to date has been 86,900,000 tons. Maximum practical capacity of existing facilities is estimated at 144,500,000 tons. The major growth factor will be caused by an increase in Pacific Rim trade.

3. To satisfy expected growth, the Ports have undertaken a long-range cooperative planning effort known as the 2020 Plan. The principal components of the 2020 Plan are (a) landfills in outer harbor areas covering 2,400 acres and development of 600 existing acres, providing space for 38 new terminals; (b) deep-draft channels at various depths from 55 to 90 ft (providing most of the materials for the landfills); and (c) an extensive system of rail and highway connections and intermodal container transfer facilities. Construction will be done in two major phases, Phase 1 to be completed about the year 2010 followed by Phase 2 completion in 2020.

---

* A table of factors for converting non-SI to SI units of measurement is presented on page 3.

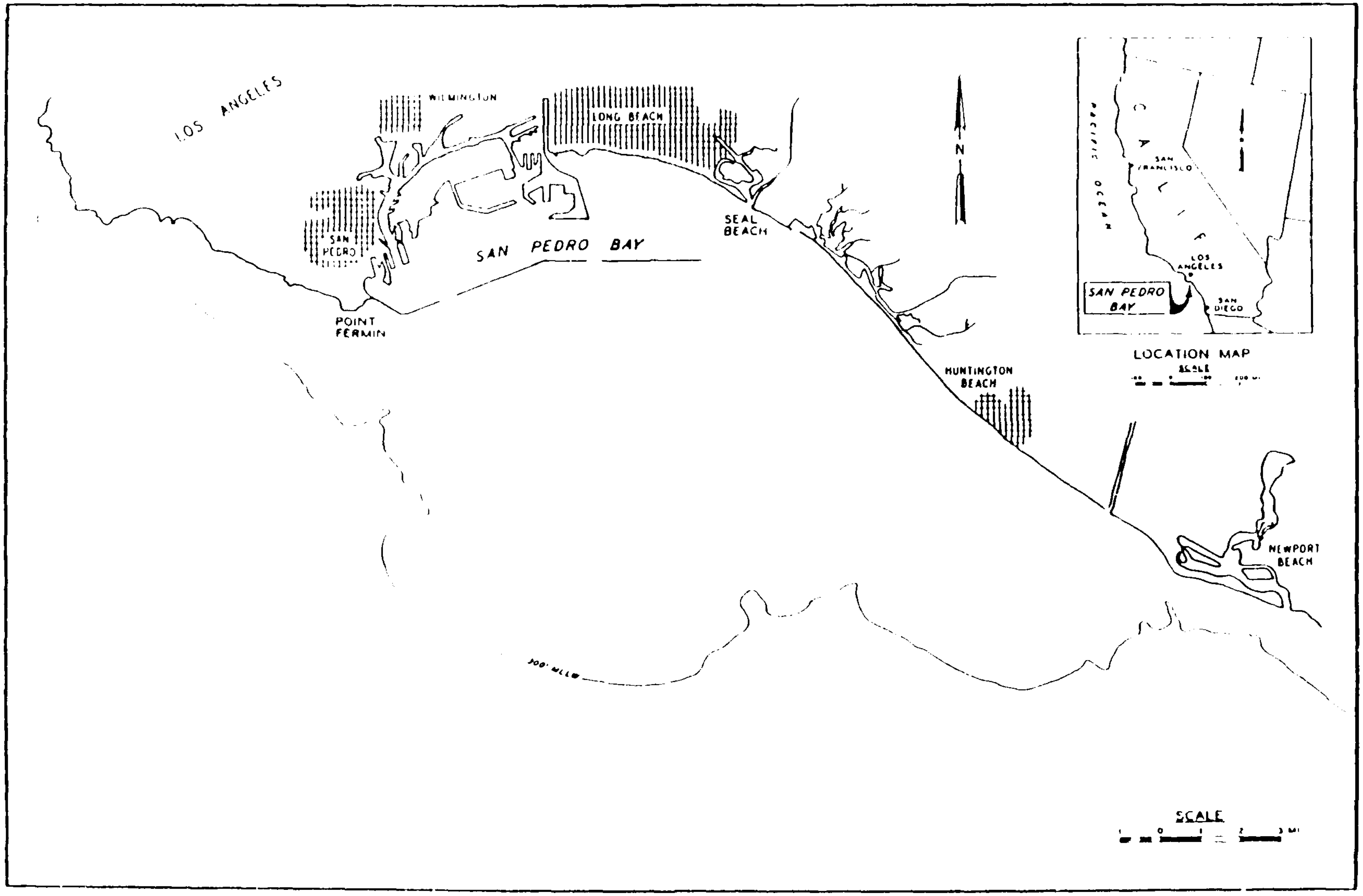

Figure 1. Project location

Purpose of Study

4. The purpose of this study was to investigate harbor oscillations excited by long waves with periods from 60 to 400 sec using a finite element numerical model. Four layouts, including existing conditions, were tested to determine whether adverse harbor oscillations would occur in existing or proposed basins. Although a ship motion analysis was not undertaken in this study, the present results can be used in a relative comparison to indicate where ship motion problems are most likely to develop. The present study is limited to the 60- to 400-sec periods and does not include energies in the 1[illegible]- to 60-sec range which may also be important in addressing ship motion.

5. Existing conditions, shown in Figure 2, were studied to provide a baseline comparison for the three alternative schemes tested. The alternative schemes consisted of two Phase 2 layouts and one Phase 1 layout. The selection of the Phase 1 layout was based on a preliminary analysis of the Phase 2 results. The Phase 1 configuration of Scheme B is shown in Figure 3. Phase 2 layouts for Scheme B and Scheme A are shown in Figures 4 and 5, respectively.

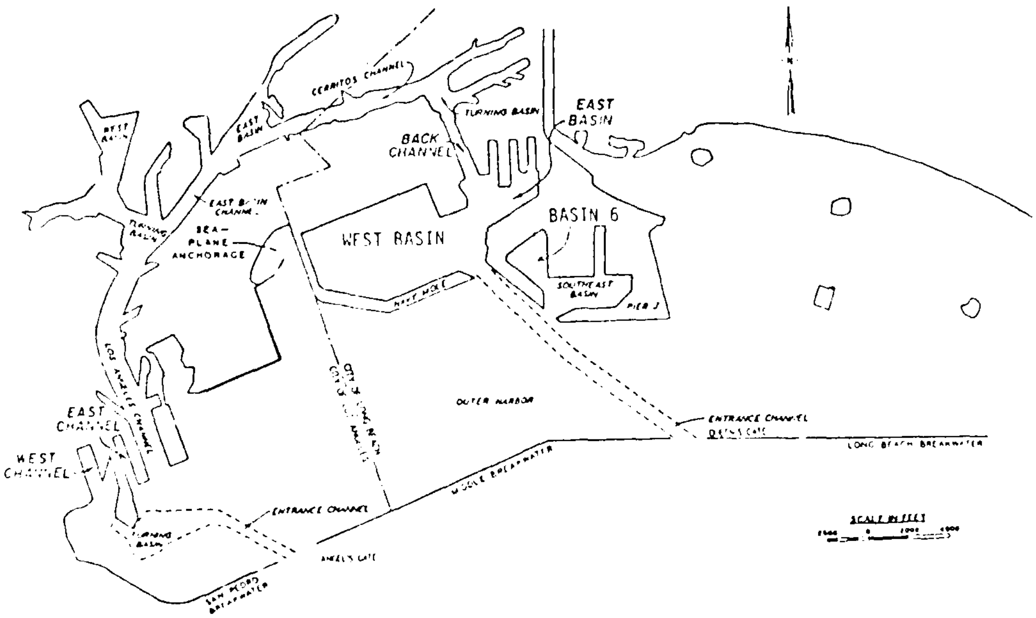

Figure 2. Existing conditions for Los Angeles - Long Beach Harbor Complex

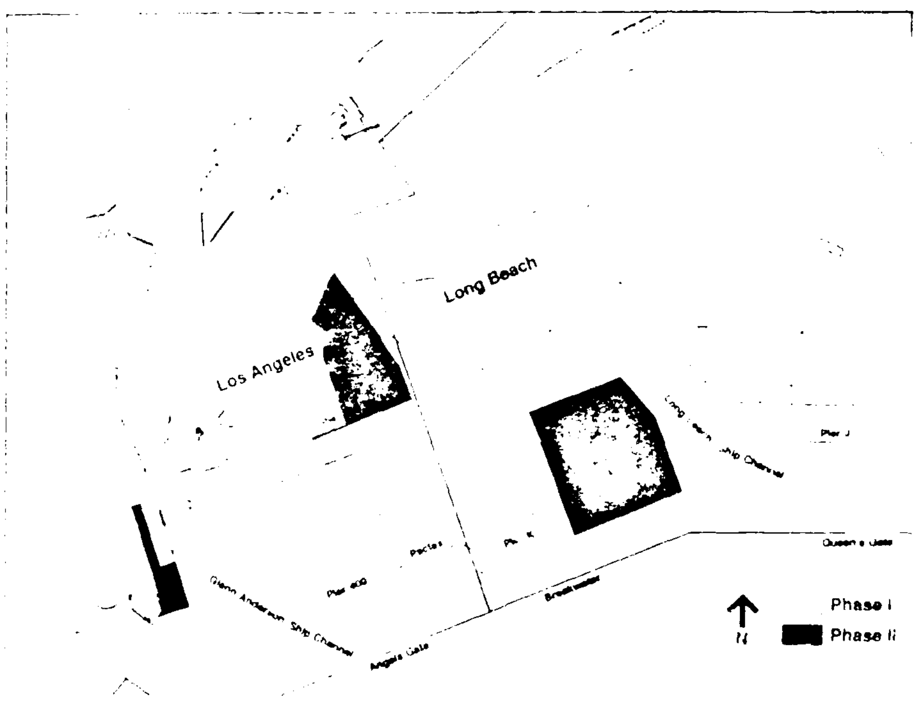

Figure 3. Scheme E Phase I harbor geometry for 2020 Plan

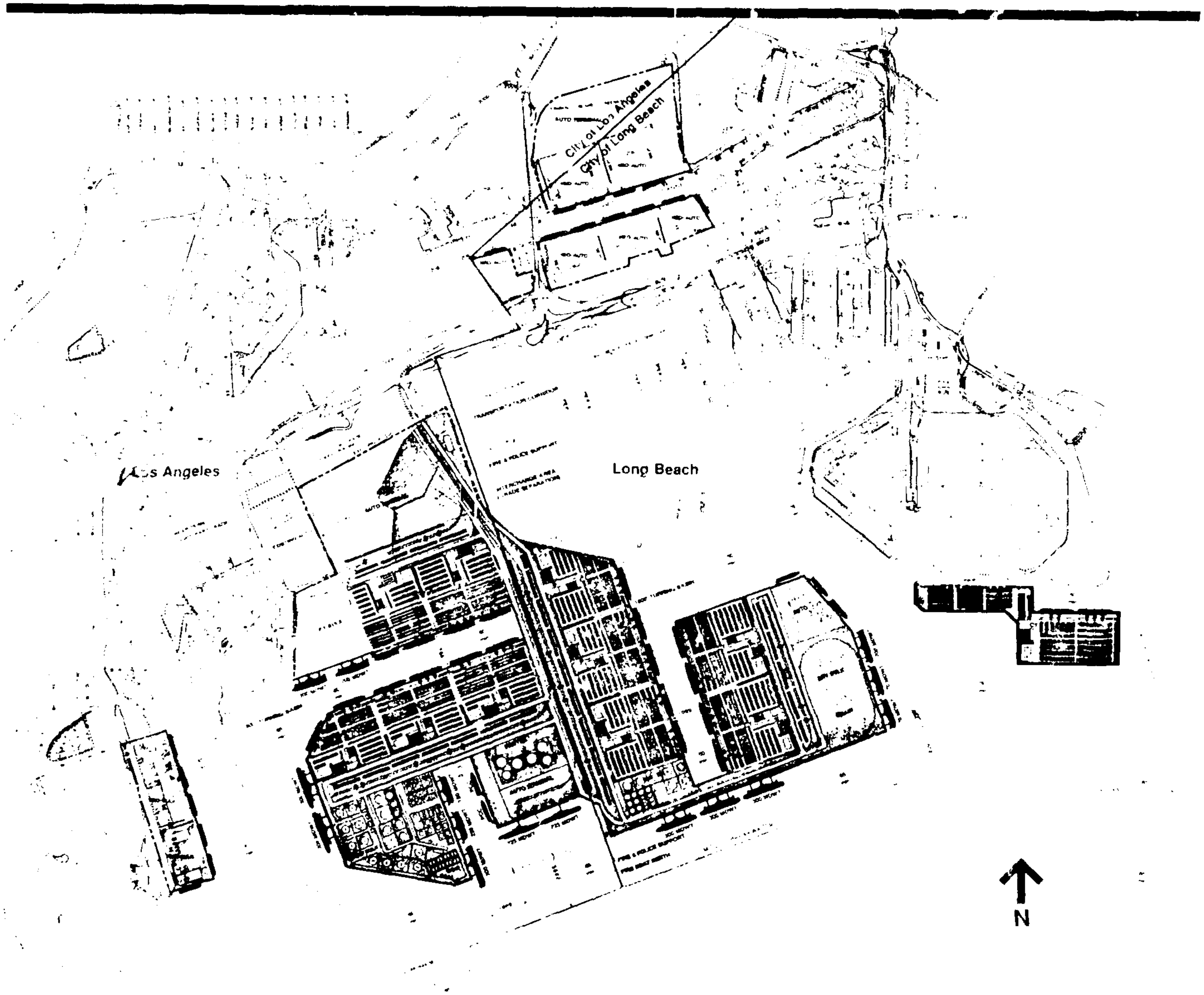

Figure 4. Scheme B Phase 2 harbor geometry for 2020 Plan

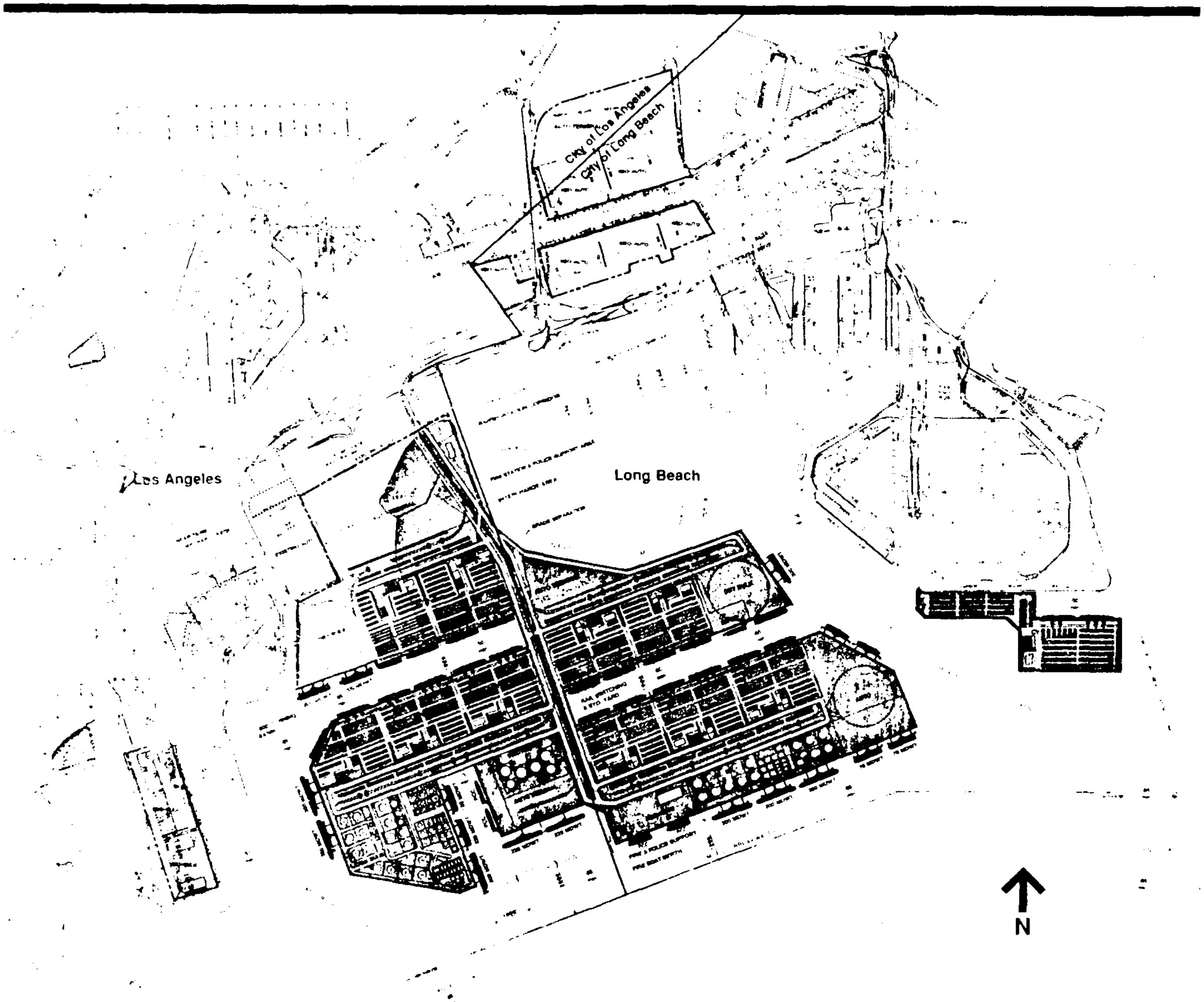

Figure 5. Scheme A Phase 2 harbor geometry for 2020 Plan

PART II: NUMERICAL MODEL

6. The numerical model, originally developed by Chen and Mei (1974), uses a hybrid finite element solution to a generalized Helmholtz equation. The model has been successfully applied to several study areas by the Coastal Engineering Research Center (CERC) (Bottin, Sargent, and Mize 1985; US Army Engineer Waterways Experiment Station (WES) 1987; Farrar and Chen 1987; and Crawford 1988). Houston (1976) included variable depth bathymetry and the dispersion relationship from linear wave theory. The effects of bottom friction and boundary absorption were incorporated into the model by Chen (1984, 1986). This more accurately models the conditions seen in prototype data and physical model testing and is consistent with theoretical arguments of energy dissipation. Chen and Houston (1987) wrote a user's manual for two versions of the model: HARBS for shallow water and HARBD for arbitrary water depth.

7. Applying linear wave theory to the governing continuity and momentum equations and noting that all the dependent variables are periodic in time with angular frequency ω yields the following governing equation (Chen 1986):

$$\nabla \cdot \lambda c c_g \nabla\phi + \frac{c_g}{c} \omega^2 \phi = 0 \tag{1}$$

where

$c = \omega/k$, phase velocity

$k = 2\pi/L$, wave number

L = wave length

$c_g = c/2 + ckh/\sinh(2kh)$, group velocity

ϕ = spatial complex velocity potential

The bottom friction factor λ is assumed proportional to the maximum flow speed at the bottom and defined as

$$\lambda = \frac{1}{1 + \dfrac{\beta a_o}{h \sinh(kh)} i e^{i\gamma}} \tag{2}$$

where

β = dimensionless parameter that varies spatially

a_o = incident wave amplitude

h = local water depth

γ = phase shift between bottom stress and flow velocity

For example, when $\beta = 0$ then $\lambda = 1$, and Equation 1 reduces to Chen and Mei's (1974) original equation without bottom friction.

8. The absorptive boundary condition on the solid boundaries adopts the impedance condition used in acoustics in terms of the boundary reflection coefficient k_r to be

$$\frac{\partial \phi}{\partial \eta} - \alpha \phi = 0 \tag{3}$$

along the boundary with

$$\alpha = ik \frac{1 - k_r}{1 + k_r} \tag{4}$$

and η is the unit normal vector outward from the fluid domain. Similar to the friction coefficient, when $\alpha = 0$, Equation 3 reduces to a statement of zero velocity normal to the boundary, which is implicit in Chen and Mei's original formulation.

9. A conventional finite element approximation with triangular elements of nodal type is used in the near region, while an analytical solution with unknown coefficients is used to describe the far region as an element of coefficient type. A variational principle using a proper functional is established so that the near and far fields are matched along an outer semicircle (or circle) bounded within a semi-infinite (or infinite) domain. The coefficients on the semicircle are obtained from the analytical solution for the specified wave direction. The analytical solution assumes a constant depth or very mild slope in the far region and neglects bottom friction in the far region.

10. Within the bounding semicircle the region is discretized into a finite number of coordinate pairs called node points. These node points are related to adjacent nodes via triangular elements (three nodes per element).

The local depth h and bottom friction factor β are defined at the element level. The reflection coefficients k_r are specified at boundary elements which are defined as a subset of the element data. Once the physical geometry of the finite element mesh is defined, a series of values for wave period T, wave direction θ, and wave amplitude a_0 can be supplied as input to the model.

11. The finite element solution is obtained from a global matrix of nodal coefficients that is assembled at the element level with respect to the governing equations and specified boundary conditions. The element matrices are symmetric with global bandwidths equal to the maximum numerical difference between adjacent node indices. It follows that the assembled matrix is symmetric with a bandwidth (maximum extent of nonzero coefficients from the diagonal) equal to the largest element bandwidth. The size of an element is dependent on the depth and minimum wave period tested which define the minimum wavelength via the dispersion relationship. Quantitative accuracy can be obtained when the number of node points per wavelength exceeds 4.* Elements with equilateral sides are most convenient since this minimizes the nodal density in addition to maximizing computational accuracy.

12. The assembled matrix is solved using Gaussian elimination with a solution time proportional to the number of unknowns (nodes) times the bandwidth squared. With the exception of calculating λ for each element, the solution is normalized with respect to an incident wave of unit amplitude. The resulting complex velocity potential ϕ at each node is then represented as an amplification factor and corresponding phase angle. In general, the solution consists of standing and progressive wave components.

---

* Personal communication, 1988, H. S. Chen, CERC, WES.

PART III: APPLICATION OF NUMERICAL MODEL

Numerical Data Analysis

13. A vectorized version of the HARBD model was run on a CDC Cyber 205 for this study (Crawford 1988). Initial runs indicated a disproportionally large amount of computational time was expended in computing k for each element. This problem was solved by using an algorithm presented by Wu and Thornton (1986). The resulting model can be used efficiently for all wave periods from shallow-water to deepwater conditions.

14. For purposes of this study, results from the model were reduced to a data set consisting of boundary element (or "panel") amplification factors. These factors are the most relevant with respect to moored ship motion. The mean panel amplification is defined as

$$A_{12} = \int_0^1 |\phi_{12}| \, dr \qquad (5)$$

where

$$|\phi_{12}| = \left\{\left[a_1 + r(a_2 - a_1)\right]^2 + \left[b_1 + r(b_2 - b_1)\right]^2\right\}^{1/2} \qquad (6)$$

$$\phi_1 = a_1 + ib_1 \quad , \quad \phi_2 = a_2 + ib_2 \qquad (7\ a,b)$$

and r is the normalized position along the boundary element. Equation 6 is simply the amplification factor at any point along the boundary. Once analyzed, particular panels or sequences of panels representing particular basins were selected for graphical and tabular presentation. Basin response is calculated by taking a weighted average of the respective panel factors. Further analysis of the selected basins was then done by averaging the basin response curves into several period bands varying in length from 30 to 100 sec.

Grid and Boundary Conditions

15. Plates 1-4 show the grid geometries for existing and planned layouts. The harbor geometries were determined from National Oceanographic and Atmospheric Administration (NOAA) charts, information provided by the Ports of Los Angeles and Long Beach. and several other auxiliary data sources. The elements vary in size to reflect local changes in water depth. Nodal spacing varied from 200 ft for the minimum water depth of 9 to 800 ft for depths exceeding 75 ft. This spacing provided a minimum of 4 nodes/wavelength for the 60-sec minimum wave period tested.

16. The bottom friction coefficient was 0.1 for all elements except the 80 elements representing the San Pedro and Middle Breakwaters. The friction coefficient for the breakwater elements was 50. Water depths were determined from NOAA charts and information provided by the ports. The water depth for the breakwater elements was 29.5 ft. The model was run for a fixed water depth of +3 ft mean lower low water.

17. The boundary reflection coefficients varied from 0.965 for depths below 10 ft to 0.995 for depths exceeding 60 ft. The coefficient was incremented 0.005 for each 10-ft increase in depth. For each configuration, a total of 121 wave periods was selected between 60 and 400 sec. The period varied in 2-sec increments from 60 to 200 sec and 4-sec increments from 200 to 400 sec. For comparison purposes, the wave amplitude was fixed at 0.065 ft for friction computations, and the wave direction was set at 210 deg from true north.

18. Plates 5-8 show the boundary locations selected for data presentation. Several line segments, representing prominent basins or slips, were selected from the Los Angeles, Long Beach, and proposed 2020 landfill areas. Results for these segments were obtained as outlined in Paragraph 14.

PART IV: RESULTS

19. Plates 9-68 show the mean amplification response factors as a function of wave period for the line segments defined on Plates 5-8. In addition to the numbering scheme, a descriptive title is included on each plate to aid in identifying the location. For each location the results are presented on two successive plates for the 60- to 180- and 180- to 400-sec wave period bands, respectively. To adequately compare the four data sets shown on each plate, the amplification response (vertical) axis varies in magnitude from plate to plate.

20. A summary of results for Plates 9-68 is shown in Table 1. The values in Table 1 are time averaged response factors for the indicated period bands. For brevity, the four basin geometries will be referenced as existing conditions (EC), Scheme A - Phase II (A2), Scheme B - Phase II (B2), and Scheme B - Phase I (B1). Unless stated otherwise, all comparisons made are with reference to EC.

Long Beach

Pier J extension

21. This area is not presently used for shipping, and all three modifications to it are identical in geometry. Results shown in Plates 9-10 are markedly similar for the proposed changes below 240 sec, while some variation in amplification is seen in the principal mode occurring at 280 sec. Smaller amplification peaks of 2.5 and 1.5 occur at 65 and 90 sec, respectively. These results are similar to those presented in a report by Tekmarine, Inc. (1987), for the Port of Long Beach.

Southeast Basin

22. Plates 11-12 show the overall response of Southeast Basin, with B2 showing the largest increase. A2 increases above 300 sec, while it decreases below this point; and B1 decreases, with the exception of the 140- to 170-sec period range. Table 1 shows that between 60 to 180 sec, A2, B2, and B1 change -11, +23, and +11 percent, respectively. Above 180 sec, the response of the basin is largely a function of a 220-sec peak developing in the pier G-J areas and a 380 peak developing throughout the basin. While A2, B2, and B1 all show significant reduction of the 220-sec peak, B2 increases 103 percent in the

240- to 300-sec band. For the 360- to 400-sec range, A2 and B2 have an approximately fourfold increase in response, while B1 has an approximate twofold increase. Plates 13-18 show the response for three subsections of Southeast Basin.

East Basin

23. Plates 19-20 show the overall East Basin response, and Plates 21-22 and 23-24 show subsections located in the Pier B and Pier D areas, respectively. In the 60- to 180-sec band, East Basin response decreases under the proposed plans with changes of -24, -28, and -13 percent for A2, B2, and B1, respectively. For the modified plans, response between 60- to 180-sec never exceeds 2.0 in the Pier B or Pier D areas, as shown on Plates 21 and 23. East Basin response above 180 sec is dominated by a 200-sec peak which develops for B2 and B1 in the Pier D slip and a broad 300 to 400 sec response in the Pier B and Pier C slips for the three proposed plans. East Basin changes in the 180- to 240-sec band are -20, +51, and +31 percent for A2, B2, and B1, respectively. Similarly, changes in the 300- to 400-sec band are +115, +101, and +157 percent for A2, B2, and B1, respectively.

Naval Basin

24. Response curves for the entire Naval Basin and its west end are shown on Plates 25-26 and 27-28, respectively. Changes in Naval Basin response for the 60 to 150 band are -35, -9, and -17 percent for A2, B2, and B1, respectively. The response above 150 sec is characterized by a sharp peak at 162 sec for all four plans, smaller peaks at 188 sec and 208-12 sec, and a broad response in the 300- to 400-sec band for the three proposed plans. Changes in the 150- to 180-sec band are +49, +32, and +83 percent for A2, B2, and B1, respectively. Changes in the 300- to 400-sec band are +107, +93, and +170 percent for A2, B2, and B1, respectively.

2020 Landfill

25. The overall response of the Long Beach 2020 landfill can be seen on Plates 63-64. Plates 65-66 show the overall response of the landfill slip, and Plates 67-68 the response at the slip's end. The curves show large variations in response between A2, B2, and B1, not unusual considering the major differences in plan geometries.

26. With reference to Plates 67-68, the response curves are dominated by B1, which has a large peak of 5.62 at 86 sec, a broad peak between 120 and 145 sec averaging 3.5, and a large response above 240 sec averaging 4.4. The

B2 response is somewhat similar to B1 between 120 and 240 and usually of lower magnitude outside this range. The A2 response, typically the lowest, has a narrow peak at 122 sec reaching to 4.9 and, relative to B1 or B2, a larger response between 176 and 206 sec. Between 60 and 180 sec, the change in response from B1 to B2 is -37 percent, and from B2 to A2 is -30 percent.

Los Angeles

Main Channel slips/West Basin

27. The Slip 5 response curves (Plates 29-30) show the four plans have a fairly low response below 180 sec and a significant reduction occurring in the 240- to 300-sec band for the three proposed plans.

28. Plates 31-32 are the Slip 1 response curves which show principal peaks occurring at 78 sec, 130 to 150 sec, 276 sec, and 356 to 388 sec. The curves for A2 and B2 are very similar, which, as will be seen, is typical for most of the Los Angeles locations. Changes in the 60- to 180-sec band are +13, +14, and -7 percent for A2, B2, and B1, respectively. Above 180 sec, response decreases for the three proposed plans with major reductions from EC peaks at 276 sec and 388 sec.

29. West Basin response curves on Plates 33-34 show little change occurring under the proposed modifications. The maximum response never exceeds 1.6 for any of the four plans.

30. Response curves for Slip 93, on Plates 35-6, show a large peak forming at 110 to 130 sec for A2 and B2, and smaller peaks appearing at 140 to 160 sec and 210 to 220 sec for A2, B2, and B1. The 110- to 130-sec peak would appear to be a contribution of the East Channel landfill, a feature of A2 and B2 but not included in B1. Changes in response in the 90- to 150-sec and 180- to 240-sec bands are +45 and +25 percent for B2 and -4 and +27 percent for B1, respectively.

31. The SP Slip response curves on Plates 37-38 show changes occurring in the 150- to 180-sec and 240- to 300-sec bands, where large reductions occur, and in the 180- to 240-sec band which has increased significantly. Changes in the 150- to 180-sec and 180- to 240-sec bands are -29 and +46 percent for B2 and -20 and +57 percent for B1, respectively.

32. Plates 45-46 show Slip 240 responds mostly in the 150- to 300-sec range where peaks occur at 156 sec and 186 to 202 sec with magnitudes

close to 5. Response changes in the 150- to 180-sec and 180- to 240-sec bands are -22 and +38 percent for B2, and -15 and +47 percent for B1, respectively.

East Channel/Landfill

33. East Channel geometry remains unchanged for B1 but is replaced by a landfill for A2 and B2 geometries. Response curves for the channel/landfill, located on Plates 39-40, show A2 and B2 are nearly identical, while differences between EC and B1 are significant. Between 60 to 240 sec, B1 response increases +41 percent, and above 240 sec there is a -22 percent decrease. Within the 60- to 150-sec band, the mean response of 1.731 for EC increases to 2.565 for B1 and 1.807 for B2.

Watchorn Basin, Cabrillo Marina, and Fish Harbor

34. Response curves for these areas are shown on Plates 41-42, 43-44, and 47-48 for Watchorn Basin, Cabrillo Marina, and Fish Harbor, respectively. With the possible exception of Watchorn Basin, these areas are not expected to be adversely affected by any changes in response for the 60- to 400-sec band. Most vessels which occupy these areas have principal modes of oscillation occurring at periods below 60 sec. Changes in Watchorn Basin response between 60 and 180 sec are +11 and -3 percent for B2 and B1, respectively. Changes in Cabrillo Marina response between 60 and 180 sec are +10 and -3 percent for B2 and B1, respectively. Fish Harbor shows significant reductions in response for the three proposed plans throughout the 60- to 400-sec band, with the 60- to 180-sec band showing changes of -48 and -54 percent for B2 and B1, respectively.

2020 Landfill

35. Plates 54-55 show the overall response of the Los Angeles 2020 landfill, and Plates 56-62 are response curves for several subsections in this area. As noted earlier, the B2 and A2 curves are very similar, with the largest differences seen at locations in closer proximity to the Long Beach 2020 landfill. Two possibilities for similar response curves are (a) A2 and B2 Los Angeles geometries are identical and (b) orientation of, and distance to, the Long Beach 2020 slip. The two major geographical features of the landfill will be referred to as the Northern Slip and Southern Slip.

36. From Plates 57-58 the major response features of the Northern Slip are several peaks with magnitudes of 2 to 3 between 120 and 200 sec, a peak at 280 sec for B1, and a broad peak at 310 sec for B2. Between 60 to 180 sec, the change in response from B1 to B2 is +15 percent.

37. Major features of the Southern Slip response curves, shown on Plates 61-62, are an amplification peak of 2.5 to 3 between 80 and 100 sec, and a strong peak reaching 7.5 at 240 sec for B1. Between 60 to 180 sec, the change in response from B1 to B2 is +2 percent.

Los Angeles-Long Beach Complex and 2020 Landfill

38. Plates 49-50 show the space-averaged response of the harbors, while Plates 51-52 show the response for the Los Angeles-Long Beach 2020 Landfill. Referring to Table 1, the harbor response below 180 sec decreases for all three proposed plans, whereas above 300 sec just the opposite occurs. Relative to B2, A2 has a lower response below 120 sec and essentially the same response above 120 sec. The overall changes for A2, B2, and B1 are -7.2, -3.3, and +0.1 percent, respectively. Overall changes for the landfill, relative to B2, are -7.1 and +12.2 percent for A2 and B1, respectively.

PART V: CONCLUSIONS

39. Based on the results from the numerical model, it is concluded for Long Beach Harbor that:

- a. The three landfill schemes' influence on existing areas is seen principally above 180 sec. Between 60 and 180 sec, for the Naval, East, and Southeast Basins, changes in response (relative to EC) are -17, -13, and +4 percent for A2, B2, and B1, respectively. Similarly, overall changes between 60 and 400 sec are +24, +33, and +39 percent, respectively.
- b. The Scheme B layouts show a significant increase in response for the 2020 Landfill Slip relative to the Scheme A layout; between 60 and 180 sec, changes in response are +51 and +136 percent for B2 and B1, respectively. Similarly, overall changes between 60 and 400 sec are +44 and +106 percent, respectively.
- c. The Pier J Extension Slip is not significantly influenced by the three landfill schemes.

Overall, A2 appears to be the best plan for minimizing harbor response for Long Beach. While the B2 layout has a stronger response, its effect is located primarily within the 2020 Landfill Slip. The magnitude of the B2 layout response is not sufficiently above the A2 response to consider excluding B2 from plan selection. With respect to ship motion, other factors such as response characteristics in the 10- to 60-sec period band, ship types, fender types, mooring line types and configurations, downtime criteria, and wave statistics are necessary in determining the best plan.

40. Based on the results for the numerical model, it is concluded for Los Angeles Harbor that:

- a. Response characteristics for A2 and B2 are virtually the same for all locations, the largest differences occurring with proximity to Long Beach Harbor. It appears that the similar response may be due to two factors, (1) the Los Angeles Phase 2 geometries are identical and (2) orientation and distance of differences in Long Beach Phase 2 geometries.
- b. With the exception of Slip 93, the Main Channel basins/slips do not show significant changes in response for the three proposed plans. The large increase between 90 to 150 sec at Slip 93 appears to be due to the presence of the East Channel Landfill.
- c. For the Phase 2 layouts, East Channel response between 60 to 150 sec is about the same as EC, while the B1 layout shows a significant increase. Above 150 sec, response for the three proposed plans decreases significantly (except for a substantial increase in the 180- to 240-sec band).
- d. Watchorn Basin and Cabrillo marina do not change significantly. The changes that occur are not expected to adversely affect

typical vessels in these areas since principal ship motion response periods are below the most significant changes (or in fact below 60-sec minimum period studied here).

e. Fish Harbor shows significant reduction in response for all three proposed plans.

f. Although the 2020 Northern Slip shows significant changes in response between Phases 1 and 2, the overall responses are relatively small (compared with East Channel or 2020 Southern Slip).

g. The 2020 Southern Slip shows strong response between 80 to 100 sec and above 180 sec for the three proposed plans. The response above 180 sec is largest for B1, in particular between 200 to 270 sec, where the amplification factor approaches 8 at the slip's end.

The critical areas for Los Angeles Harbor appear to be the B1 configuration for East Channel and the three proposed plans for the 2020 Southern Slip. Relative to EC for East Channel, the 2020 Southern Slip shows a smaller response below 180 sec and a larger response above this point. The relative exposure of these locations and their proximity to Angle's Gate, coupled with incident wave energies in the 10- to 60-sec period band, could lead to adverse ship motion events under extreme wave conditions.

41. The overall response of the Los Angeles - Long Beach Harbor Complex and proposed 2020 landfill areas show that A2 has the lowest response followed by B2 and B1, respectively.

REFERENCES

Bottin, Robert R., Jr. 1988. "Case Histories of Corps Breakwater and Jetty Structures; Report 1, South Pacific Division," Technical Report REMR-CO-3, US Army Engineer Waterways Experiment Station, Vicksburg, MS.

Bottin, Robert R., Jr., Sargent, Francis E., and Mize, Marvin G. 1985. "Fisherman's Wharf Area, San Francisco Bay, California, Design for Wave Protection: Physical and Numerical Model Investigation," Technical Report CERC-85-7, US Army Engineer Waterways Experiment Station, Vicksburg, MS.

Chen, H. S. 1984. "Hybrid Element Modeling of Harbor Resonance," Fourth International Conference on Applied Numerical Modeling, Tainan, Taiwan, R.O.C.

__________. 1986. "Effects of Bottom Friction and Boundary Absorption on Water Wave Scattering," Applied Ocean Research, Vol 8, No. 2, pp 99-104.

Chen, H. S., and Houston, J. R. 1987. "Calculation of Water Oscillation in Coastal Harbors, HARBS and HARBD User's Manual," Instruction Report CERC-87-2, US Army Engineer Waterways Experiment Station, Vicksburg, MS.

Chen, H. S., and Mei, C. C. 1974 (Aug). "Oscillations and Wave Forces in an Offshore Harbor," Ralph M. Parsons Laboratory Report No. 190, Massachusetts Institute of Technology, Cambridge, MA.

Crawford, Peter L. 1988. "Comparison of Numerical and Physical Models of Wave Response in a Harbor," Miscellaneous Paper CERC-88-11, US Army Engineer Waterways Experiment Station, Vicksburg, MS.

Farrar Paul D., and Chen, H. S. 1987. "Wave Response of the Proposed Harbor at Agat, Guam," Technical Report CERC-87-4, US Army Engineer Waterways Experiment Station, Vicksburg, MS.

Houston, James R. 1976. "Long Beach Harbor Numerical Analysis of Harbor Oscillations; Report 1, Existing Conditions and Proposed Improvements," Miscellaneous Paper H-76-20, US Army Engineer Waterways Experiment Station, Vicksburg, MS.

Tekmarine, Inc. 1987. "Ship Motion and Harbor Response Study for Pier J Expansion Project," Tekmarine Report No. TCN-108, Pasadena, CA.

US Army Engineer Waterways Experiment Station. 1987. "Disposal Alternatives for PCB-Contaminated Sediments from Indiana Harbor, Indiana; Volumes 1 and 2," Miscellaneous Paper EL-87-9, Environmental Laboratory, Vicksburg, MS.

Vickerman Zachary Miller, Inc. 1988. "2020 OFI Study Summary, San Pedro Bay Ports of Los Angeles and Long Beach," Oakland, CA.

Wu, Chung-Shang, and Thornton, E. B. 1986 (Jul). "Wave Numbers of Linear Progressive Waves," Journal of Waterways, Port, Coastal and Ocean Engineering, Vol 112, No. 4, pp 536-40.

BIBLIOGRAPHY

Burington, Richard S. 1965. Handbook of Mathematical Tables and Formulas, 4th Edition, McGraw-Hill, New York.

Gallagher, Richard H. 1975. Finite Element Analysis: Fundamentals, Prentice-Hall, Inc., Englewood Cliffs, NJ.

US Army Corps of Engineers. 1985. The Ports of Los Angeles, Long Beach, and Port Hueneme, California, Port Series No. 28, Water Resources Support Center, Fort Belvoir, VA.

Table 1

Mean Amplification Response Factors

LOCATION	PLATES	BOUNDARY FROM	BOUNDARY TO	SCHEME	LENGTH (FEET)	PERIOD BANDS (SECONDS) 060-090	090-120	120-150	150-180	180-240	240-300	300-400	060-400
LA SLII 5	29,30	14	15										
				EXISTING	5717	.283	.296	.133	.272	.748	1.769	.202	.590
				A:PHASE II	5717	.268	.303	.162	.229	.780	1.032	.324	.500
				B:PHASE II	5717	.256	.310	.150	.230	.861	1.079	.282	.509
				B:PHASE I	5717	.220	.319	.142	.210	.845	.928	.383	.504
LA SLIP 1	31,32	16	17										
				EXISTING	7874	.648	.351	.838	.526	.472	1.870	1.365	1.023
				A:PHASE II	7874	.711	.516	1.005	.443	.534	1.137	1.017	.830
				B:PHASE II	7874	.709	.518	1.010	.449	.547	1.109	1.058	.841
				B:PHASE I	7874	.502	.343	.912	.441	.563	1.084	.870	.740
LA WEST BASIN	33,34	18	19										
				EXISTING	8828	.366	.358	.115	.243	.563	.344	.112	.288
				A:PHASE II	8828	.316	.426	.145	.237	.691	.210	.058	.275
				B:PHASE II	8828	.302	.426	.147	.238	.707	.204	.060	.277
				B:PHASE I	8828	.288	.316	.124	.232	.684	.191	.059	.257
LA SLIP 93	35,36	20	21										
				EXISTING	2726	.341	1.203	2.312	1.377	1.351	1.278	.767	1.151
				A:PHASE II	2726	.358	2.203	2.908	1.384	1.692	.781	.700	1.247
				B:PHASE II	2726	.353	2.202	2.923	1.387	1.695	.794	.713	1.255
				B:PHASE I	2726	.268	.993	2.373	1.295	1.714	.748	.530	1.025
LA SP SLIP	37,38	22	23										
				EXISTING	3797	1.347	.334	1.302	3.116	2.384	2.203	.748	1.568
				A:PHASE II	3797	1.513	.454	1.463	2.206	3.481	1.310	.753	1.564
				B:PHASE II	3797	1.510	.451	1.475	2.207	3.484	1.302	.765	1.567
				B:PHASE I	3797	1.051	.258	1.310	2.508	3.731	1.203	.535	1.481
LA EAST CHANNEL/LANDFILL	39,40	24	25										
				EXISTING	7685	1.525	1.722	1.927	2.095	.886	2.845	2.953	2.168
				A:PHASE II	3076	1.792	1.774	1.839	1.427	1.626	1.867	.606	1.397
				B:PHASE II	3076	1.784	1.768	1.847	1.432	1.619	1.868	.607	1.397
				B:PHASE I	7685	2.269	2.826	2.574	1.898	1.582	2.243	2.283	2.190
LA WATCHORN BASIN	41,42	26	27										
				EXISTING	4097	1.794	.682	2.240	1.677	2.086	.239	.328	1.071
				A:PHASE II	4097	1.659	1.115	2.055	2.253	1.702	.149	.501	1.099
				B:PHASE II	4097	1.661	1.120	2.057	2.253	1.698	.151	.491	1.096
				B:PHASE I	4097	1.728	.983	2.090	1.423	1.272	.152	.487	.944
LA CABRILLO MARINA	43,44	28	29										
				EXISTING	3672	1.061	.198	.780	.515	1.755	.635	1.330	1.038
				A:PHASE II	3672	.906	.315	.810	.768	1.322	.632	2.010	1.183
				B:PHASE II	3672	.910	.316	.812	.770	1.317	.633	1.972	1.172
				B:PHASE I	3672	.959	.262	.768	.482	.983	.589	1.915	1.059
LA SLIP 240	45,46	34	35										
				EXISTING	3736	.694	.550	1.312	3.401	2.231	2.097	.623	1.473
				A:PHASE II	3736	.666	.879	1.507	2.662	3.068	1.259	.675	1.466
				B:PHASE II	3736	.666	.881	1.518	2.670	3.077	1.265	.684	1.474
				B:PHASE I	3736	.483	.500	1.288	2.881	3.271	1.188	.470	1.380
LA FISH HARBOR	47,48	36	37										
				EXISTING	8630	1.827	1.561	1.656	1.562	1.855	2.004	1.979	1.846
				A:PHASE II	8630	.736	1.031	.283	1.416	.943	.878	1.059	.939
				B:PHASE II	8630	.728	1.023	.285	1.416	.937	.865	1.075	.939
				B:PHASE I	8630	.538	1.095	.661	.718	.612	.651	.763	.713

(Continued)

(Sheet 1 of 3)

Table 1 (Continued)

LOCATION	PLATES	BOUNDARY FROM	BOUNDARY TO	SCHEME	LENGTH (FEET)	PERIOD BANDS (SECONDS) 060-090	090-120	120-150	150-180	180-240	240-300	300-400	060-400
LA/LB HARBOR COMPLEX	49,50	1	50										
				EXISTING	287613	.903	.883	.891	.939	1.137	1.033	.883	.962
				A:PHASE II	333926	.682	.722	.745	.807	1.013	.859	1.026	.893
				B:PHASE II	336711	.779	.821	.742	.812	1.123	.865	1.022	.930
				B:PHASE I	342947	.756	.797	.828	.886	1.104	.929	1.073	.963
LA/LB 2020 LANDFILL	51,52	39	50										
				A:PHASE II	57373	.855	.811	.866	.774	1.178	1.252	1.583	1.186
				B:PHASE II	56280	.917	.788	1.044	.935	1.126	1.393	1.722	1.276
				B:PHASE I	48239	1.133	1.013	1.259	.938	1.332	1.729	1.730	1.432
LA 2020 LANDFILL	53,54	39	45										
				A:PHASE II	26051	.909	.906	.803	.828	1.092	1.323	1.699	1.230
				B:PHASE II	26051	.903	.914	.802	.823	1.087	1.338	1.673	1.224
				B:PHASE I	26051	.892	.948	.908	.772	1.319	1.532	1.507	1.257
LA NORTHERN SLIP	55,56	39	41										
				A:PHASE II	6760	.393	.427	.609	.570	.693	1.018	.886	.739
				B:PHASE II	6760	.391	.429	.615	.570	.709	1.004	.898	.743
				B:PHASE I	6760	.286	.484	.932	.427	.402	1.064	.603	.624
LA NORTHERN SLIP(END)	57,58	39	40										
				A:PHASE II	832	.618	.669	.937	.905	.995	1.514	1.431	1.140
				B:PHASE II	832	.616	.671	.946	.905	1.018	1.492	1.450	1.146
				B:PHASE I	832	.382	.627	1.317	.401	.451	1.428	.401	.690
LA SOUTHERN SLIP	59,60	42	45										
				A:PHASE II	10823	1.326	1.308	.913	1.074	1.562	1.961	2.998	1.911
				B:PHASE II	10823	1.319	1.326	.898	1.063	1.539	2.017	2.922	1.893
				B:PHASE I	10823	1.295	1.326	.830	1.020	2.331	2.473	2.760	2.054
LA SOUTHERN SLIP(END)	61,62	43	44										
				A:PHASE II	1359	1.972	1.713	1.038	1.459	2.674	3.421	4.128	2.835
				B:PHASE II	1359	1.955	1.772	.995	1.414	2.633	3.555	4.014	2.814
				B:PHASE I	1359	1.986	1.937	.889	1.198	3.881	4.327	3.881	3.120
LB 2020 LANDFILL	63,64	45	50										
				A:PHASE II	31322	.810	.731	.918	.730	1.249	1.193	1.487	1.150
				B:PHASE II	30229	.930	.680	1.253	1.032	1.160	1.441	1.764	1.322
				B:PHASE I	22188	1.415	1.089	1.671	1.133	1.347	1.960	1.993	1.638
LB 2020 SLIP	65,66	46	49										
				A:PHASE II	15695	.551	.574	.845	.365	1.231	.887	1.279	.956
				B:PHASE II	10568	.569	.297	1.674	.990	.918	1.344	2.272	1.379
				B:PHASE I	10568	1.529	.810	2.155	1.015	1.218	2.267	2.937	1.965
LB 2020 SLIP(END)	67,68	47	48										
				A:PHASE II	1241	.892	.908	1.262	.581	1.842	1.318	2.125	1.504
				B:PHASE II	1267	.876	.460	2.425	1.419	1.457	2.249	3.462	2.129
				B:PHASE I	1267	2.364	1.265	3.115	1.457	1.932	3.798	4.508	3.061

(Continued)

Table 1 (Concluded)

LOCATION	PLATES	BOUNDARY FROM	BOUNDARY TO	SCHEME	LENGTH (FEET)	PERIOD BANDS (SECONDS) 060-090	090-120	120-150	150-180	180-240	240-300	300-400	060-400
LB PIER J EXTENSION SLIP	9,10	2	3										
				EXISTING	2407	1.911	1.823	1.943	1.373	1.811	1.634	1.441	1.654
				A:PHASE II	5758	[illegible].488	1.573	.472	1.042	2.309	4.620	1.743	2.139
				B:PHASE II	5758	1 406	1.600	.494	.975	2.112	5.684	1.894	2.328
				B:PHASE I	5758	1 411	1.585	.504	.980	2.106	5.027	1.685	2.150
LB SOUTHEAST BASIN	11,12	4	8										
				EXISTING	20562	.734	.437	.577	1.018	1.391	.343	.623	.733
				A:PHASE II	20562	.729	.266	.495	.958	.767	.238	1.445	.818
				B:PHASE II	20562	1.15[illegible]	.479	.670	1.108	.963	.695	1.295	.975
				B:PHASE I	20562	.716	.397	.740	1.219	.847	.233	.873	.718
LB PIER J SLIP	13,14	4	5										
				EXISTING	5536	.827	.635	.973	1.620	1.566	.137	.337	.757
				A:PHASE II	5536	.763	.371	.838	1.536	.904	.108	.910	.756
				B:PHASE II	5536	1.188	.695	1.129	1.773	.960	.256	.827	.880
				B:PHASE I	5536	.717	.513	1.254	1.956	.830	.084	.533	.710
LB PIER G SLIP	15,16	5	6										
				EXISTING	5527	.512	.260	.092	.514	2.660	.570	.643	.881
				A:PHASE II	5527	.507	.137	.080	.421	1.398	.353	1.555	.867
				B:PHASE II	5527	.782	.302	.121	.508	1.838	1.225	1.389	1.100
				B:PHASE I	5527	.428	.198	.133	.544	1.623	.419	.905	.742
LB BASIN 6	17,18	7	8										
				EXISTING	7234	.802	.387	.464	.828	.519	.397	.966	.665
				A:PHASE II	7234	.867	.253	.396	.790	.303	.304	2.076	.921
				B:PHASE II	7234	1.443	.425	.540	.910	.450	.752	1.852	1.049
				B:PHASE I	7234	.913	.417	.585	1.003	.399	.246	1.291	.751
LB EAST BASIN	19,20	9	13										
				EXISTING	17753	.645	.402	.742	.277	.798	.516	1.106	.740
				A:PHASE II	17753	.317	.231	.697	.324	.641	.492	2.383	1.039
				B:PHASE II	17753	.488	.421	.354	.226	1.205	.322	2.222	1.054
				B:PHASE I	17753	.470	.386	.507	.437	1.045	.376	2.843	1.246
LB PIER B SLIP	21,22	10	11										
				EXISTING	4799	.499	.519	.912	.244	.243	.431	1.692	.809
				A:PHASE II	4799	.293	.293	870	.283	.195	.464	3.685	1.353
				B:PHASE II	4799	.485	.530	.452	.196	.360	.245	3.440	1.265
				B:PHASE I	4799	.414	.509	.619	.397	.345	.394	4.366	1.585
LB PIER D SLIP	23,24	12	13										
				EXISTING	4814	.844	.362	.4[illegible]3	.296	2.267	1.048	.512	.906
				A:PHASE II	4814	.423	.218	.376	.344	1.839	.886	1.022	.902
				B:PHASE II	4814	.585	.411	.178	.240	3.431	.705	.949	1.134
				B:PHASE I	4814	.682	.330	.300	.460	2.909	.586	1.261	1.144
LB NAVAL BASIN	25,26	30	33										
				EXISTING	18425	1.241	1.081	.557	.862	.716	.614	.703	.772
				A:PHASE II	18425	.603	.599	.663	1.287	.649	.730	1.453	.949
				B:PHASE II	18425	1.005	1.197	.412	1.138	1.051	.237	1.358	.958
				B:PHASE I	18425	1.101	.833	.453	1.577	.929	.653	1.900	1.188
LB NAVAL BASIN(WEST END)	27,28	31	32										
				EXISTING	5458	1.415	1.127	.770	1.101	.916	.927	1.164	1.057
				A:PHASE II	5458	.788	.622	.888	1.717	.868	1.119	2.415	1.415
				B:PHASE II	5458	1.269	1.308	.549	1.485	1.349	.350	2.257	1.371
				B:PHASE I	5458	1.408	.975	.613	2.128	1.195	1.002	3.124	1.759

(Sheet 3 of 3)

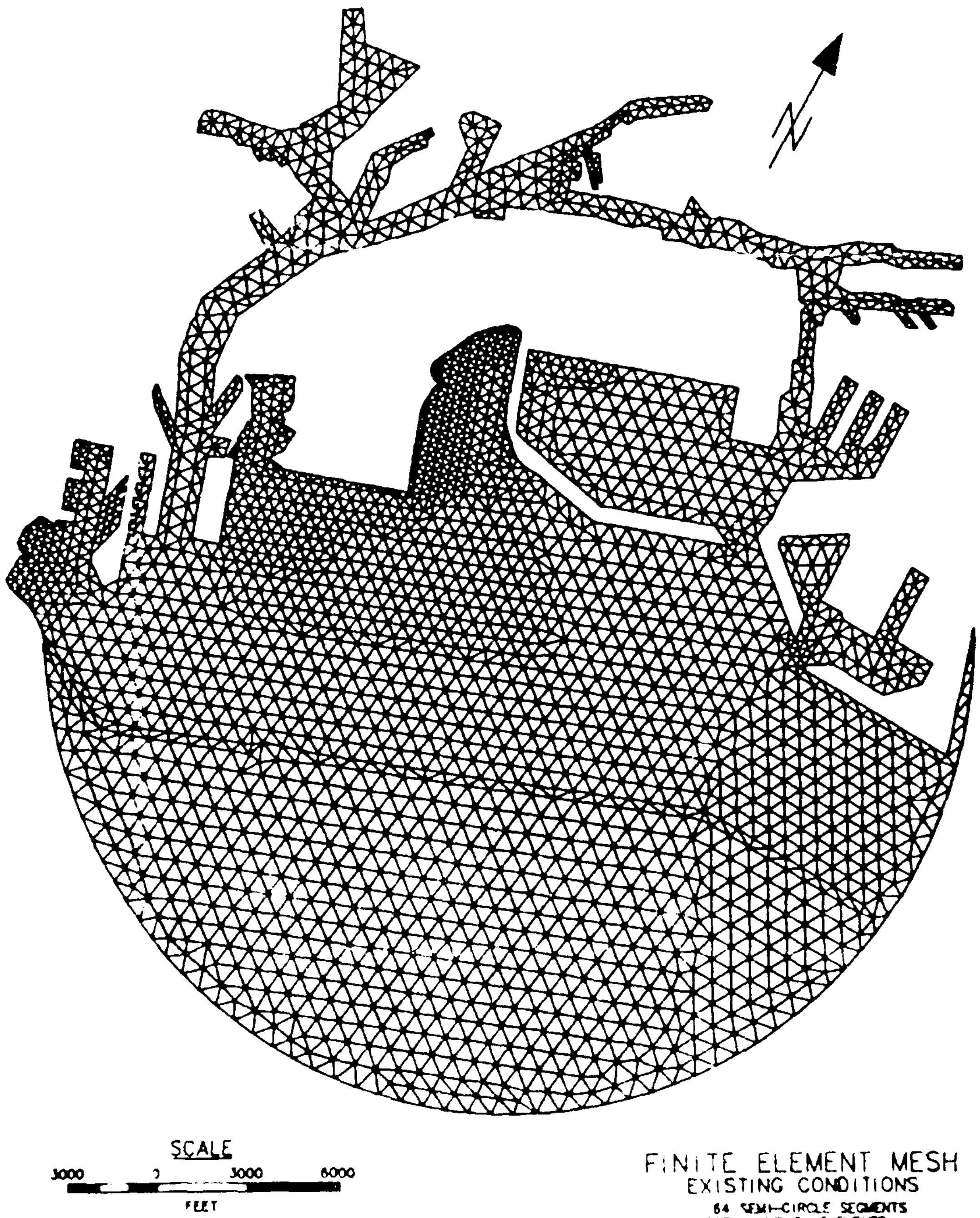

FINITE ELEMENT MESH
EXISTING CONDITIONS

64 SEMI-CIRCLE SEGMENTS
677 BOUNDARY ELEMENTS
4693 ELEMENTS
2717 NODES

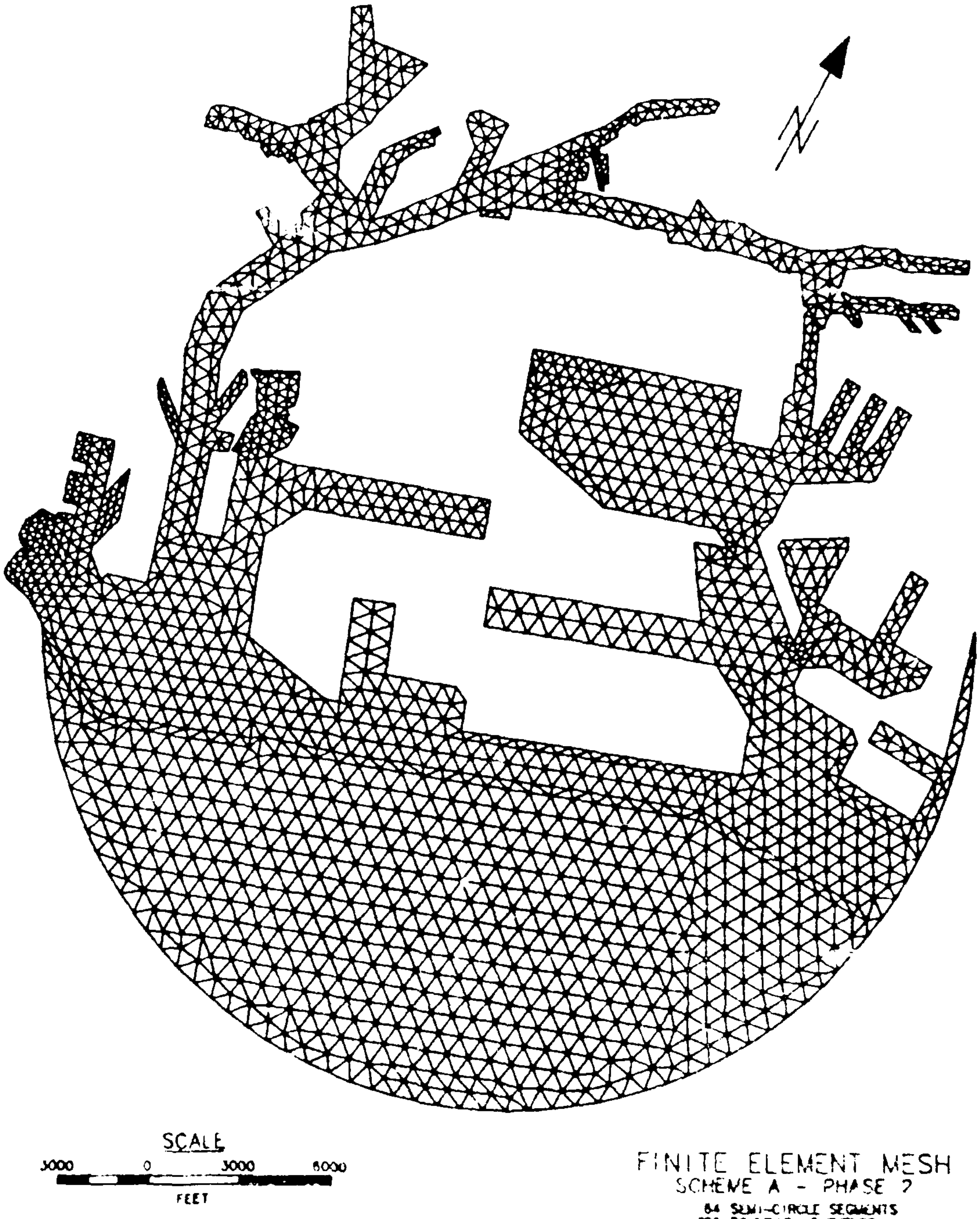

FINITE ELEMENT MESH
SCHEME A - PHASE 2
64 SEMI-CIRCLE SEGMENTS
725 BOUNDARY ELEMENTS
3317 ELEMENTS
2153 NODES

PLATE 2

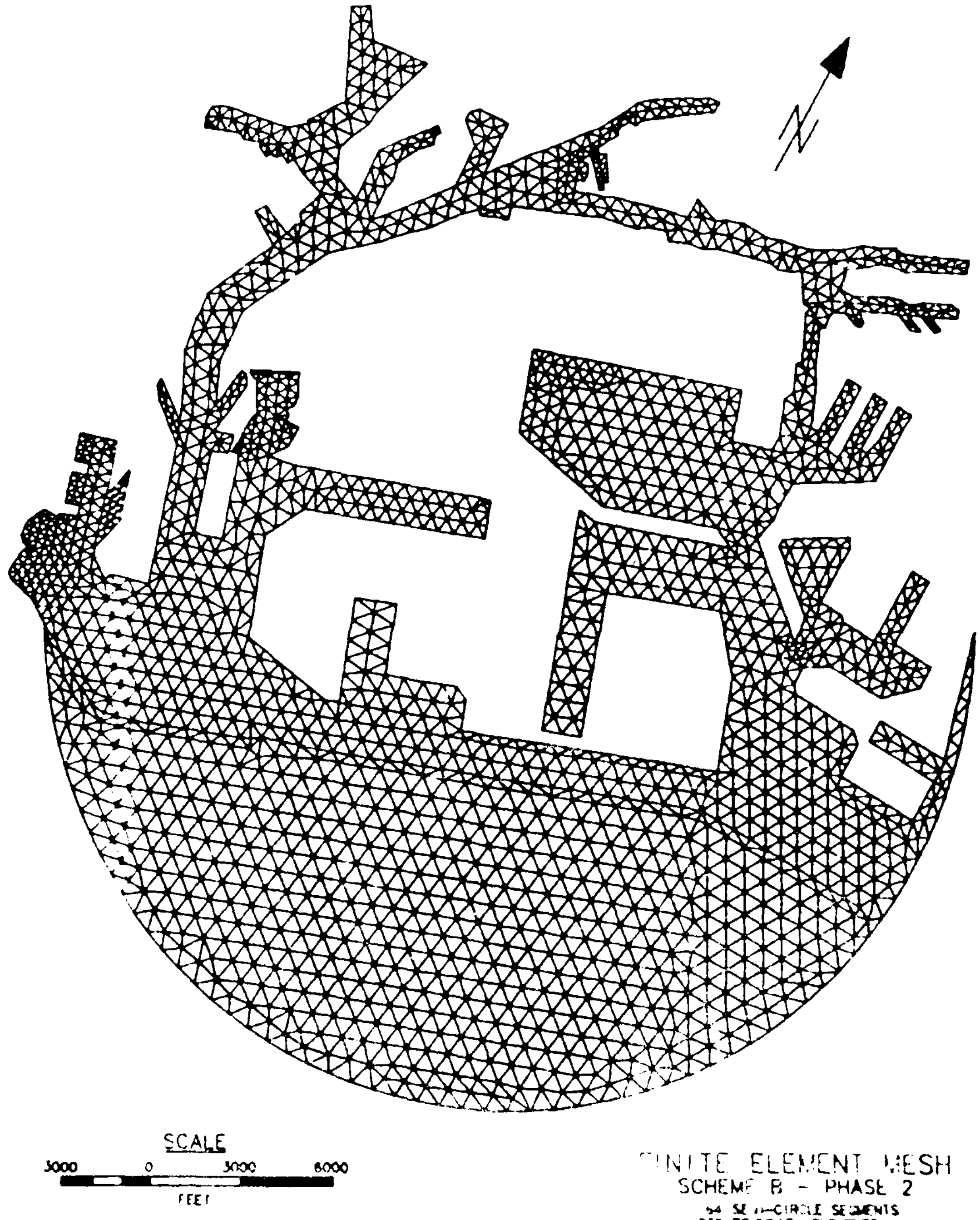

FINITE ELEMENT MESH
SCHEME B - PHASE 2
64 SEMI-CIRCLE SEGMENTS
736 BOUNDARY ELEMENTS
3373 ELEMENTS
2189 NODES

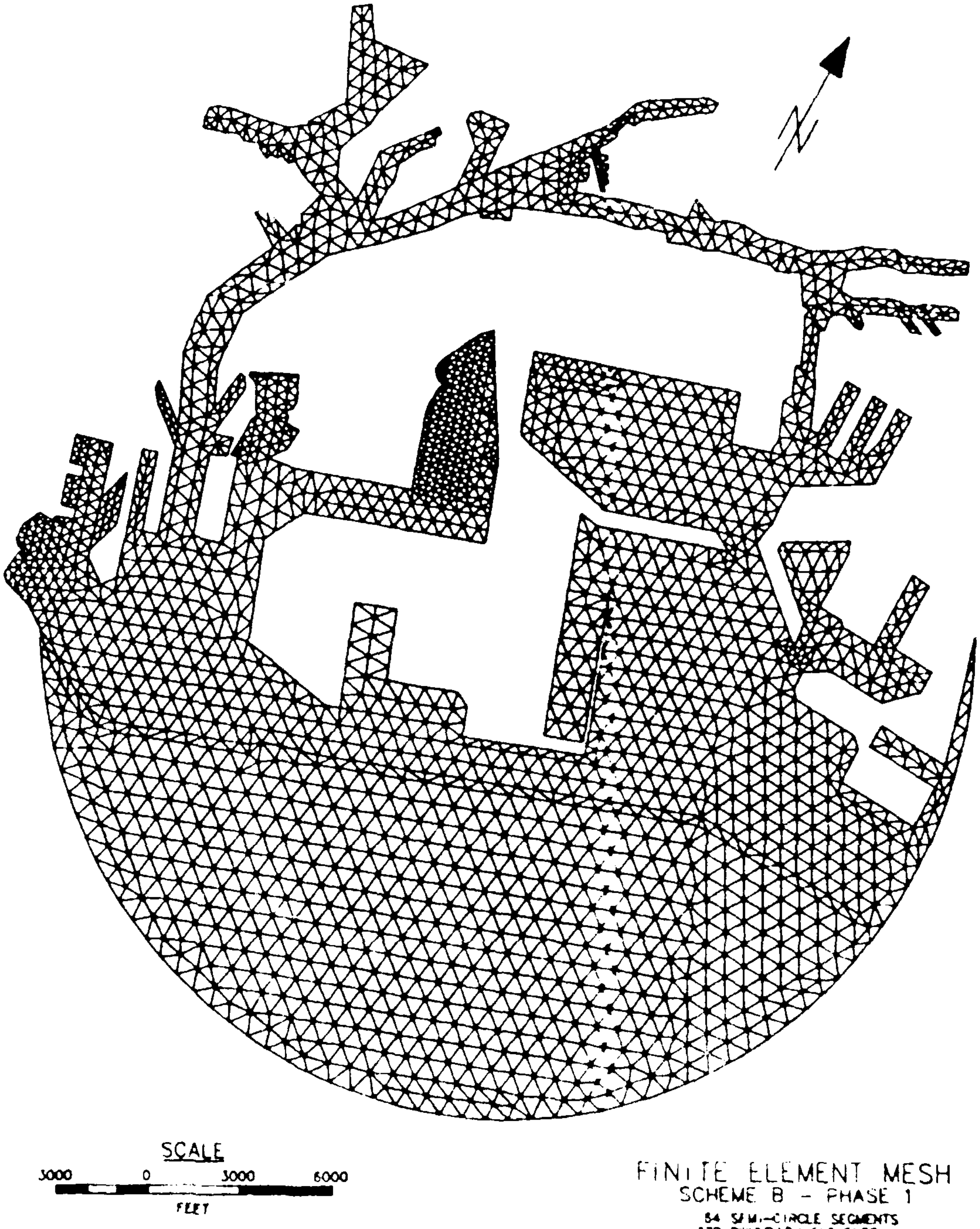

FINITE ELEMENT MESH
SCHEME B - PHASE 1

84 SEMI-CIRCLE SEGMENTS
772 BOUNDARY ELEMENTS
4030 ELEMENTS
2433 NODES

PLATE 4

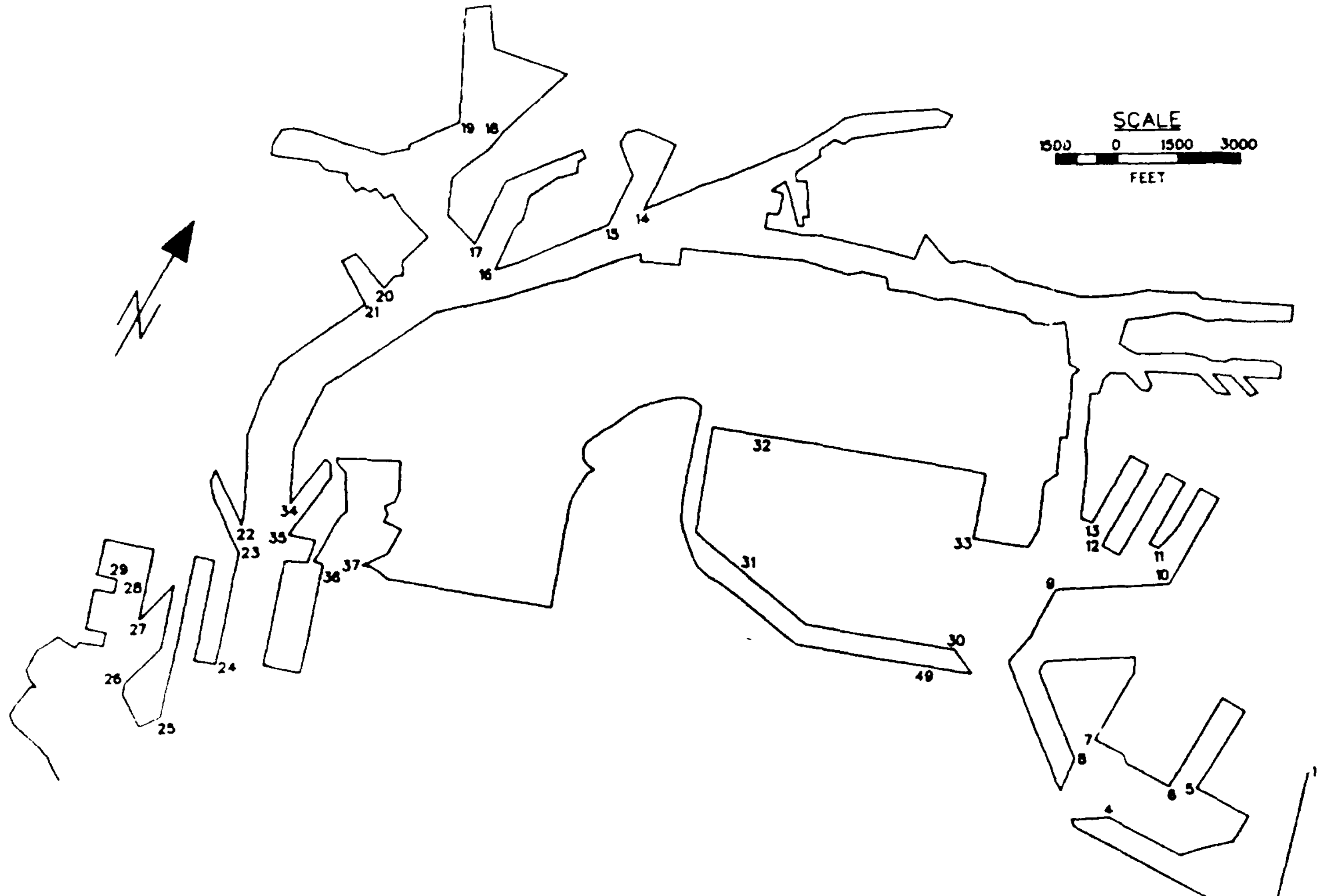

LOCATION OF BOUNDARY NODES
EXISTING CONDITIONS

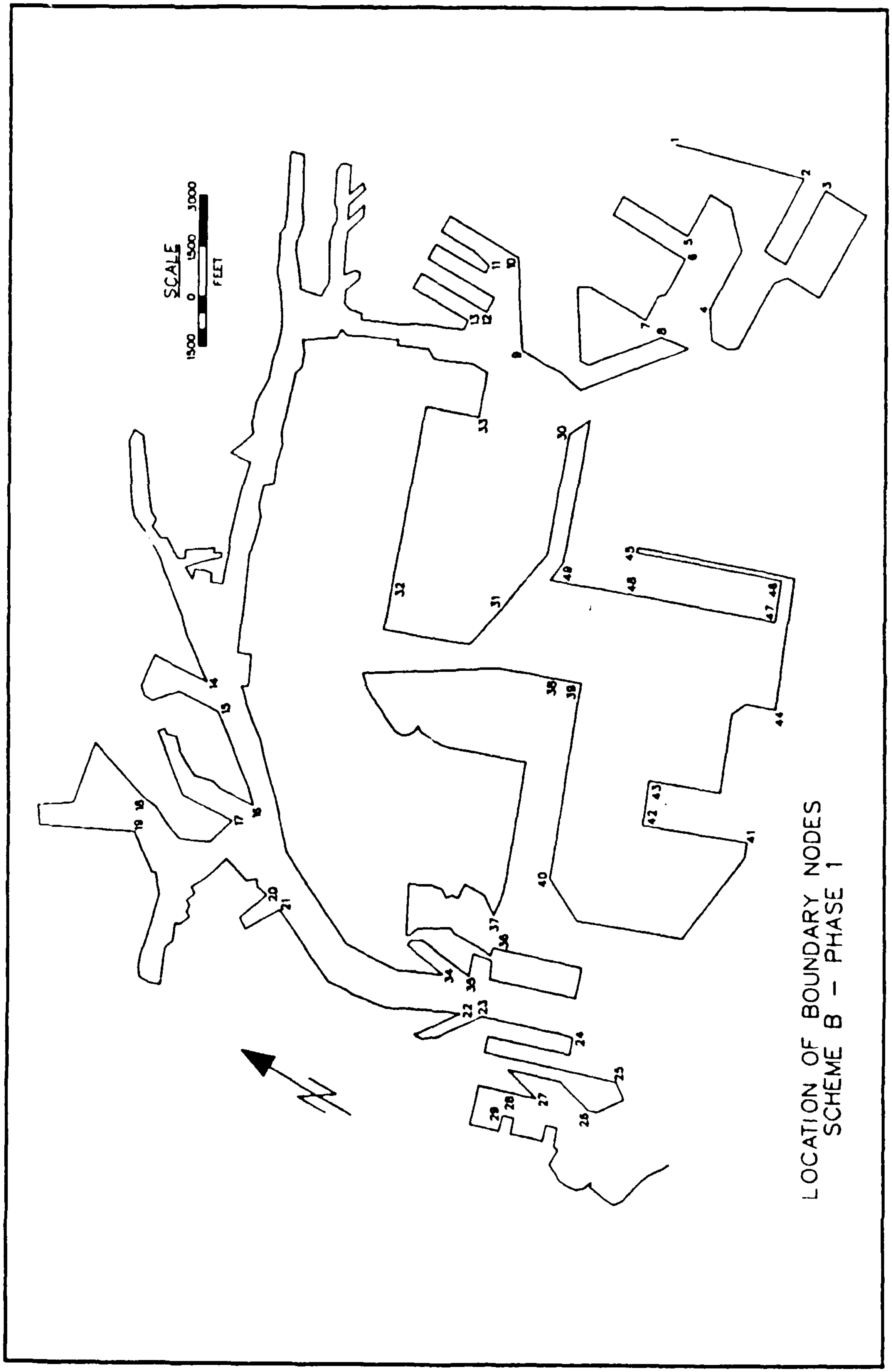
SCALE
1500 0 1500 3000
FEET
LOCATION OF BOUNDARY NODES
SCHEME B – PHASE 1

PLATE 6

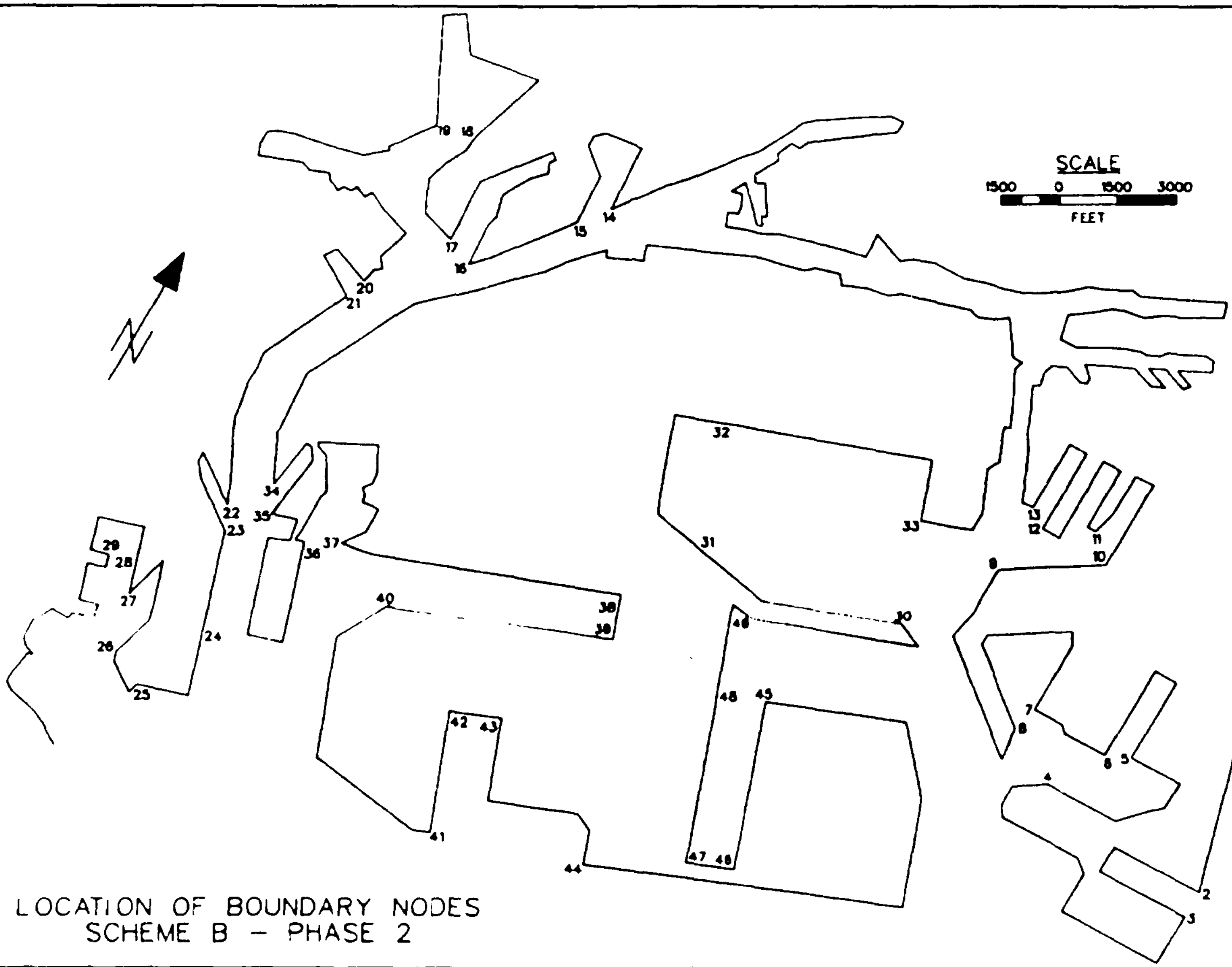

LOCATION OF BOUNDARY NODES
SCHEME B - PHASE 2

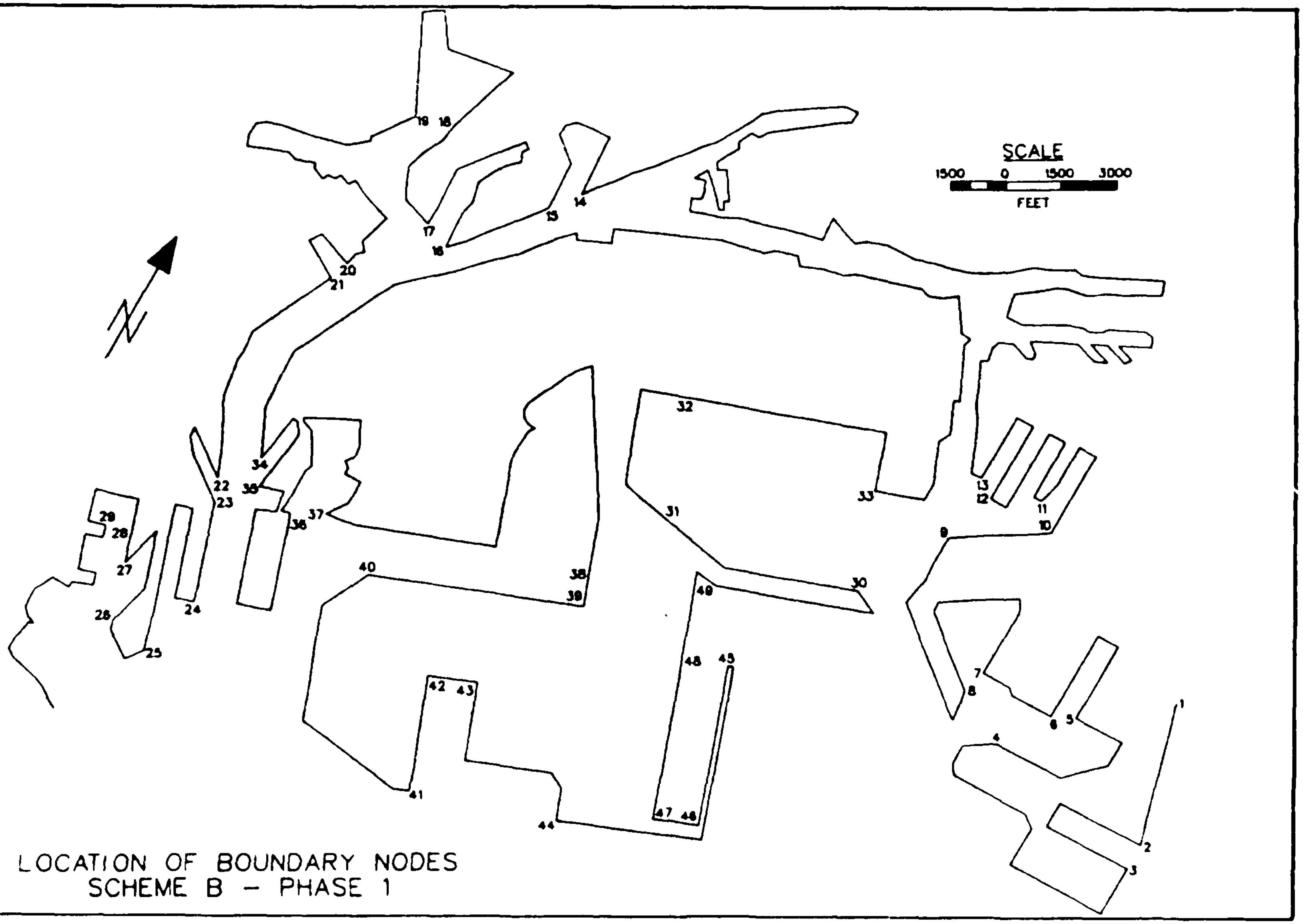

LOCATION OF BOUNDARY NODES
SCHEME B – PHASE 1

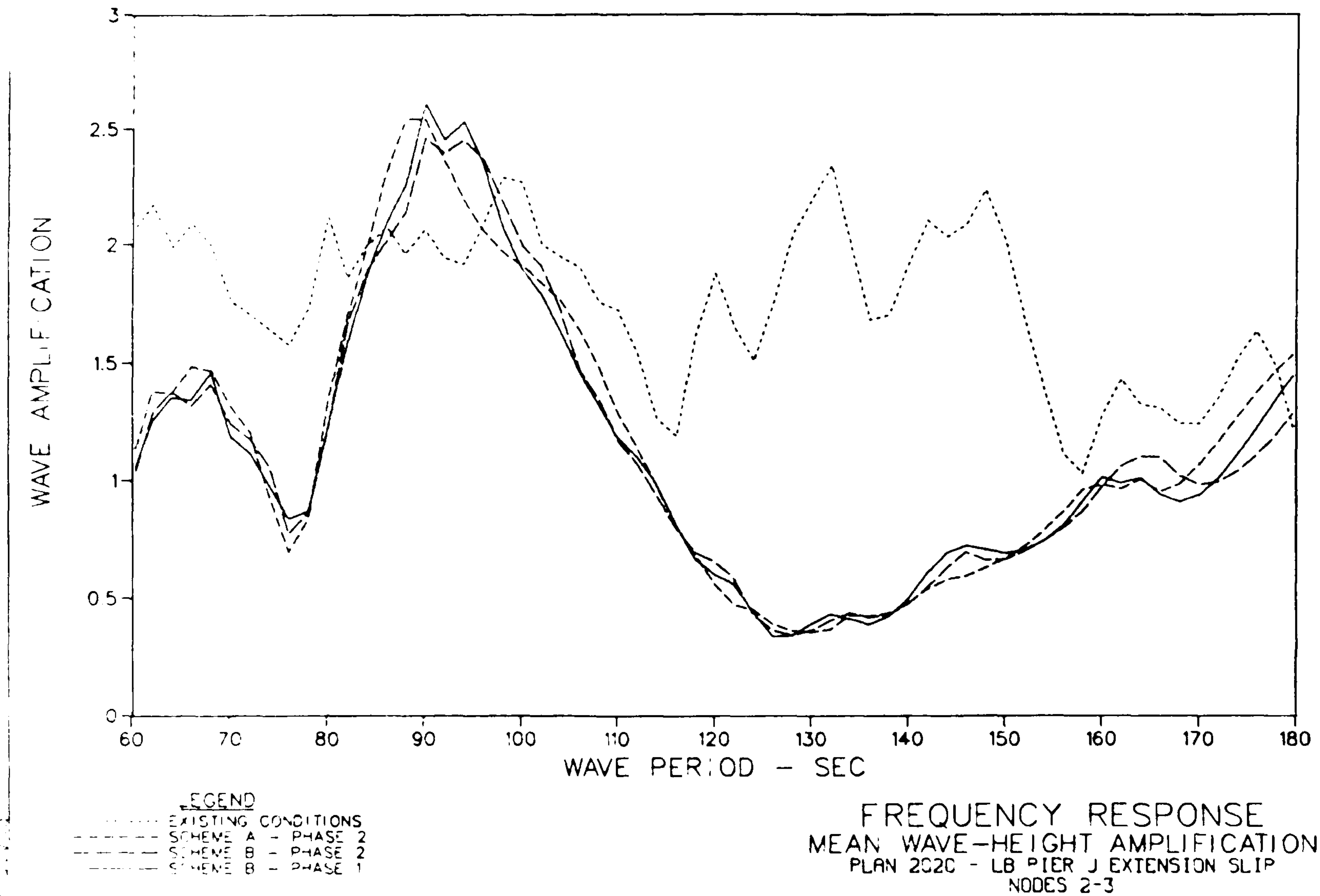

FREQUENCY RESPONSE
MEAN WAVE-HEIGHT AMPLIFICATION
PLAN 2C2C - LB PIER J EXTENSION SLIP
NODES 2-3

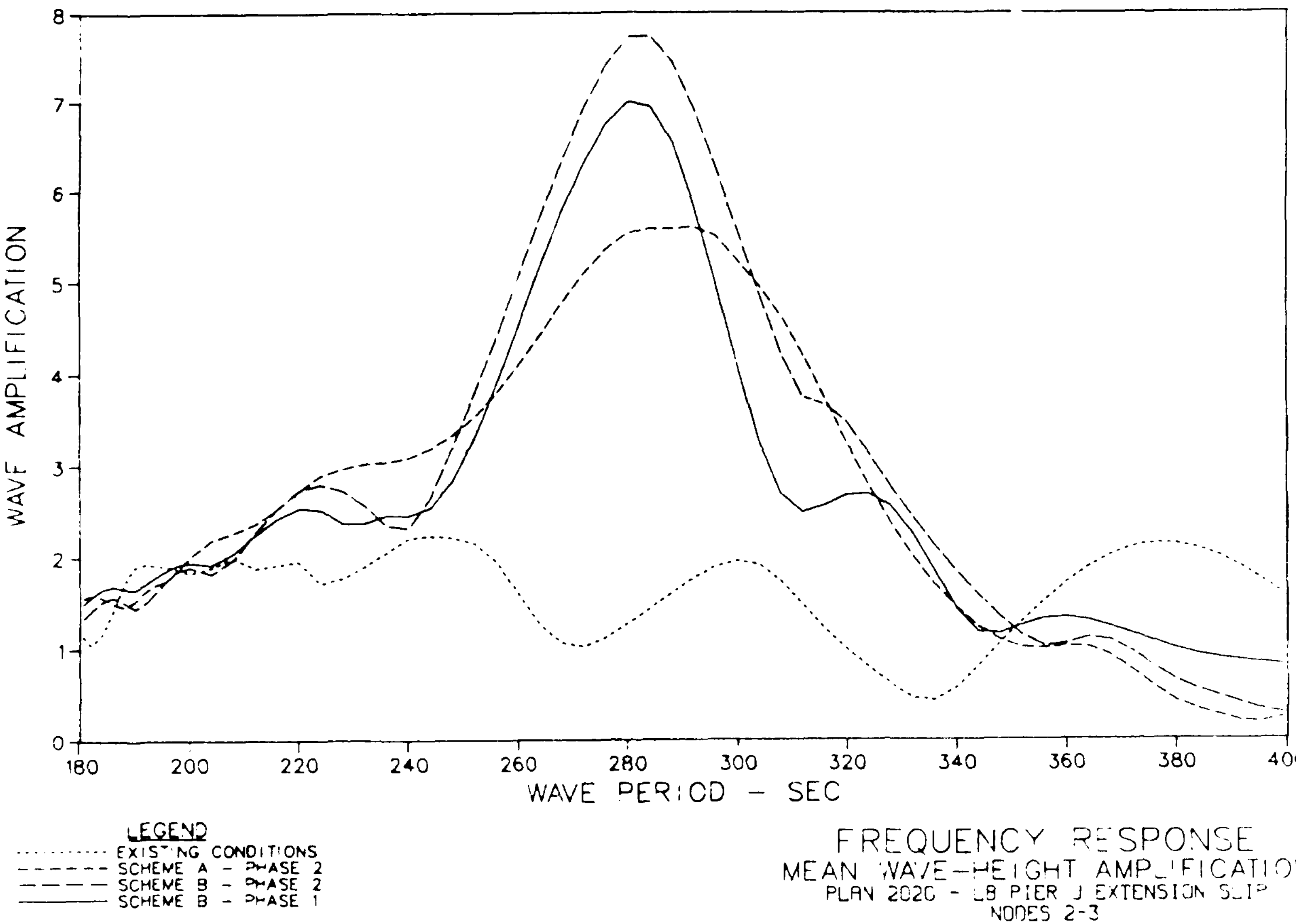

FREQUENCY RESPONSE
MEAN WAVE-HEIGHT AMPLIFICATION
PLAN 2020 - LB PIER J EXTENSION SLIP
NODES 2-3

PLATE 10

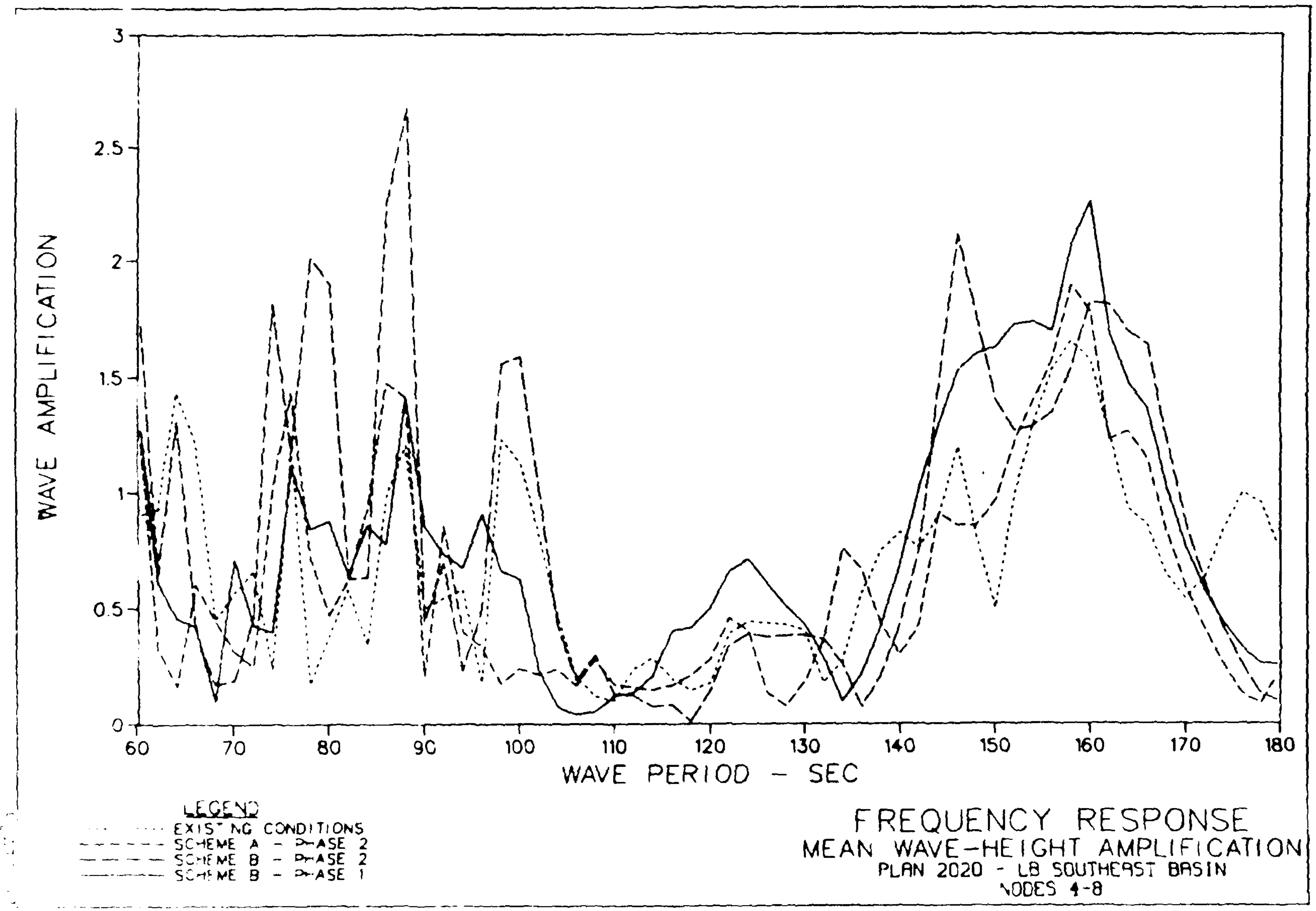
WAVE AMPLIFICATION
WAVE PERIOD - SEC
LEGEND
EXISTING CONDITIONS
SCHEME A - PHASE 2
SCHEME B - PHASE 2
SCHEME B - PHASE 1
FREQUENCY RESPONSE
MEAN WAVE-HEIGHT AMPLIFICATION
PLAN 2020 - LB SOUTHEAST BASIN
NODES 4-8

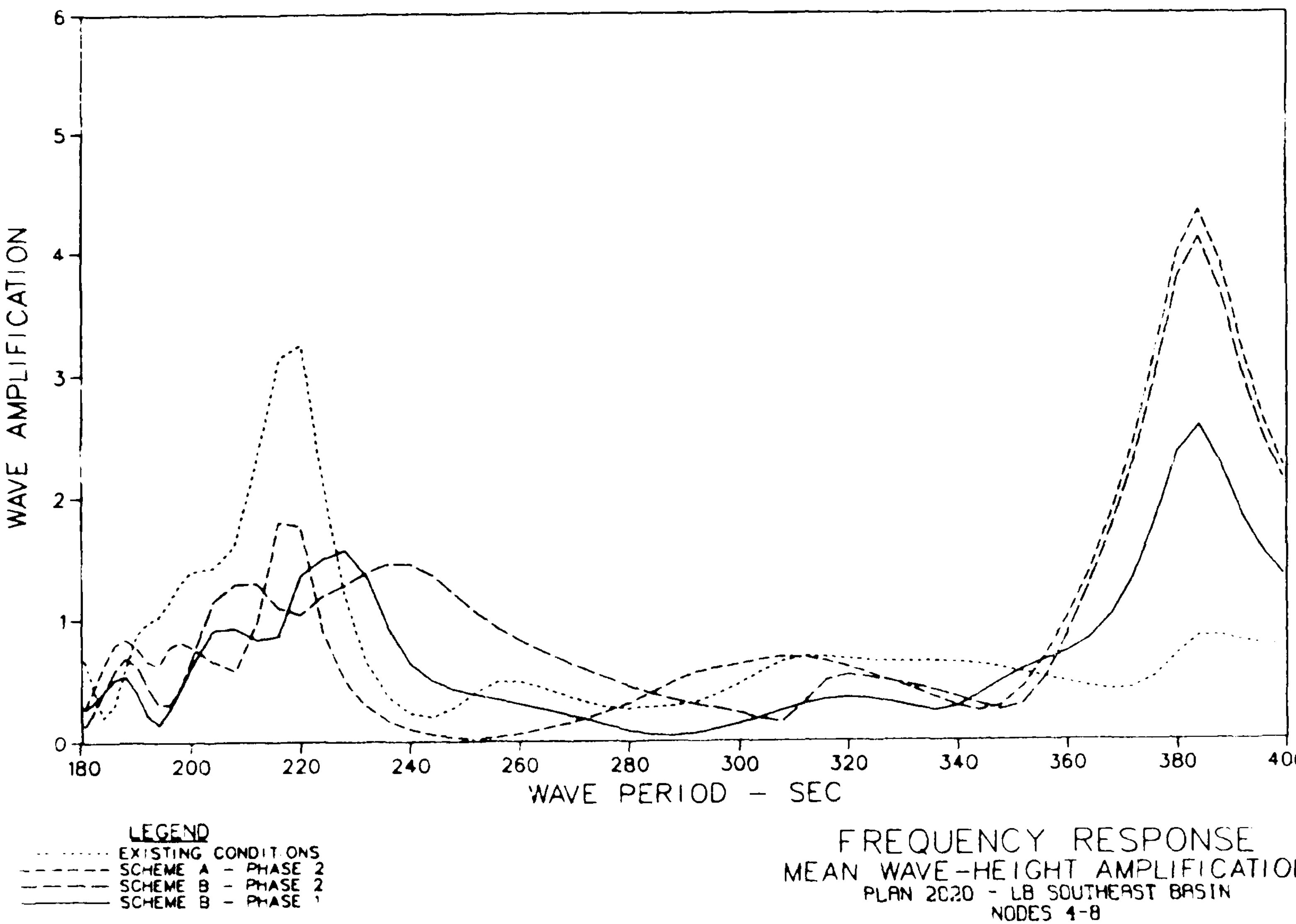

FREQUENCY RESPONSE
MEAN WAVE-HEIGHT AMPLIFICATION
PLAN 2020 - LB SOUTHEAST BASIN
NODES 4-8

PLATE 12

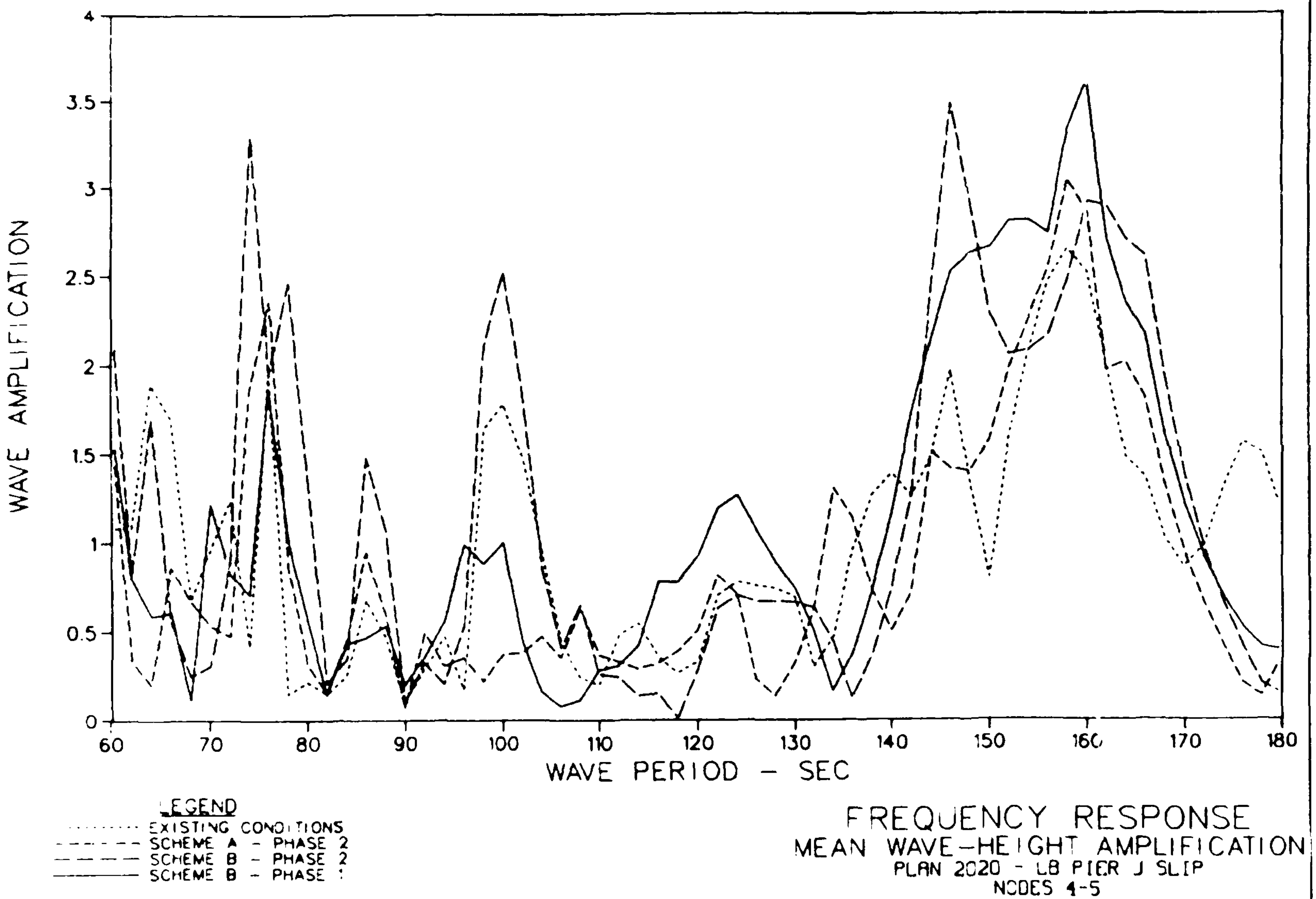

FREQUENCY RESPONSE
MEAN WAVE-HEIGHT AMPLIFICATION
PLAN 2020 - LB PIER J SLIP
NODES 4-5

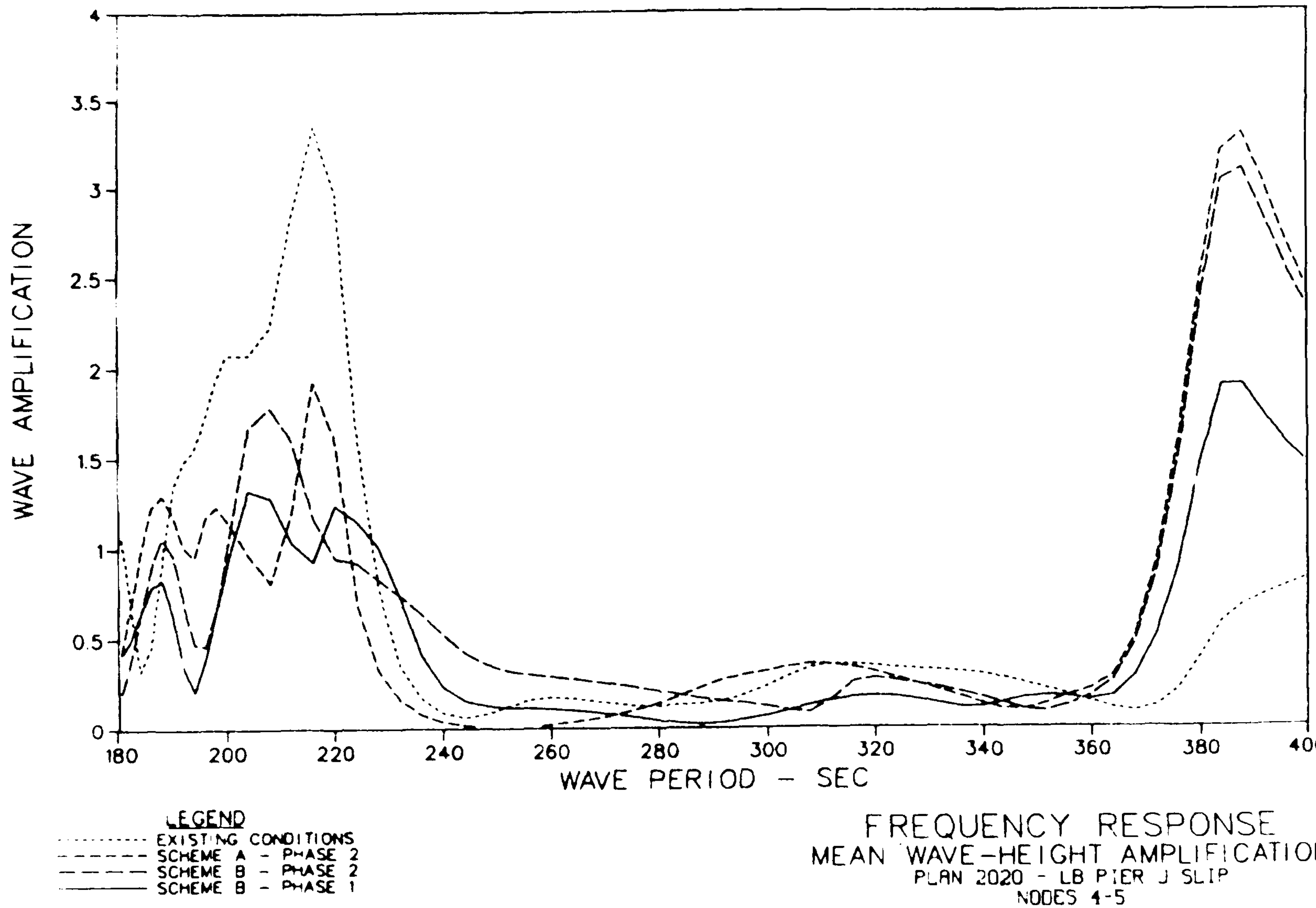

FREQUENCY RESPONSE
MEAN WAVE-HEIGHT AMPLIFICATION
PLAN 2020 - LB PIER J SLIP
NODES 4-5

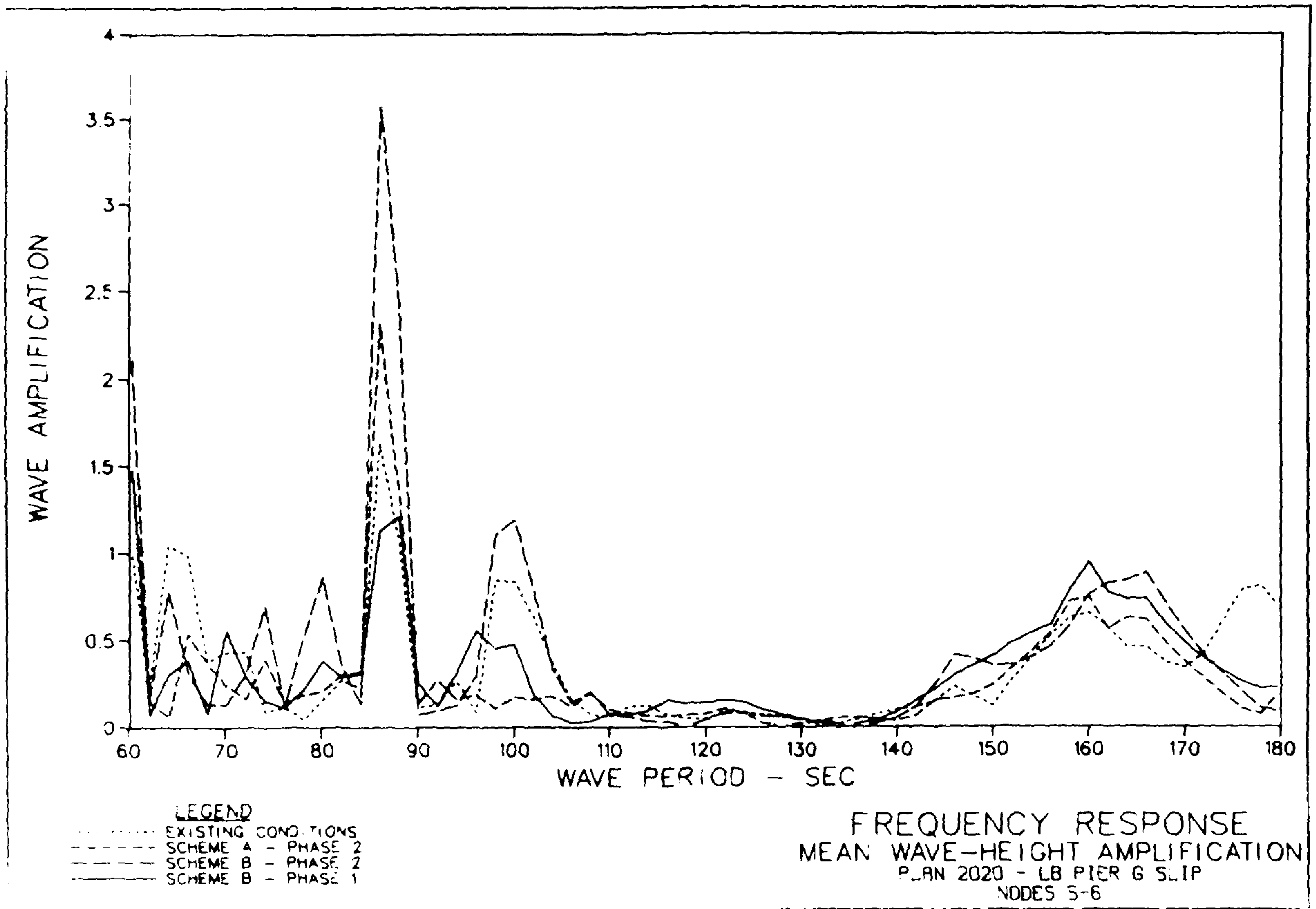
WAVE AMPLIFICATION
4
3.5
3
2.5
2
1.5
1
0.5
0
60
70
80
90
100
110
120
130
140
150
160
170
180
WAVE PERIOD - SEC
LEGEND
EXISTING CONDITIONS
SCHEME A - PHASE 2
SCHEME B - PHASE 2
SCHEME B - PHASE 1
FREQUENCY RESPONSE
MEAN WAVE-HEIGHT AMPLIFICATION
PLAN 2020 - LB PIER G SLIP
NODES 5-6

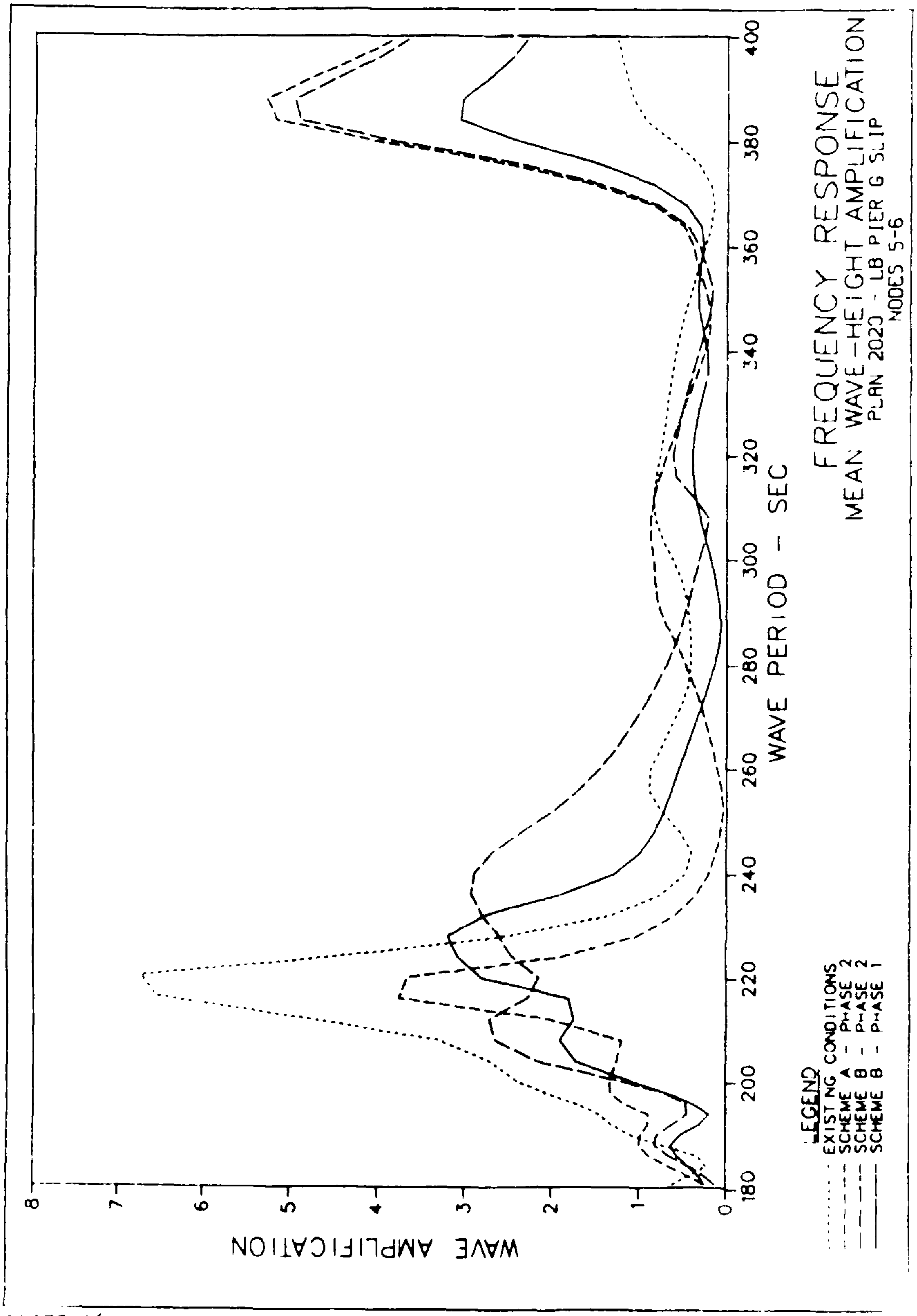
FREQUENCY RESPONSE
MEAN WAVE-HEIGHT AMPLIFICATION
PLAN 2020 - LB PIER G SLIP
NODES 5-6
WAVE PERIOD - SEC
WAVE AMPLIFICATION
180
200
220
240
260
280
300
320
340
360
380
400
0
1
2
3
4
5
6
7
8
LEGEND
EXISTING CONDITIONS
SCHEME A - PHASE 2
SCHEME B - PHASE 2
SCHEME B - PHASE 1

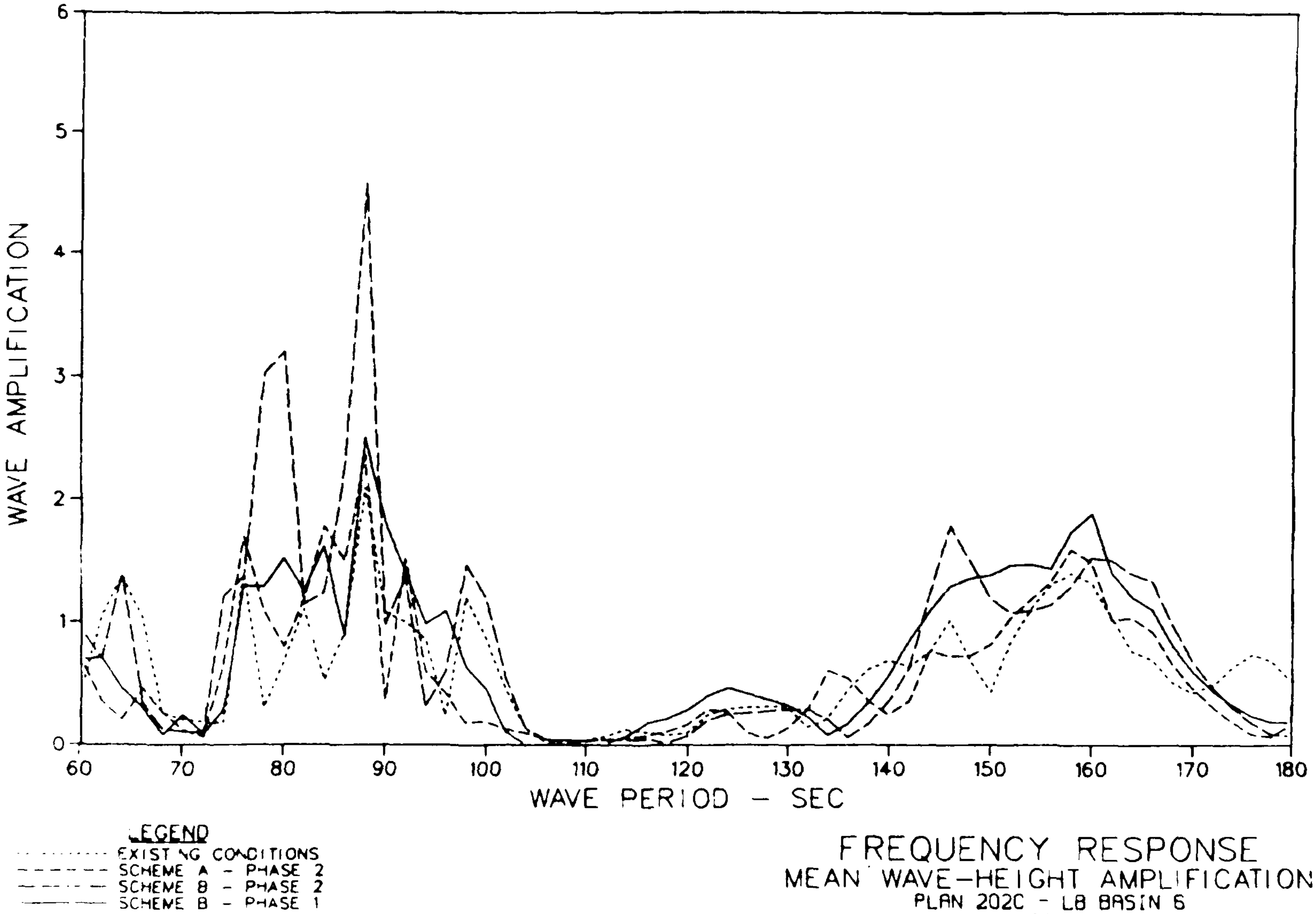

FREQUENCY RESPONSE
MEAN WAVE-HEIGHT AMPLIFICATION
PLAN 202C - LB BASIN 6
NODES 7-8

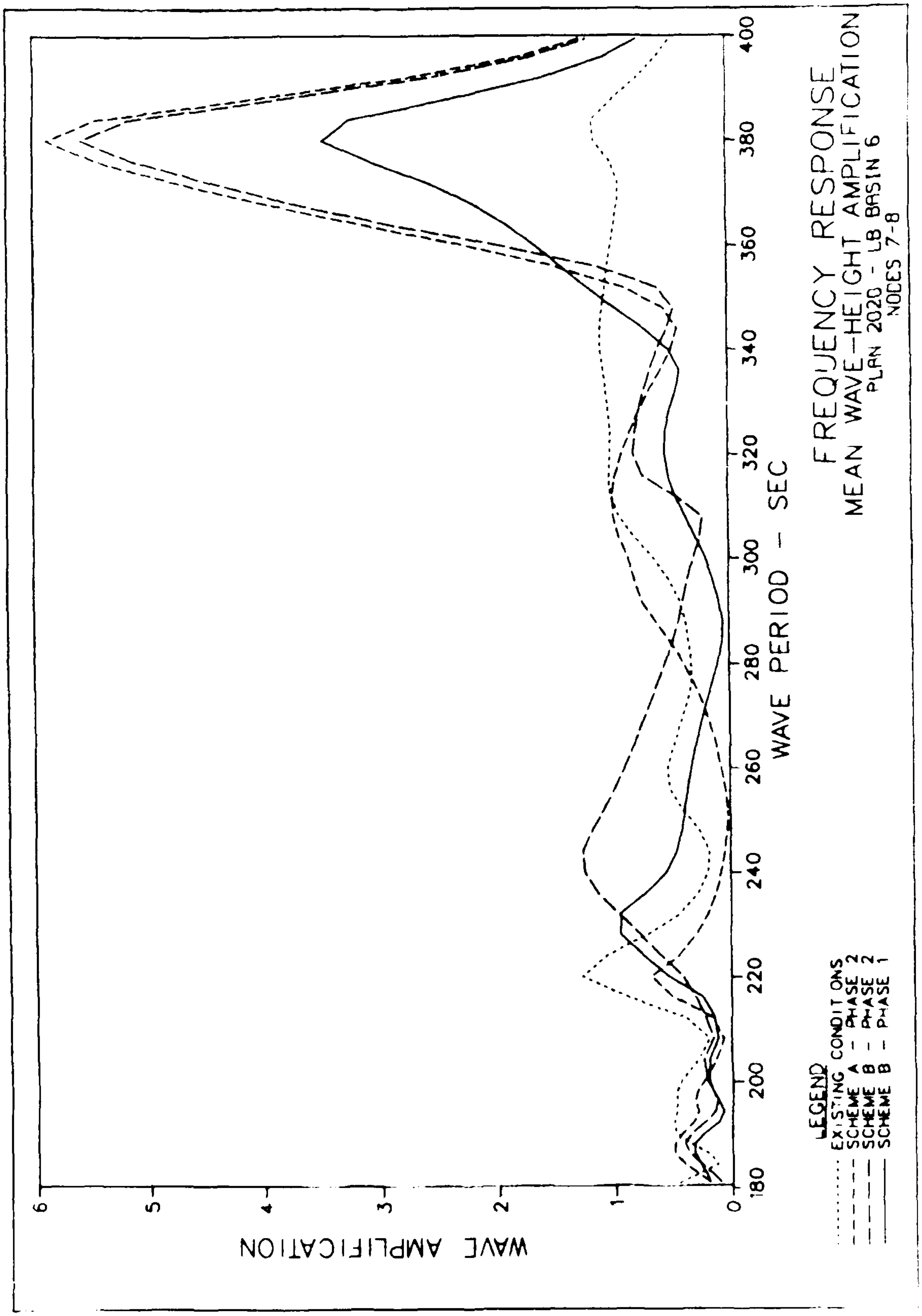

FREQUENCY RESPONSE
MEAN WAVE-HEIGHT AMPLIFICATION
PLAN 2020 - LB BASIN 6
NODES 7-8
WAVE AMPLIFICATION
WAVE PERIOD - SEC
0
1
2
3
4
5
6
180
200
220
240
260
280
300
320
340
360
380
400
LEGEND
EXISTING CONDITIONS
SCHEME A - PHASE 2
SCHEME B - PHASE 2
SCHEME B - PHASE 1

PLATE 18

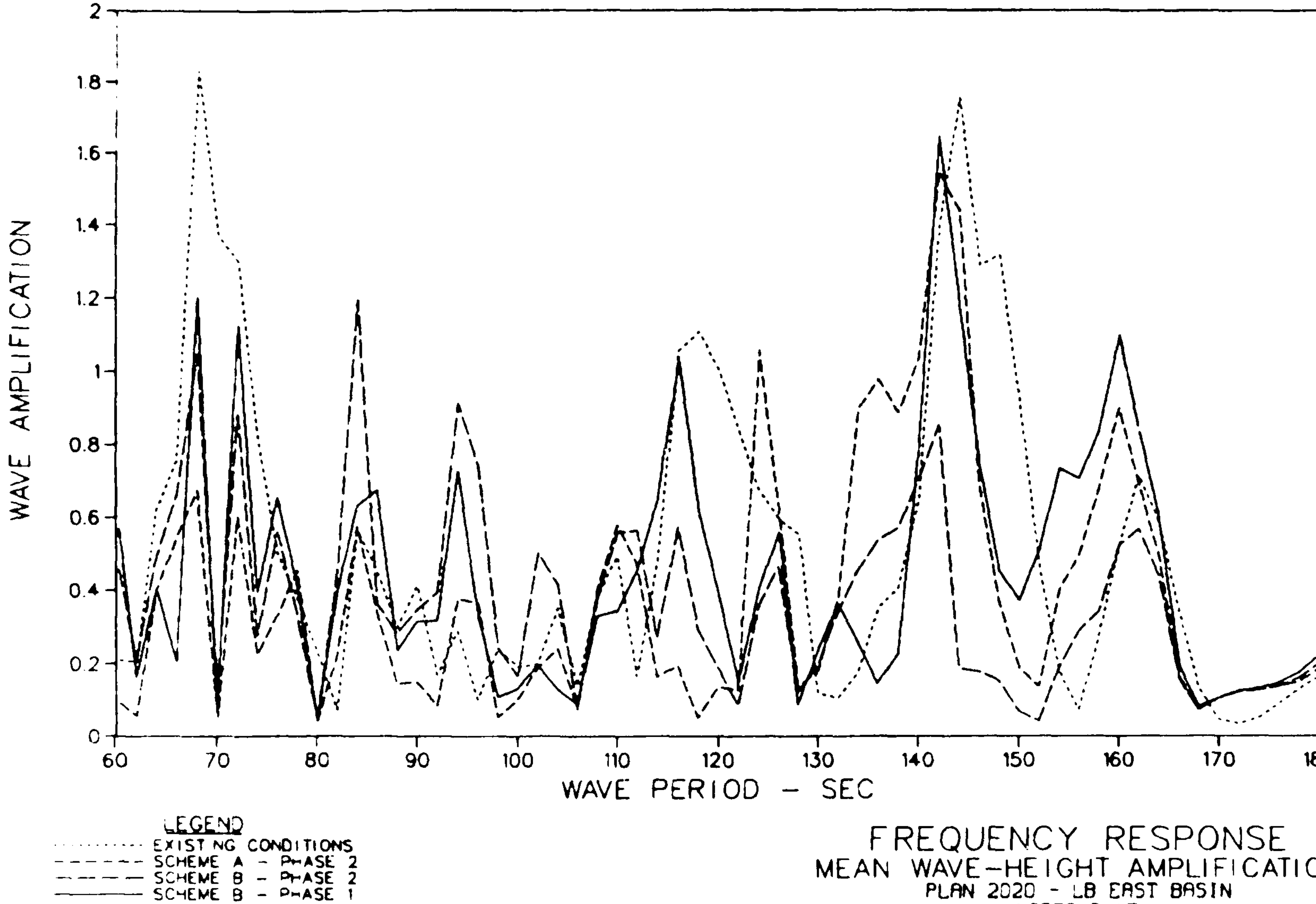

FREQUENCY RESPONSE
MEAN WAVE-HEIGHT AMPLIFICATION
PLAN 2020 - LB EAST BASIN
NODES 9-13

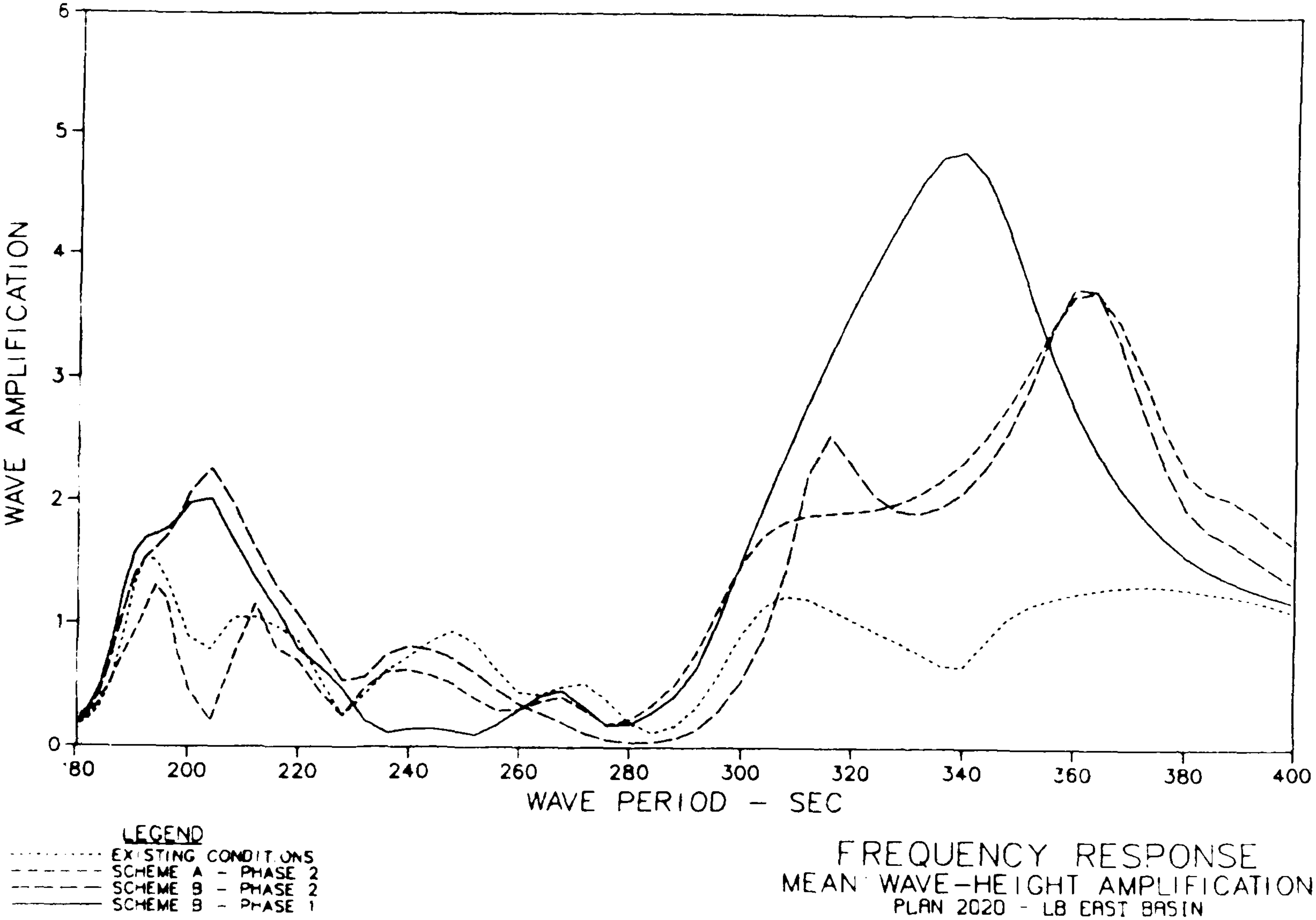

FREQUENCY RESPONSE
MEAN WAVE-HEIGHT AMPLIFICATION
PLAN 2020 - LB EAST BASIN
NODES 9-13

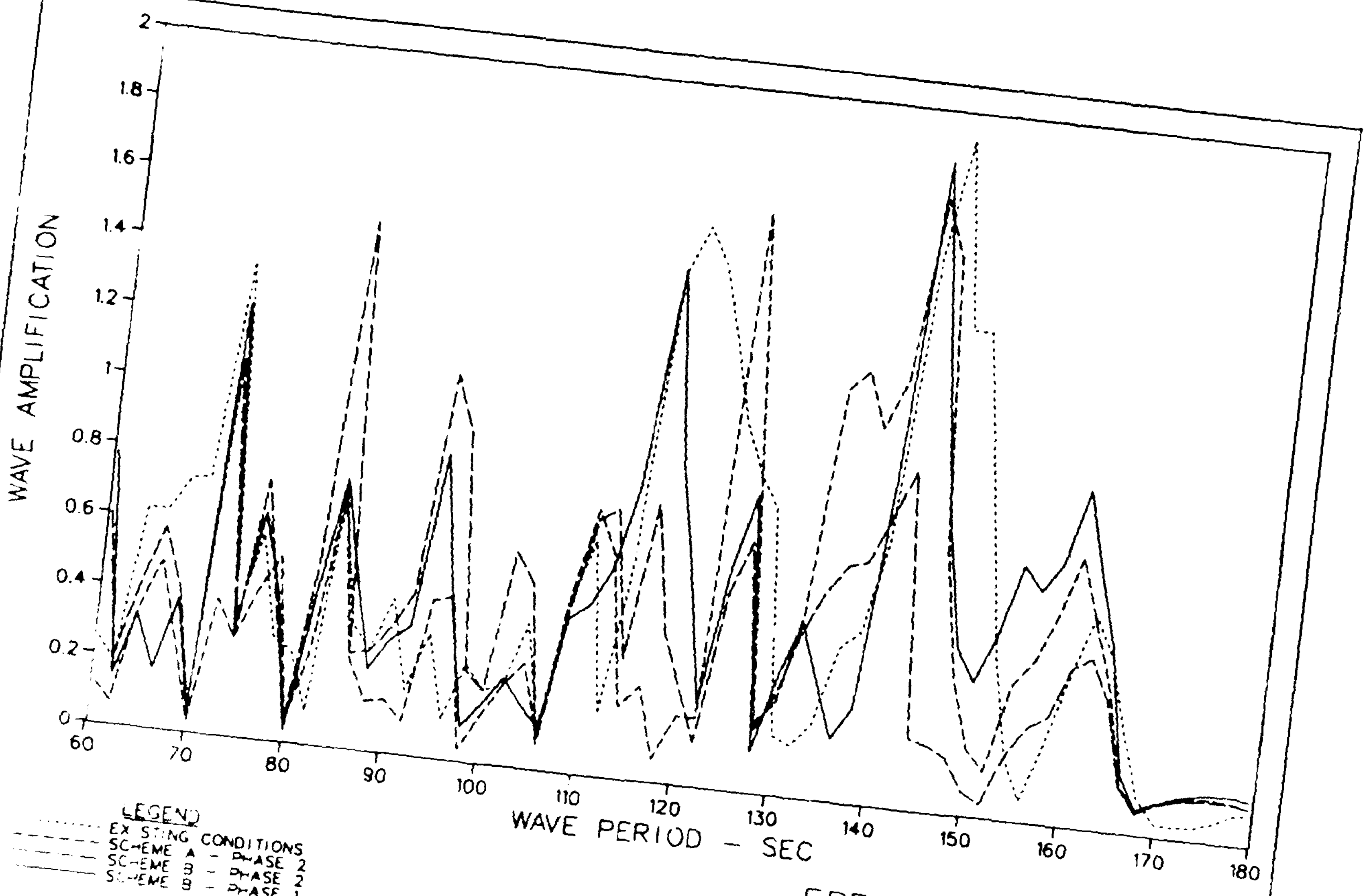

FREQUENCY RESPONSE
MEAN WAVE-HEIGHT AMPLIFICATION
PLAN 2020 - LB PIER B SLIP
NODES 10-11

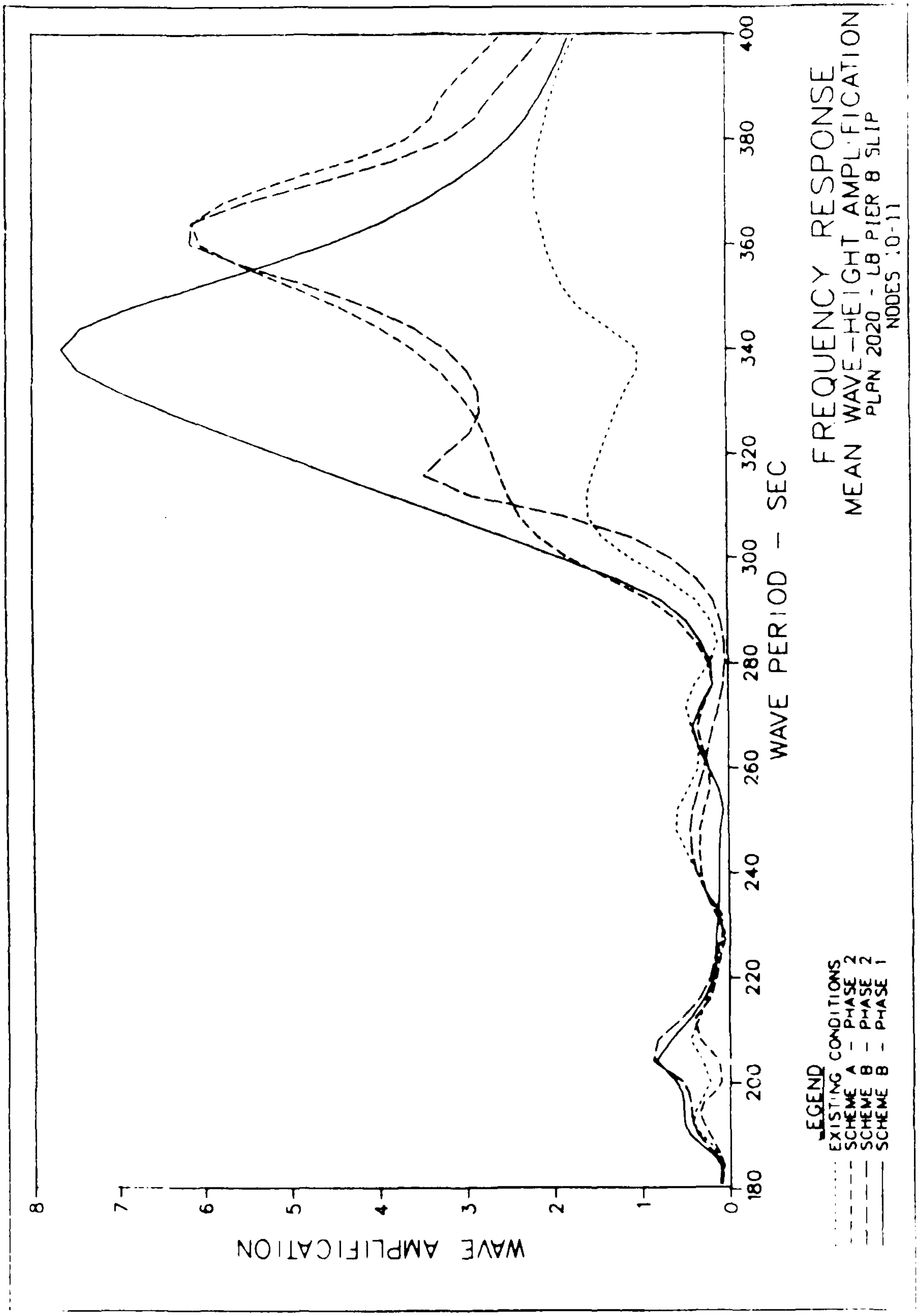
FREQUENCY RESPONSE
MEAN WAVE-HEIGHT AMPLIFICATION
PLAN 2020 - LB PIER B SLIP
NODES 10-11
WAVE PERIOD - SEC
WAVE AMPLIFICATION
180
200
220
240
260
280
300
320
340
360
380
400
0
1
2
3
4
5
6
7
8
LEGEND
EXISTING CONDITIONS
SCHEME A - PHASE 2
SCHEME B - PHASE 2
SCHEME B - PHASE 1

PLATE 22

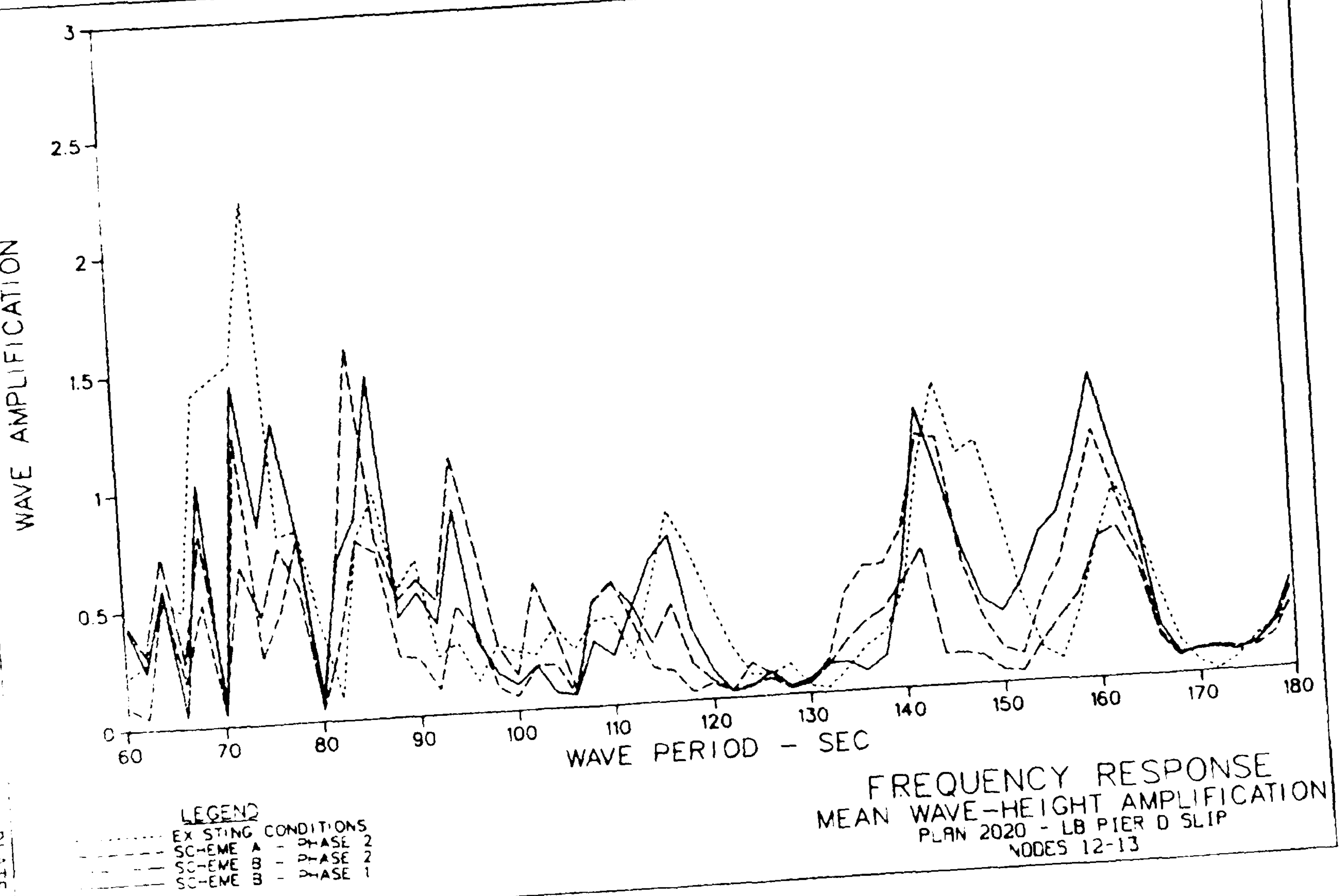

FREQUENCY RESPONSE
MEAN WAVE-HEIGHT AMPLIFICATION
PLAN 2020 - LB PIER D SLIP
NODES 12-13

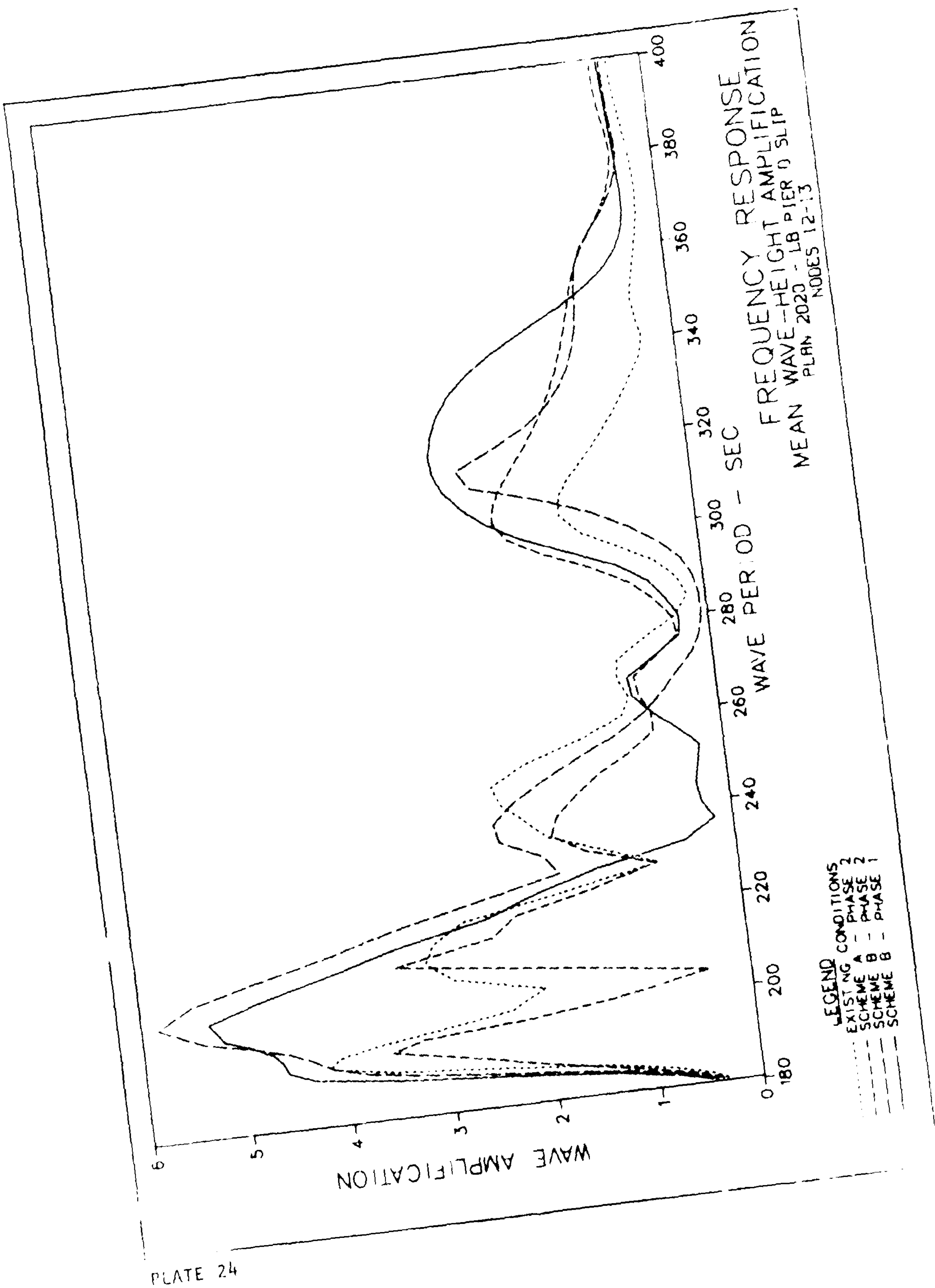
FREQUENCY RESPONSE
MEAN WAVE-HEIGHT AMPLIFICATION
PLAN 2020 - LB PIER D SLIP
NODES 12-13
WAVE PERIOD - SEC
WAVE AMPLIFICATION
LEGEND
EXISTING CONDITIONS
SCHEME A - PHASE 2
SCHEME B - PHASE 2
SCHEME B - PHASE 1

PLATE 24

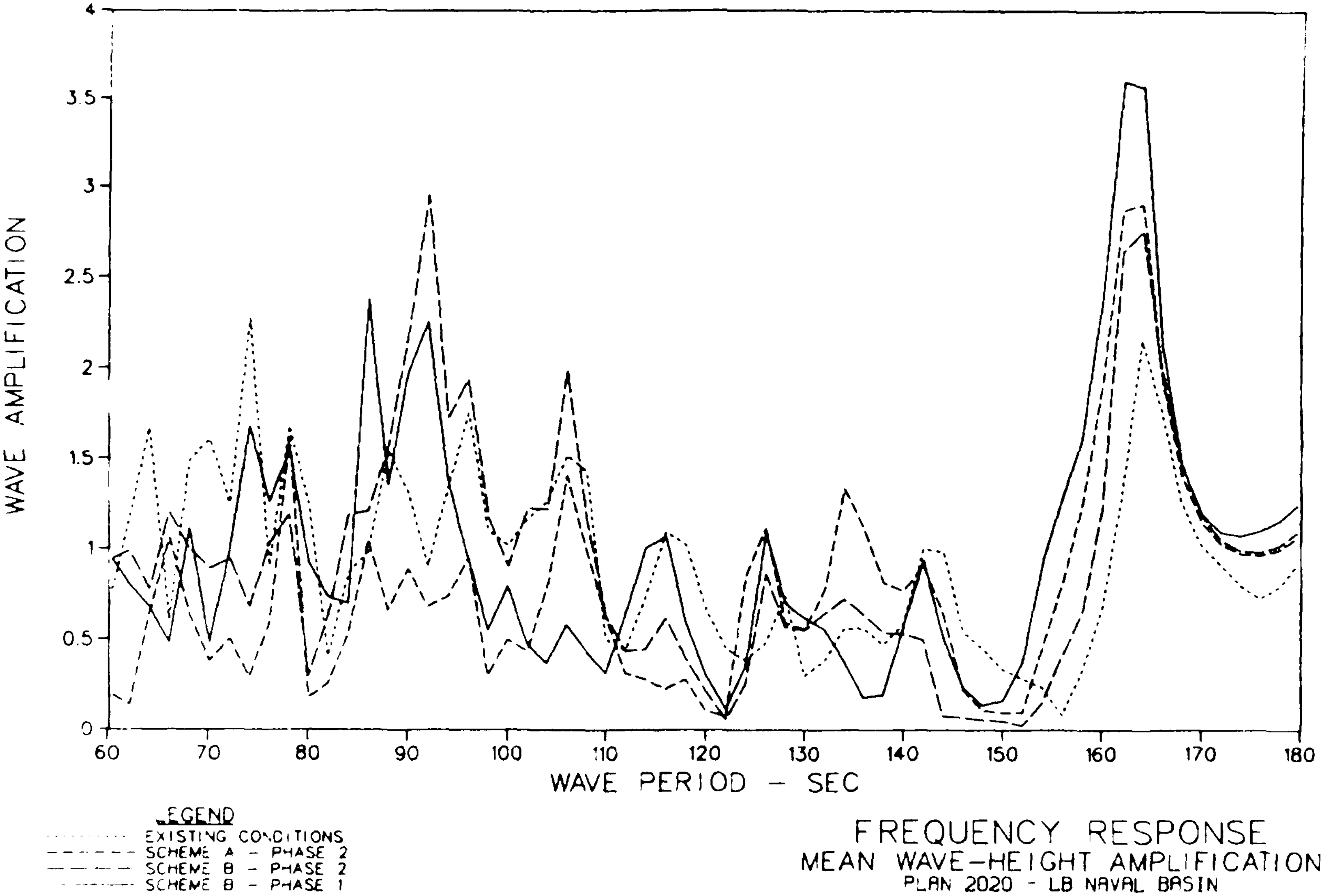

FREQUENCY RESPONSE
MEAN WAVE-HEIGHT AMPLIFICATION
PLAN 2020 - LB NAVAL BASIN
NODES 30-33

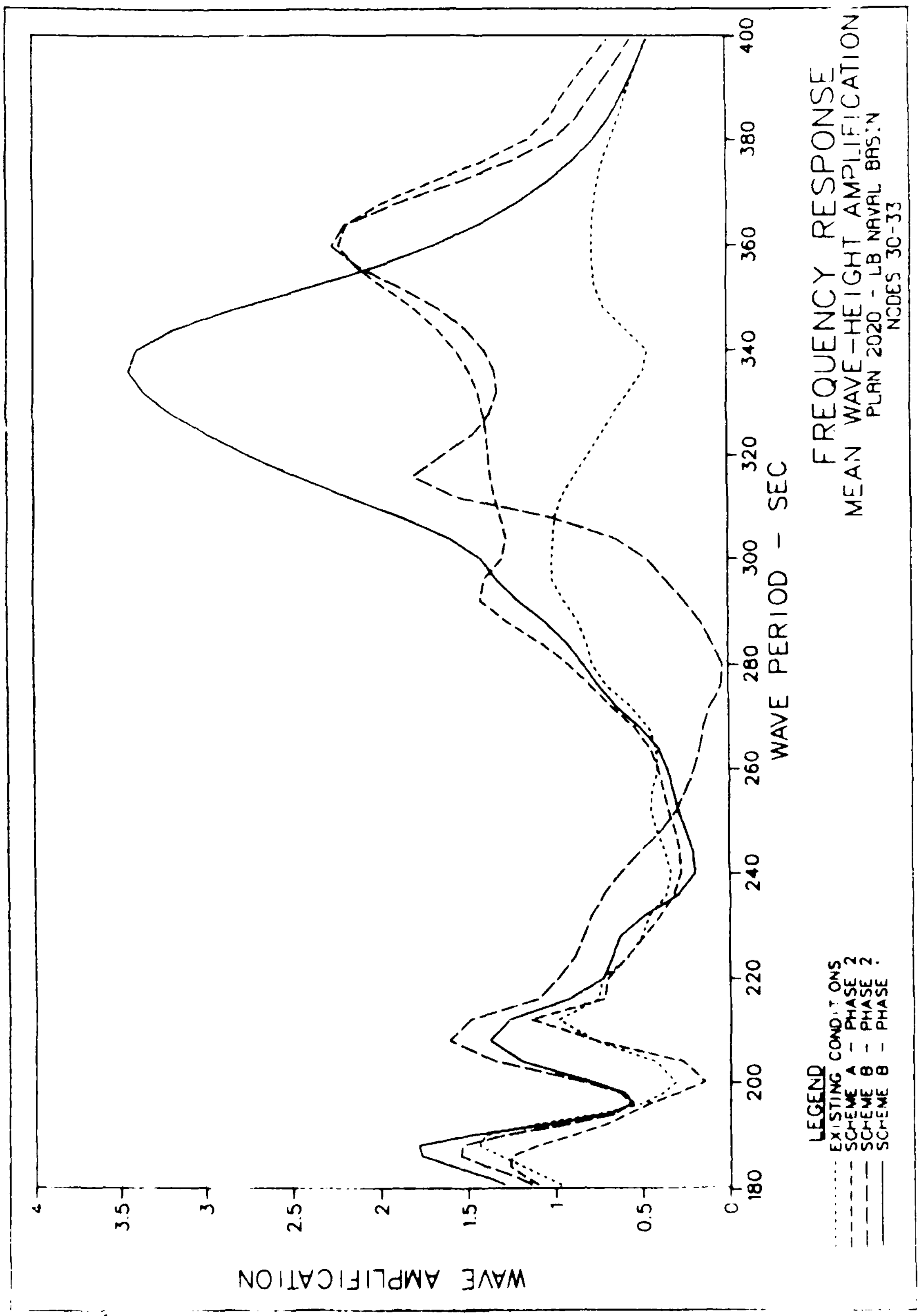
FREQUENCY RESPONSE
MEAN WAVE-HEIGHT AMPLIFICATION
PLAN 2020 - LB NAVAL BASIN
NODES 30-33
WAVE PERIOD - SEC
WAVE AMPLIFICATION
0
0.5
1
1.5
2
2.5
3
3.5
4
180
200
220
240
260
280
300
320
340
360
380
400
LEGEND
EXISTING CONDITIONS
SCHEME A - PHASE 2
SCHEME B - PHASE 2
SCHEME B - PHASE

PLATE 26

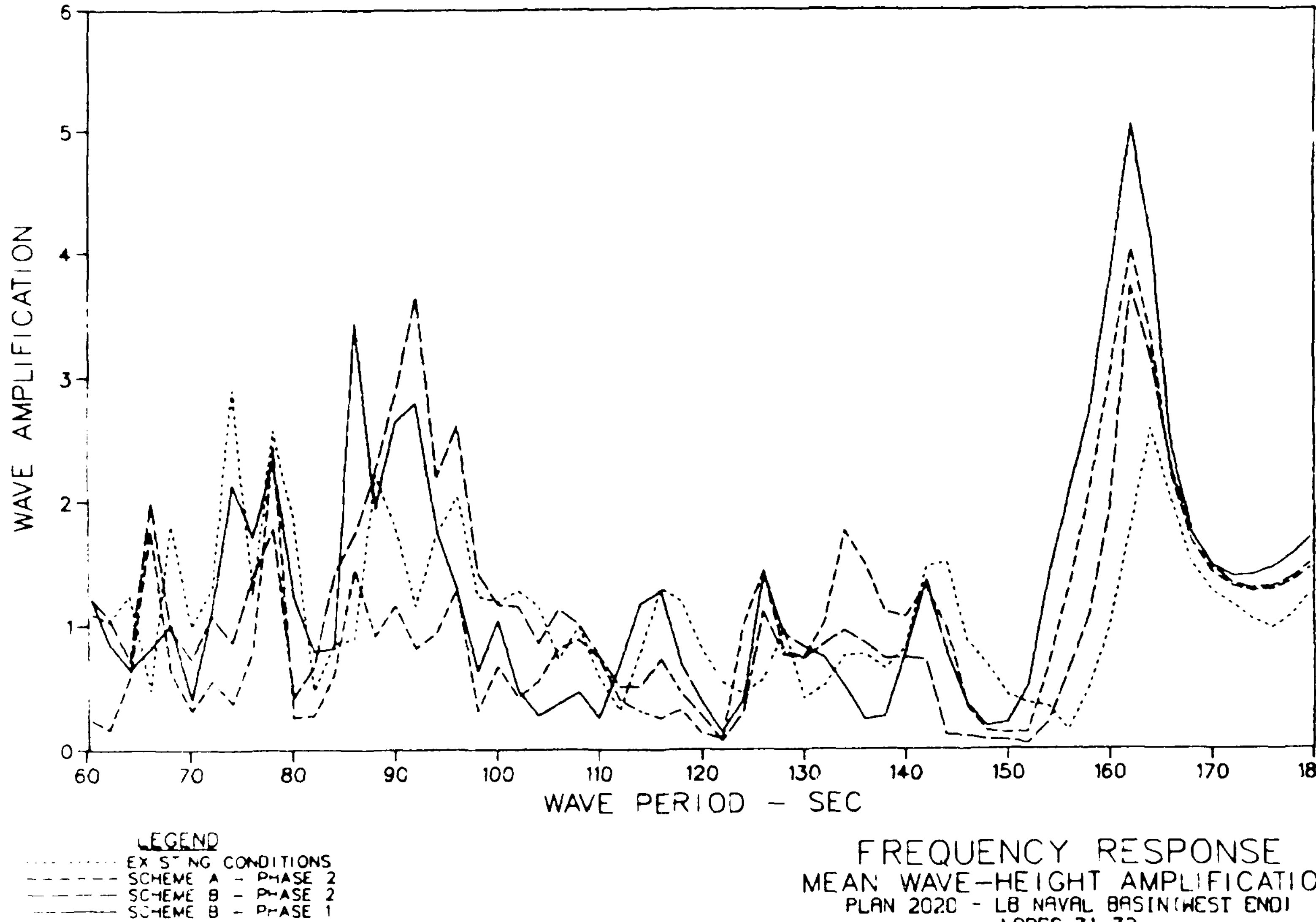

FREQUENCY RESPONSE
MEAN WAVE-HEIGHT AMPLIFICATION
PLAN 2020 - LB NAVAL BASIN(WEST END)
NODES 31-32

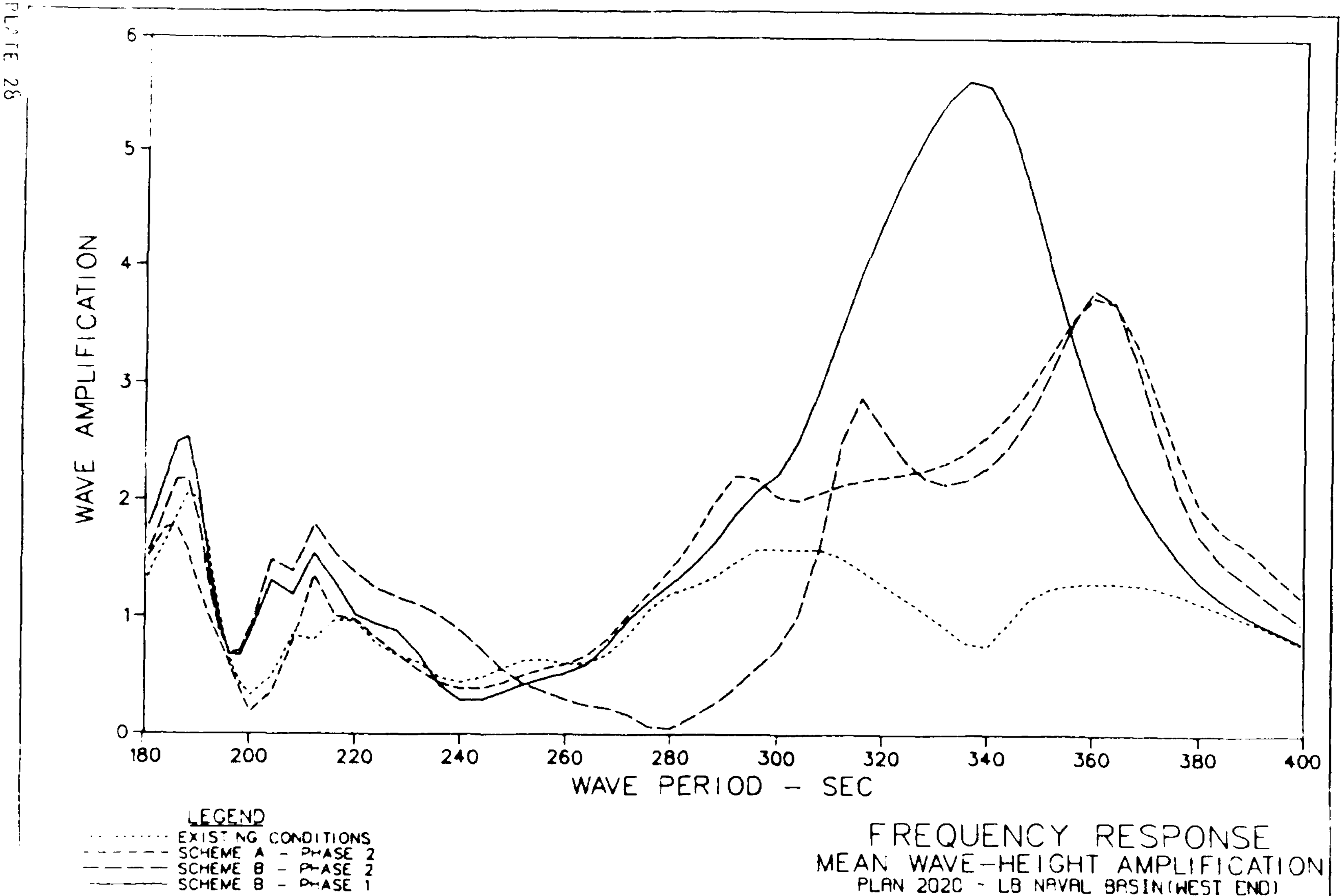

FREQUENCY RESPONSE
MEAN WAVE-HEIGHT AMPLIFICATION
PLAN 2020 - LB NAVAL BASIN (WEST END)
NODES 31-32

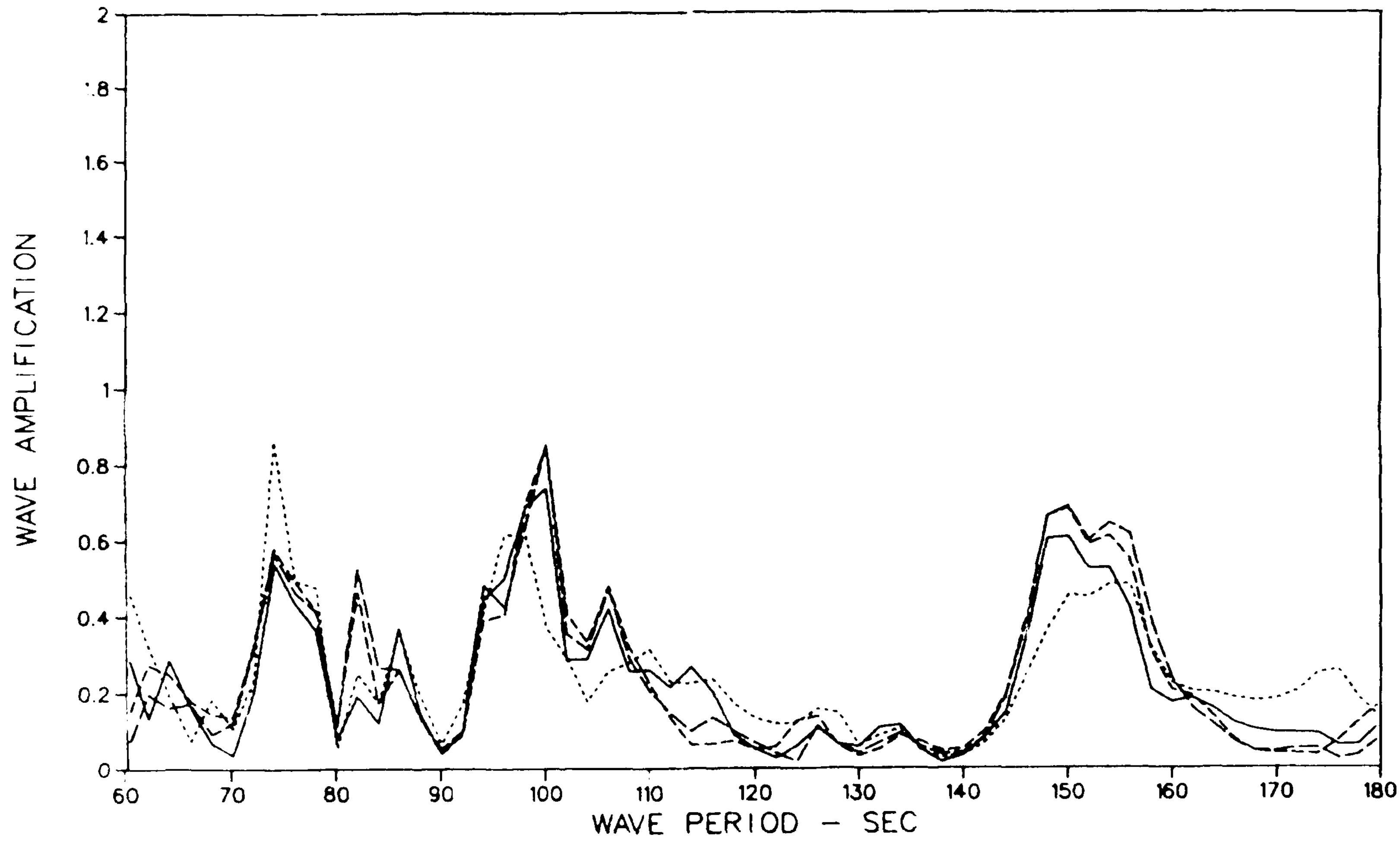

LEGEND
EXISTING CONDITIONS
SCHEME A - PHASE 2
SCHEME B - PHASE 2
SCHEME B - PHASE 1

FREQUENCY RESPONSE
MEAN WAVE-HEIGHT AMPLIFICATION
PLAN 2020 - LA SLIP 5
NODES 14-15

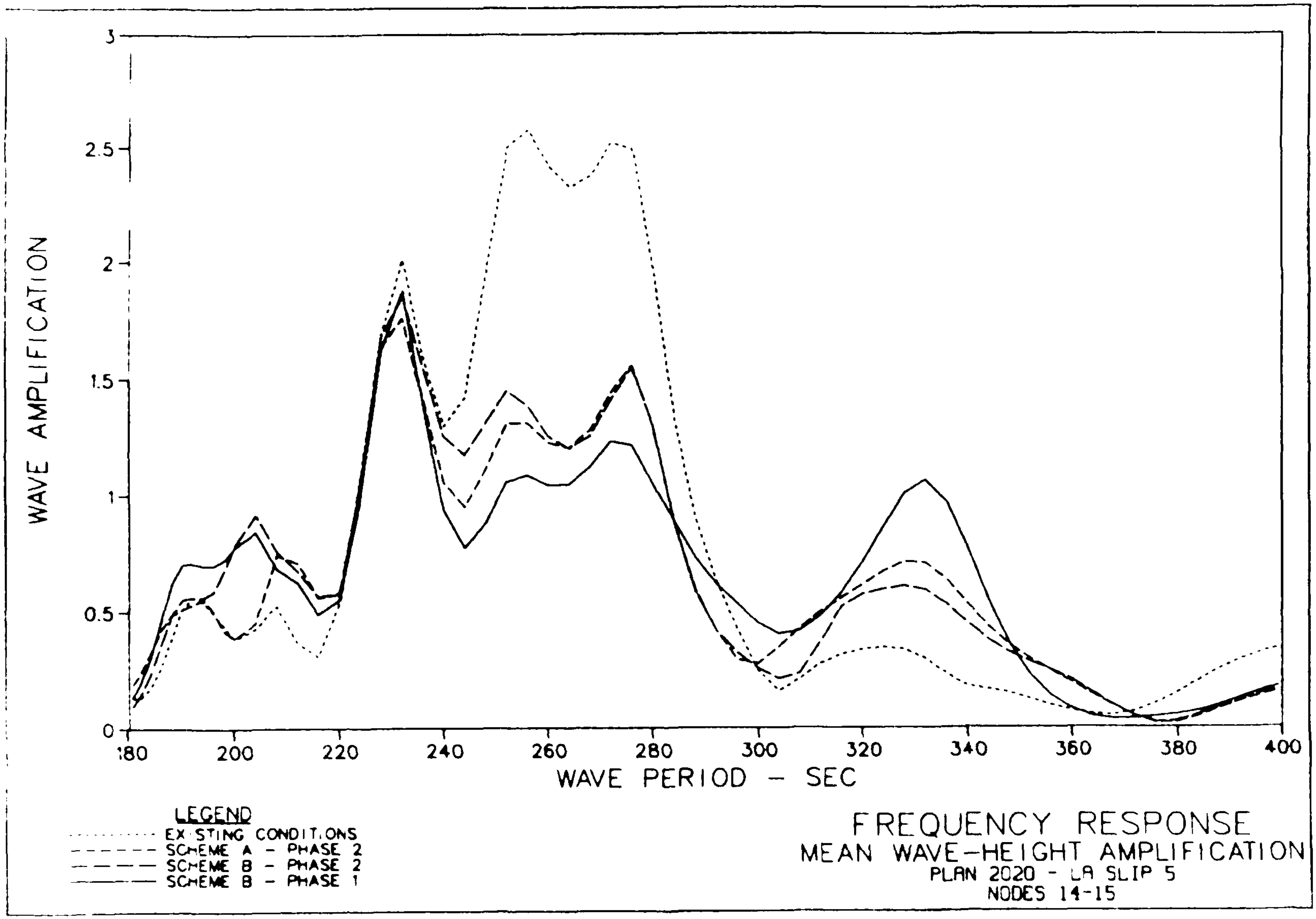
WAVE AMPLIFICATION
0
0.5
1
1.5
2
2.5
3
180
200
220
240
260
280
300
320
340
360
380
400
WAVE PERIOD - SEC
LEGEND
EXISTING CONDITIONS
SCHEME A - PHASE 2
SCHEME B - PHASE 2
SCHEME B - PHASE 1
FREQUENCY RESPONSE
MEAN WAVE-HEIGHT AMPLIFICATION
PLAN 2020 - LA SLIP 5
NODES 14-15

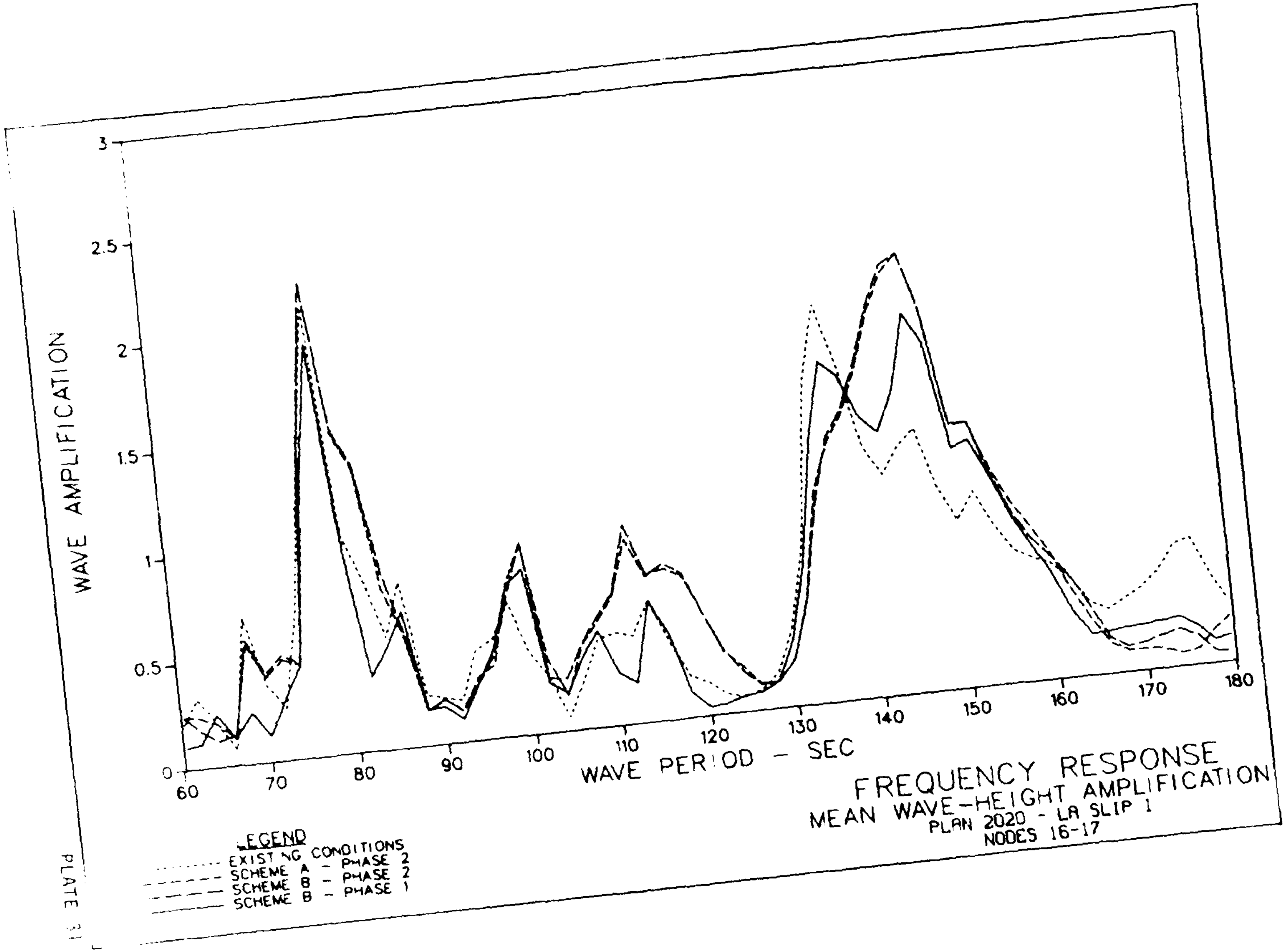

FREQUENCY RESPONSE
MEAN WAVE-HEIGHT AMPLIFICATION
PLAN 2020 - LA SLIP 1
NODES 16-17

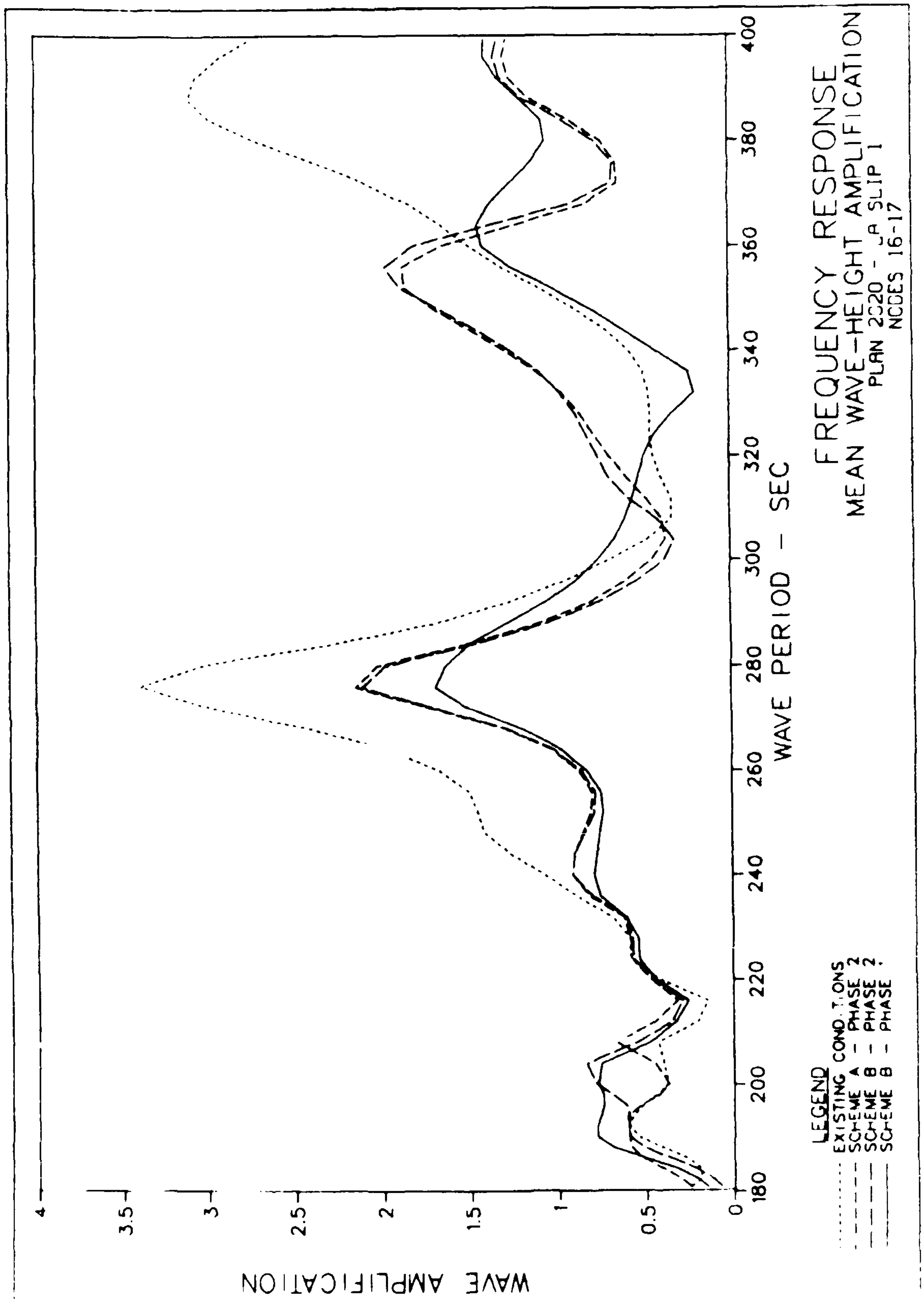
FREQUENCY RESPONSE
MEAN WAVE-HEIGHT AMPLIFICATION
WAVE PERIOD - SEC
WAVE AMPLIFICATION
LEGEND
EXISTING CONDITIONS
SCHEME A - PHASE 2
SCHEME B - PHASE 2
SCHEME B - PHASE
180
200
220
240
260
280
300
320
340
360
380
400
0
0.5
1
1.5
2
2.5
3
3.5
4

PLATE 32

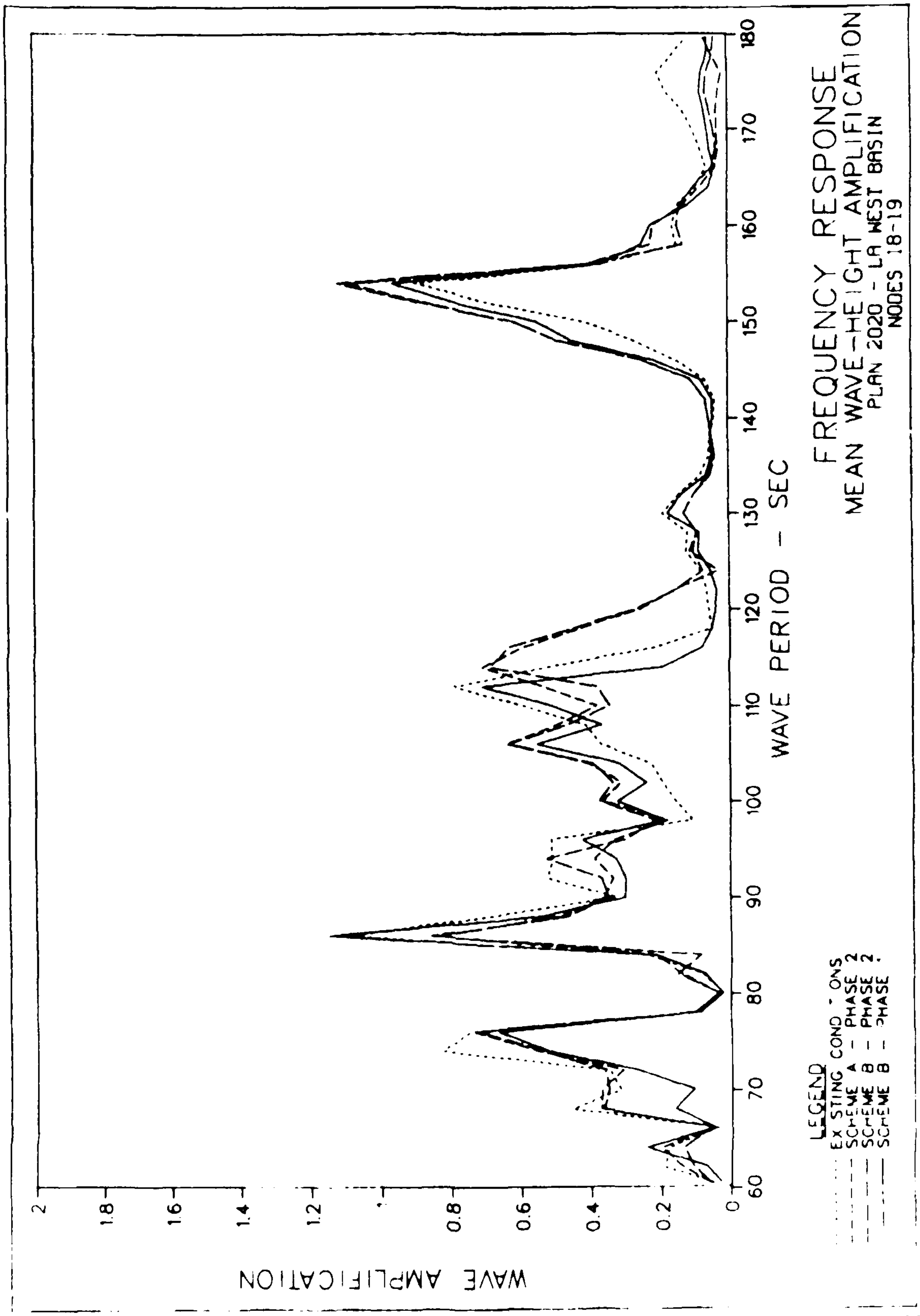

FREQUENCY RESPONSE
MEAN WAVE-HEIGHT AMPLIFICATION
PLAN 2020 - LA WEST BASIN
NODES 18-19
WAVE PERIOD - SEC
WAVE AMPLIFICATION
LEGEND
EXISTING CONDITIONS
SCHEME A - PHASE 2
SCHEME B - PHASE 2
60
70
80
90
100
110
120
130
140
150
160
170
180
0
0.2
0.4
0.6
0.8
1.2
1.4
1.6
1.8
2

PLATE 33

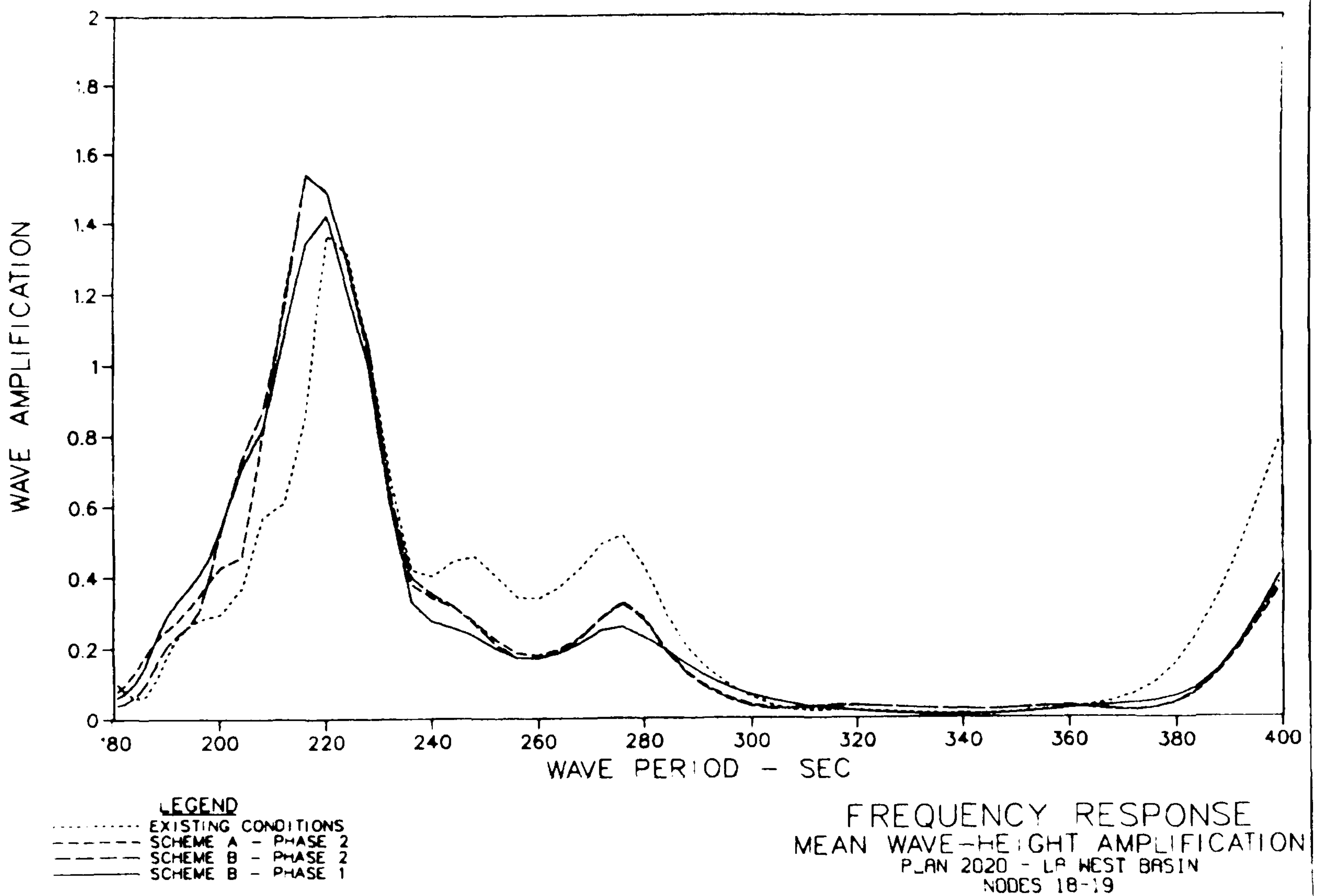

FREQUENCY RESPONSE
MEAN WAVE-HEIGHT AMPLIFICATION
PLAN 2020 - LA WEST BASIN
NODES 18-19

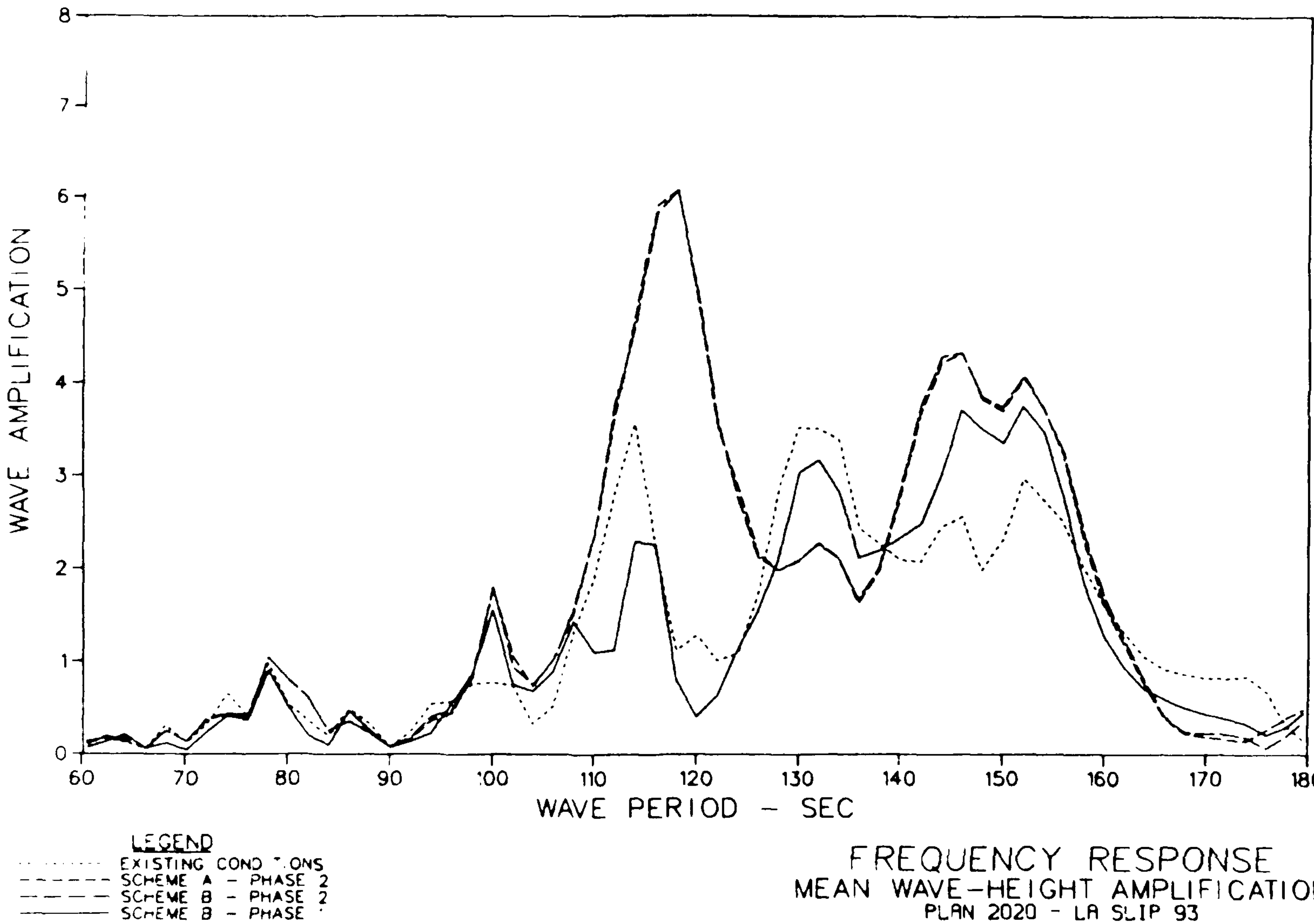

FREQUENCY RESPONSE
MEAN WAVE-HEIGHT AMPLIFICATION
PLAN 2020 - LA SLIP 93
NODES 20-21

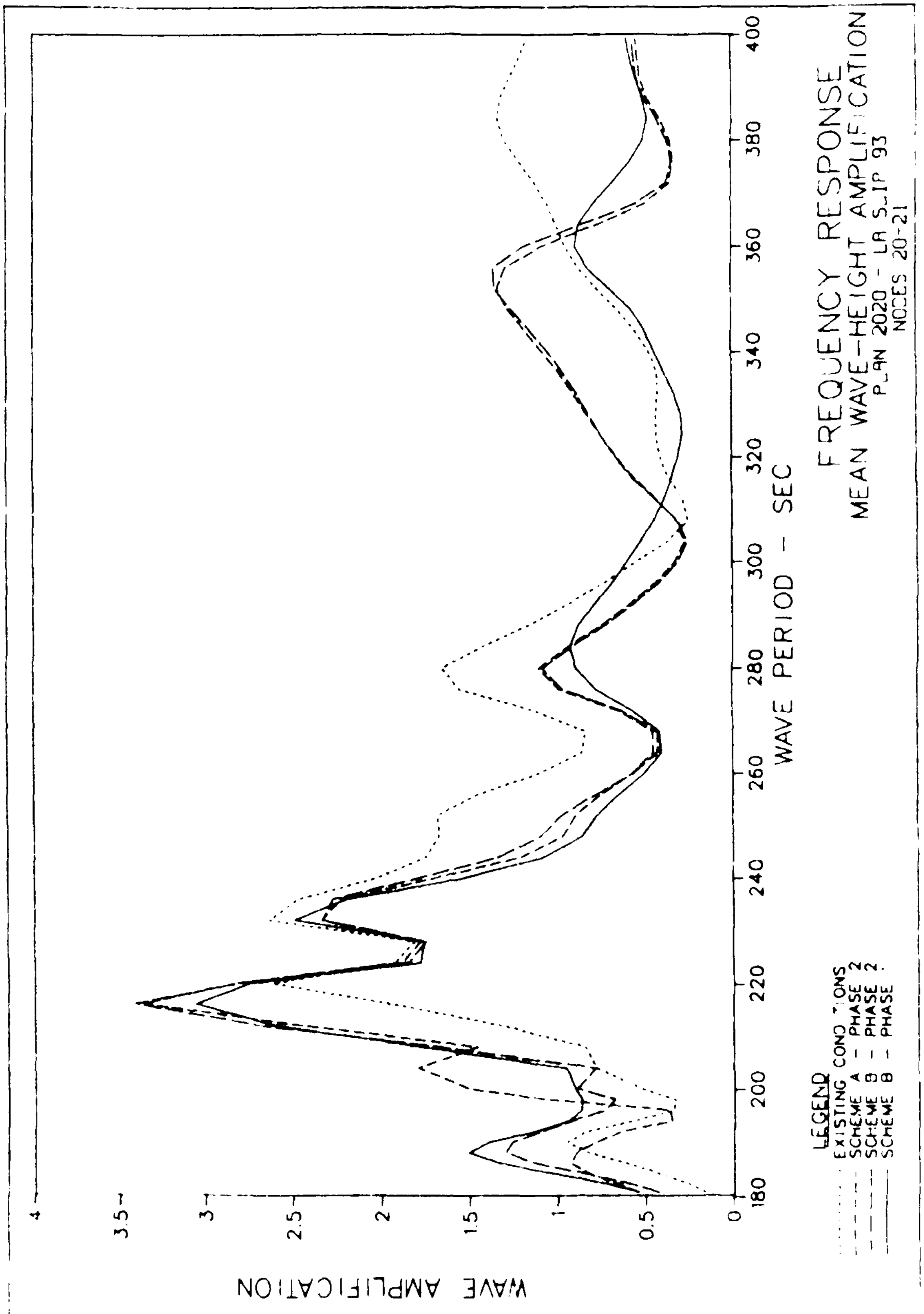
FREQUENCY RESPONSE
MEAN WAVE-HEIGHT AMPLIFICATION
PLAN 2020 - LR SLIP 93
NODES 20-21
WAVE PERIOD - SEC
WAVE AMPLIFICATION
LEGEND
EXISTING CONDITIONS
SCHEME A - PHASE 2
SCHEME B - PHASE 2
SCHEME B - PHASE
180
200
220
240
260
280
300
320
340
360
380
400
0
0.5
1
1.5
2
2.5
3
3.5
4

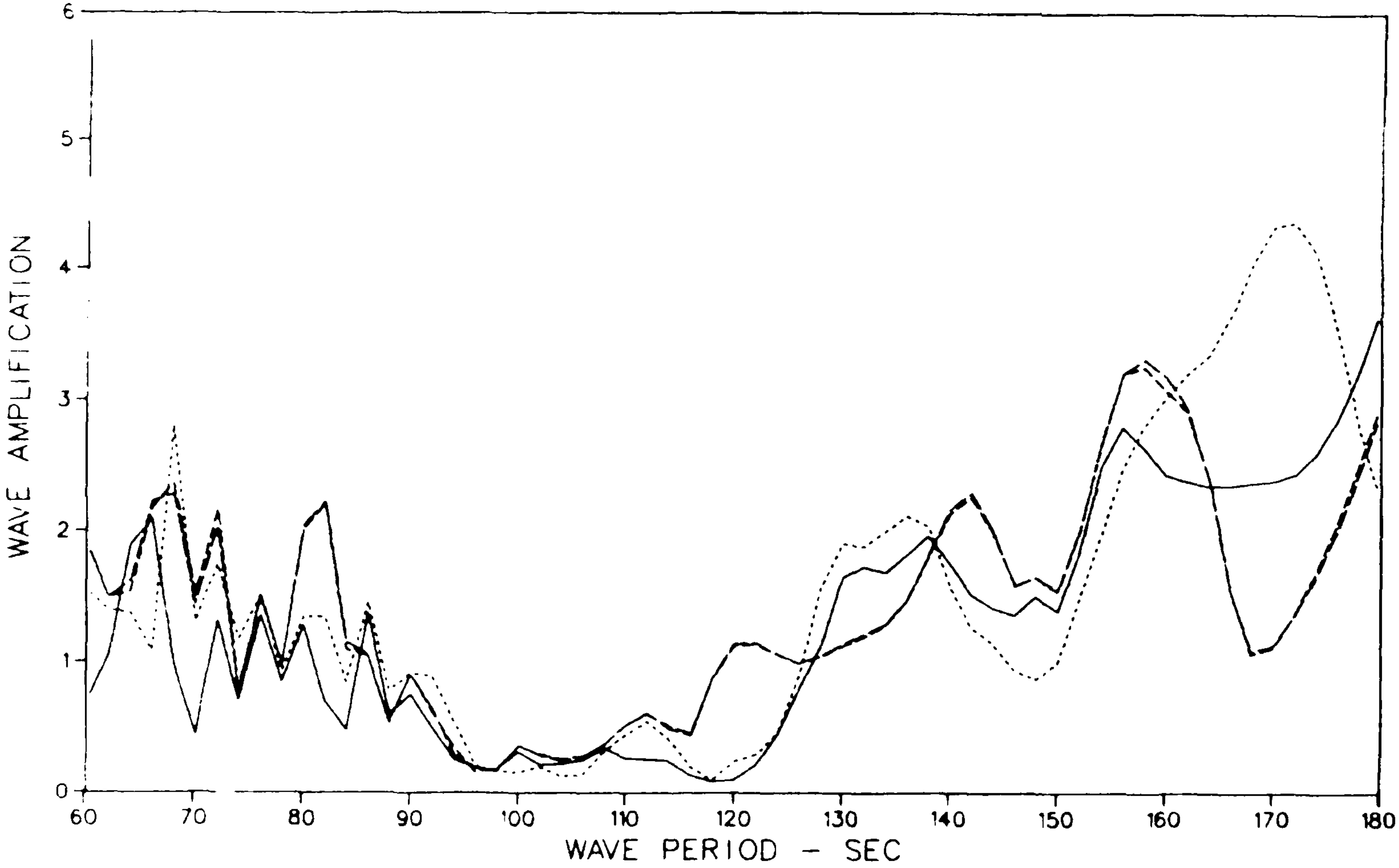

LEGEND
EXISTING COND TIONS
SCHEME A - PHASE 2
SCHEME B - PHASE 2
SCHEME B - PHASE 1

FREQUENCY RESPONSE
MEAN WAVE-HEIGHT AMPLIFICATION
PLAN 2020 - LA SP SLIP
NODES 22-23

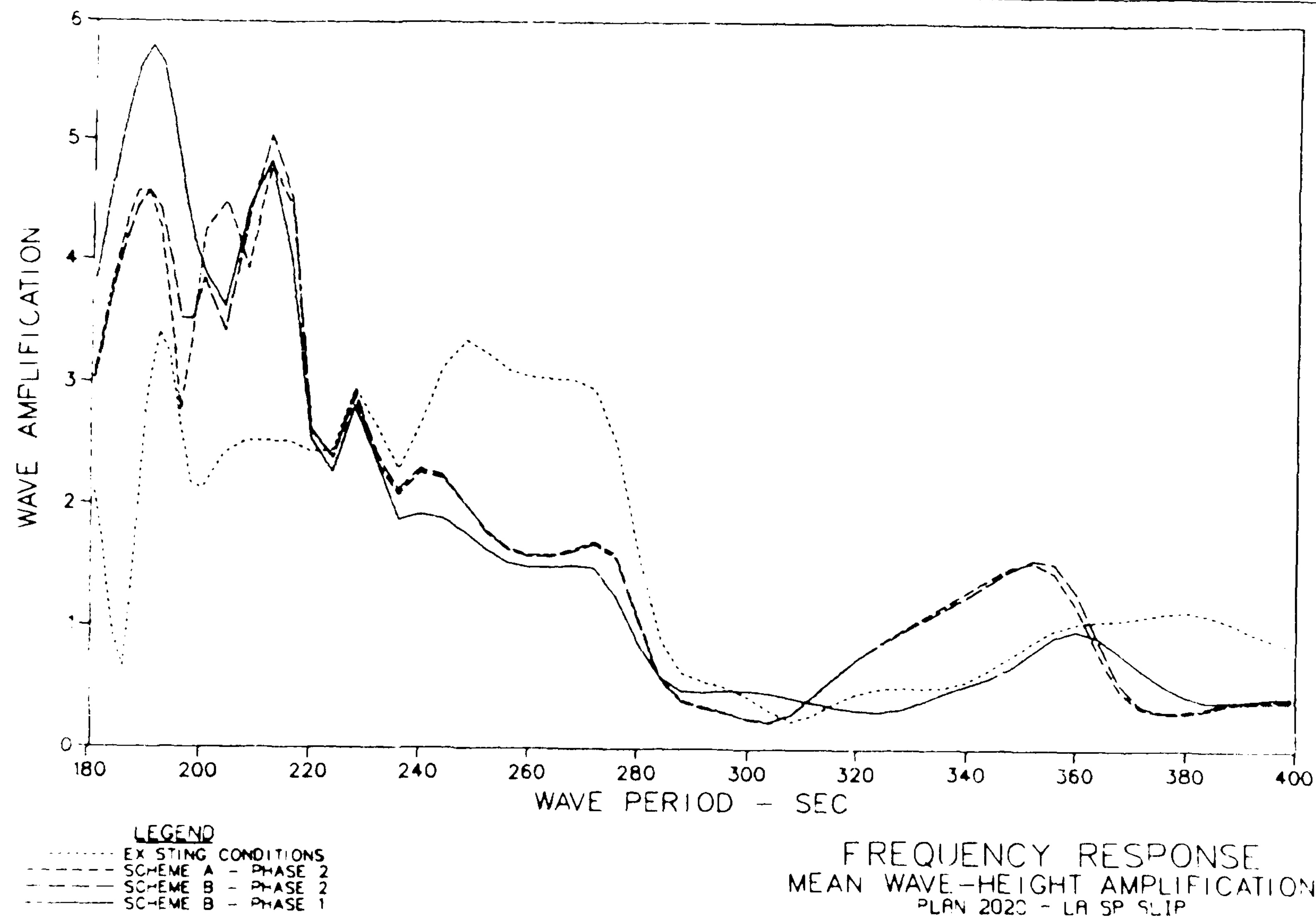

FREQUENCY RESPONSE
MEAN WAVE-HEIGHT AMPLIFICATION
PLAN 2020 - LA SP SLIP
NODES 22-23

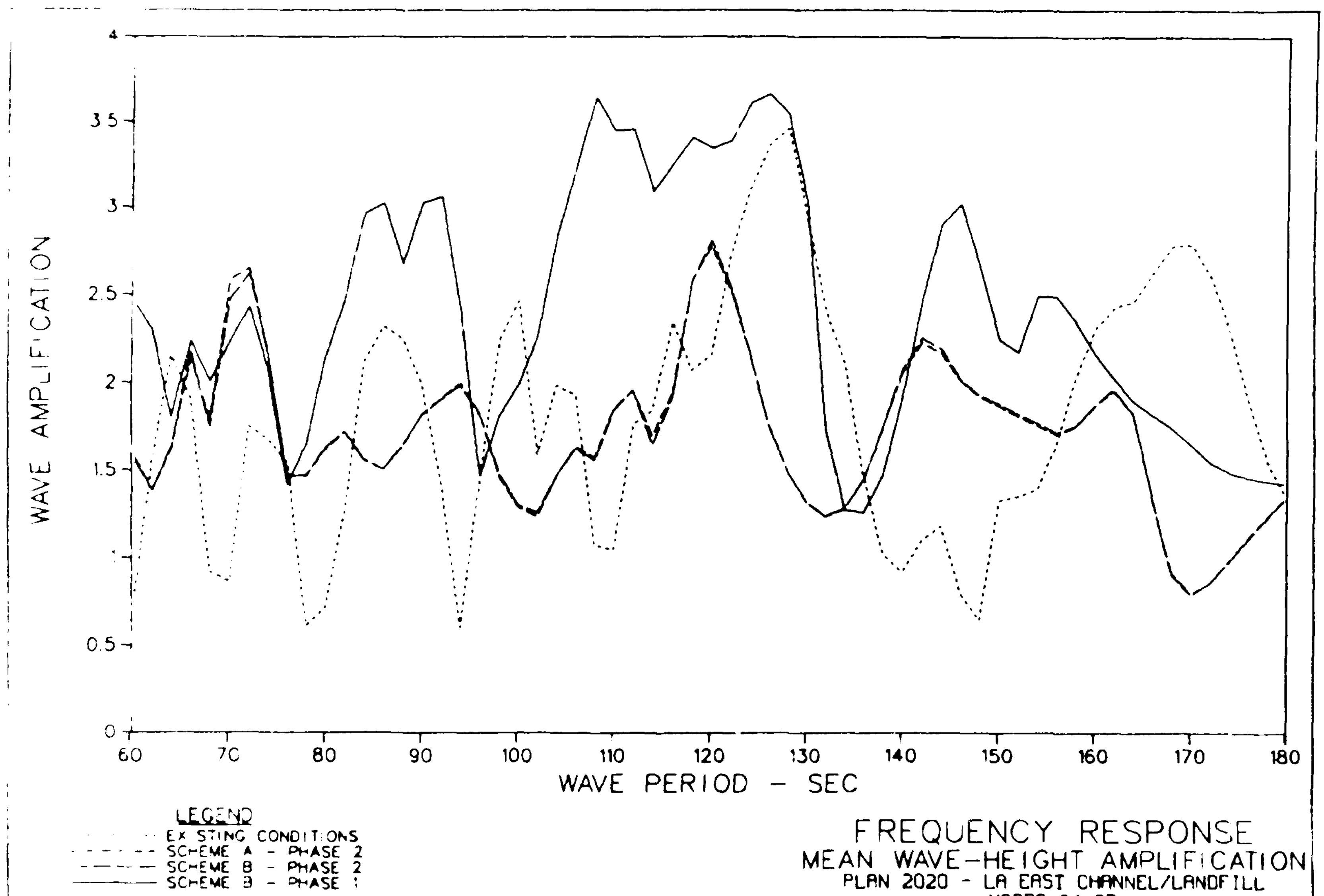

FREQUENCY RESPONSE
MEAN WAVE-HEIGHT AMPLIFICATION
PLAN 2020 - LA EAST CHANNEL/LANDFILL
NODES 24-25

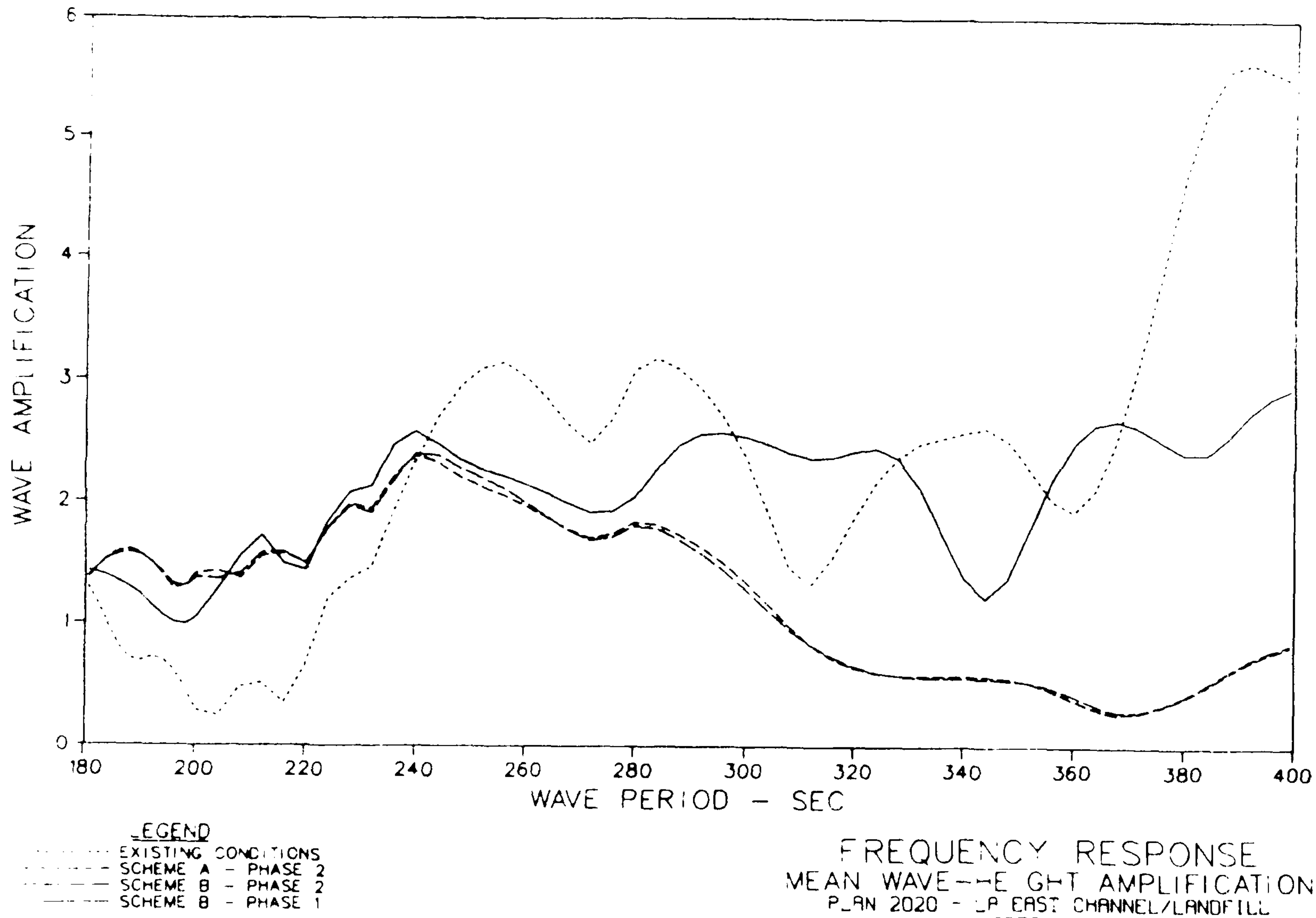

FREQUENCY RESPONSE
MEAN WAVE-HEIGHT AMPLIFICATION
PLAN 2020 - LP EAST CHANNEL/LANDFILL
NODES 24-25

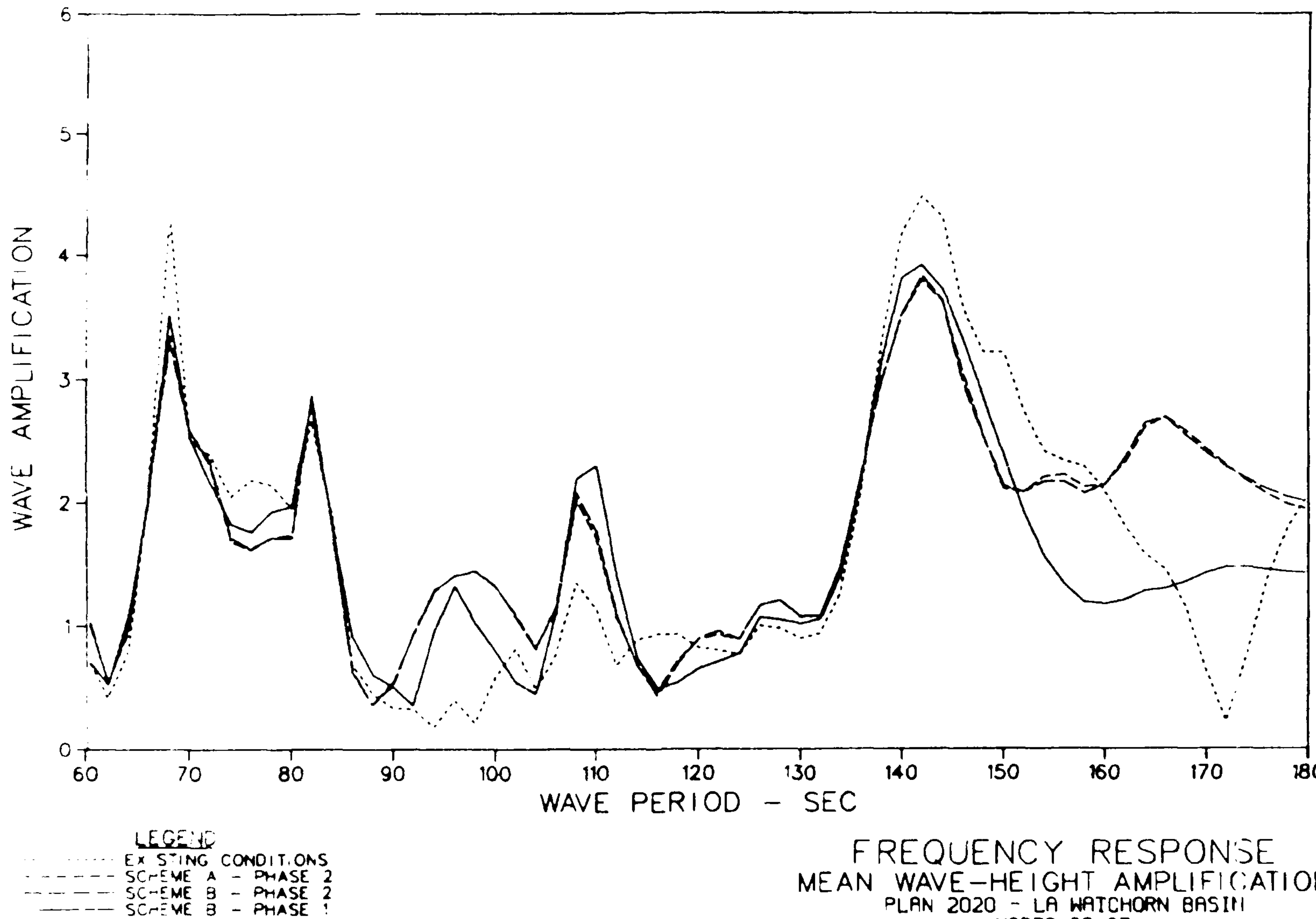

FREQUENCY RESPONSE
MEAN WAVE-HEIGHT AMPLIFICATION
PLAN 2020 - LA WATCHORN BASIN
NODES 26-27

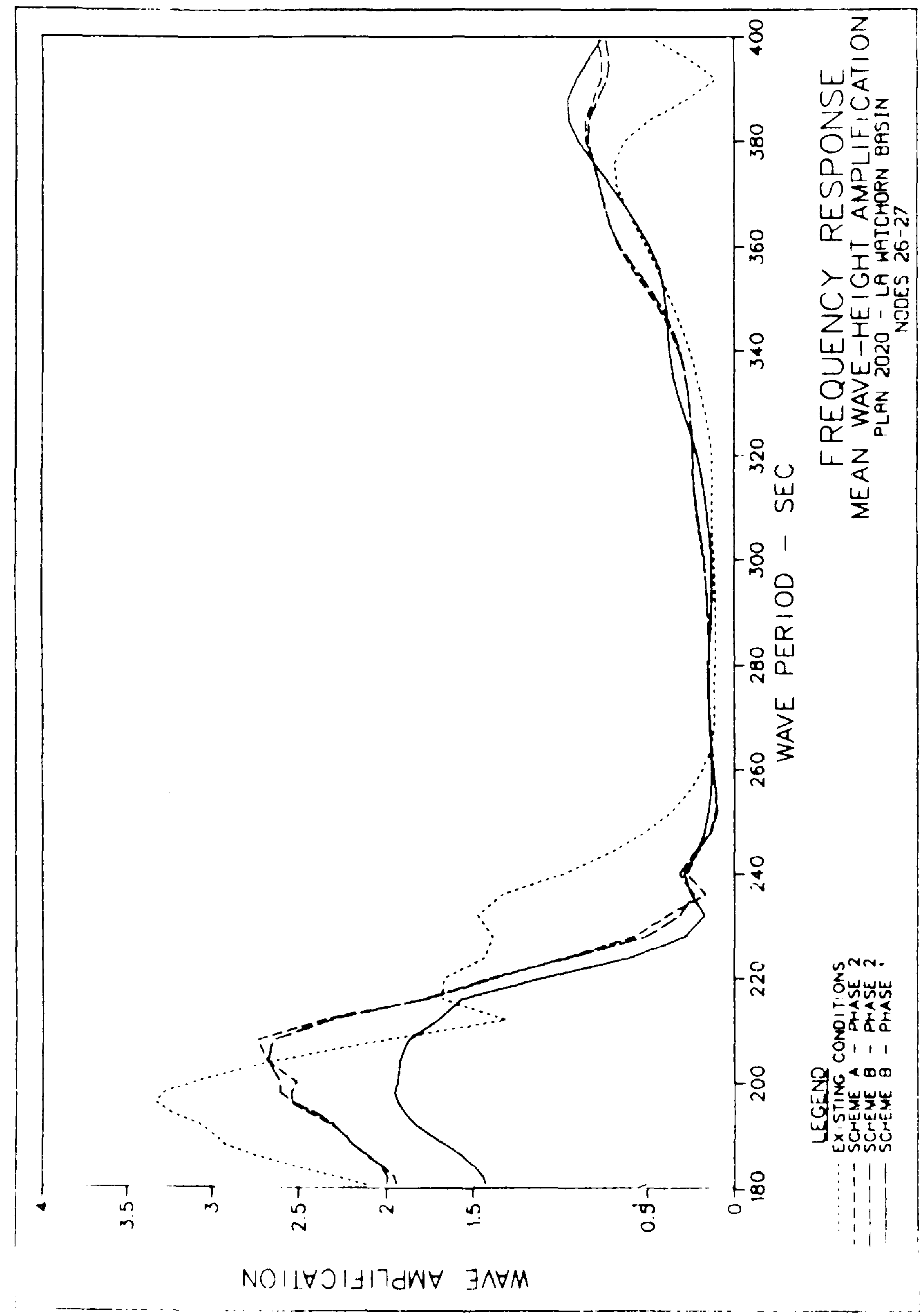
FREQUENCY RESPONSE
MEAN WAVE-HEIGHT AMPLIFICATION
PLAN 2020 - LA WATCHORN BASIN
NODES 26-27
WAVE PERIOD - SEC
WAVE AMPLIFICATION
LEGEND
EXISTING CONDITIONS
SCHEME A - PHASE 2
SCHEME B - PHASE 2
SCHEME B - PHASE 1
180
200
220
240
260
280
300
320
340
360
380
400
0
0.5
1.5
2
2.5
3
3.5
4

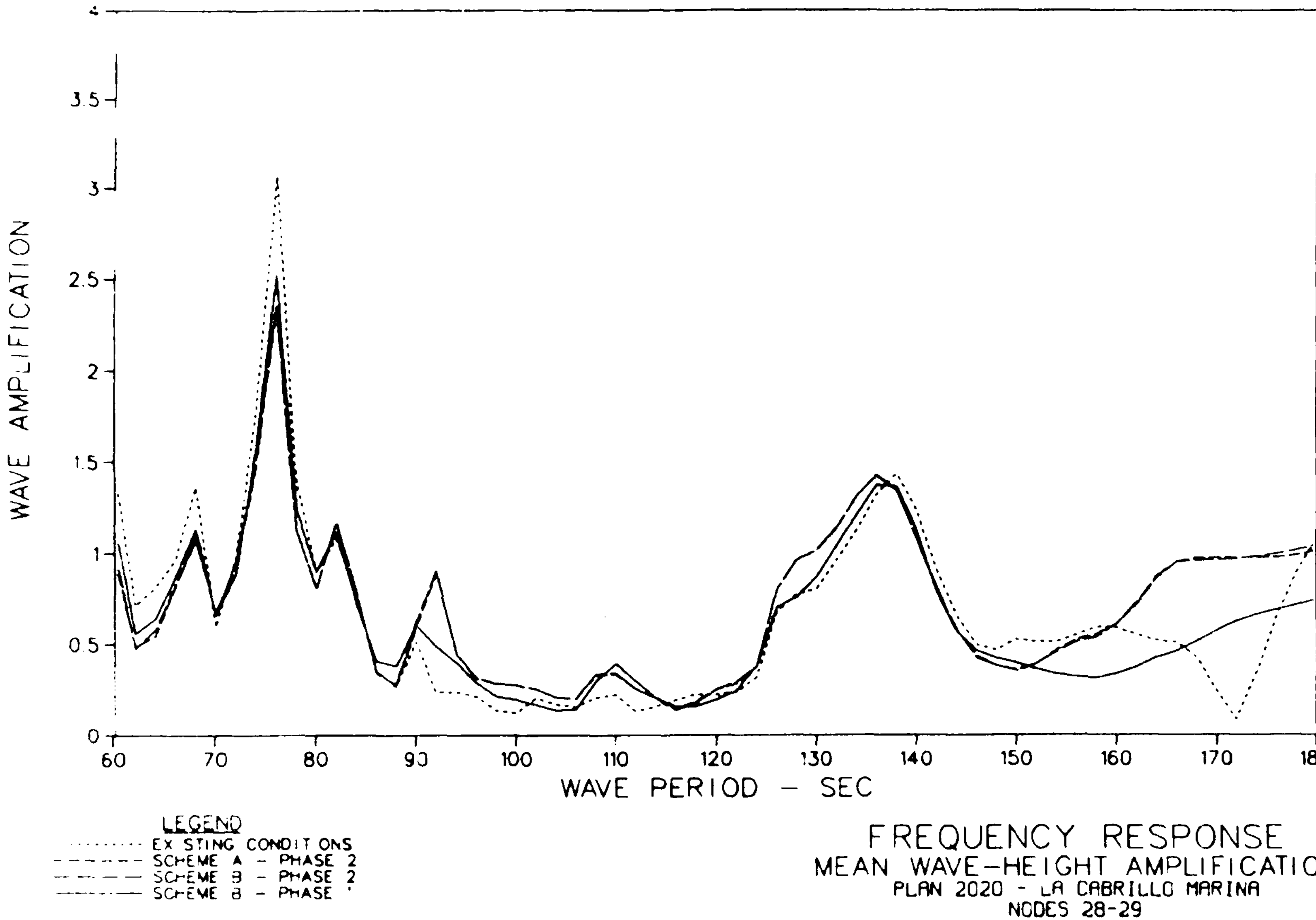

FREQUENCY RESPONSE
MEAN WAVE-HEIGHT AMPLIFICATION
PLAN 2020 - LA CABRILLO MARINA
NODES 28-29

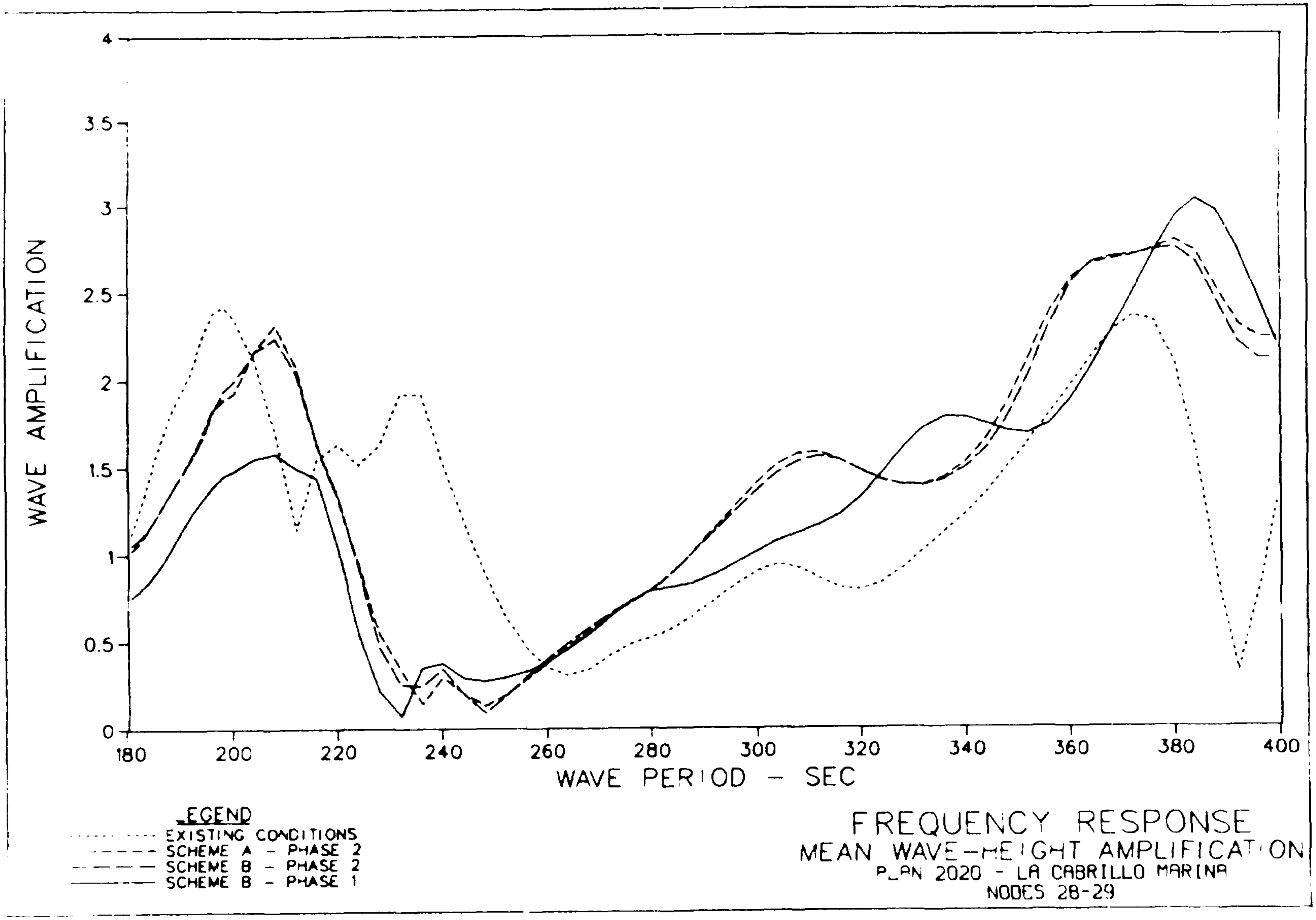

4
3.5
3
2.5
2
1.5
1
0.5
0
WAVE AMPLIFICATION
180
200
220
240
260
280
300
320
340
360
380
400
WAVE PERIOD - SEC
LEGEND
EXISTING CONDITIONS
SCHEME A - PHASE 2
SCHEME B - PHASE 2
SCHEME B - PHASE 1
FREQUENCY RESPONSE
MEAN WAVE-HEIGHT AMPLIFICATION
PLAN 2020 - LA CABRILLO MARINA
NODES 28-29

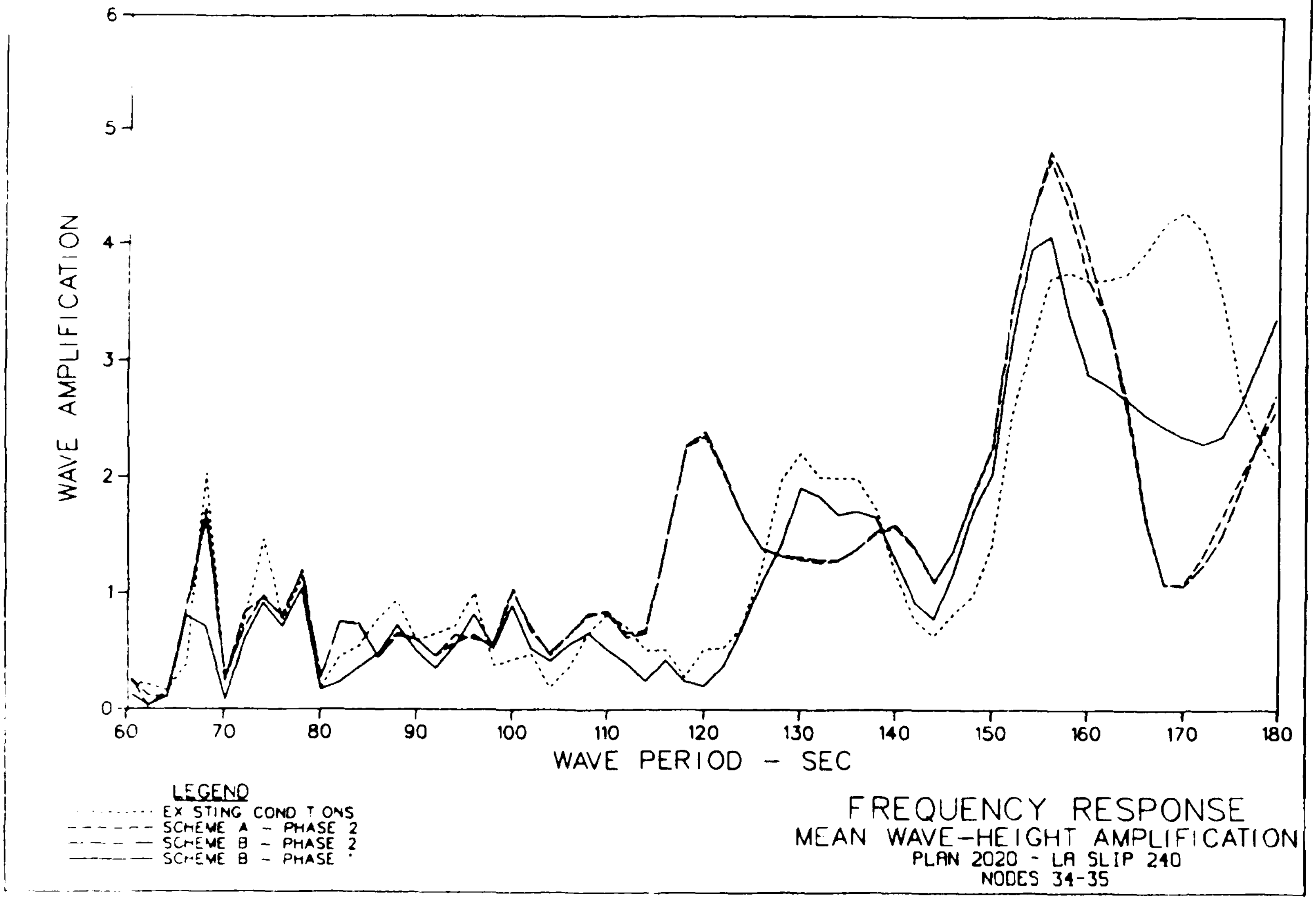

FREQUENCY RESPONSE
MEAN WAVE-HEIGHT AMPLIFICATION
PLAN 2020 - LA SLIP 240
NODES 34-35

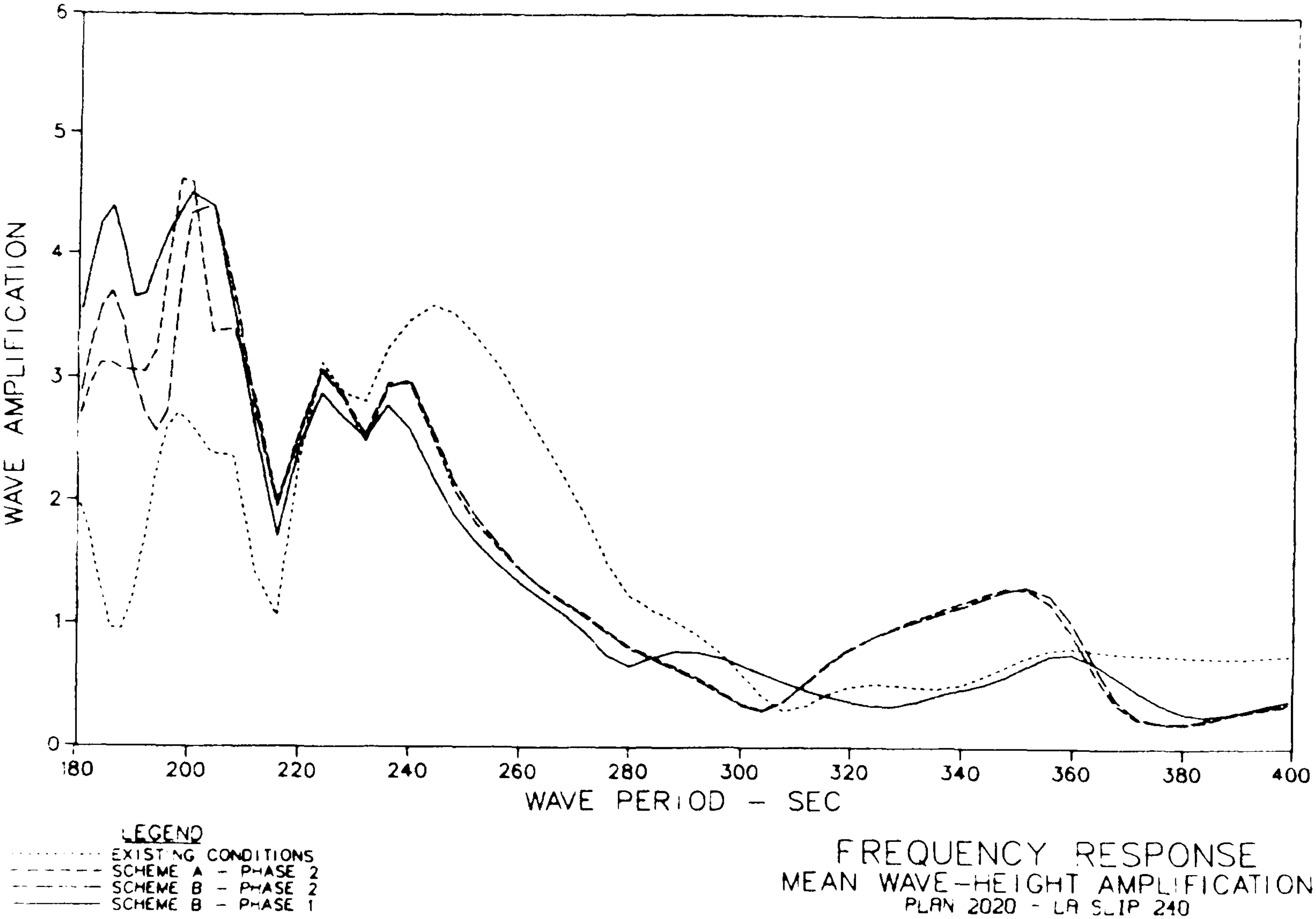

FREQUENCY RESPONSE
MEAN WAVE-HEIGHT AMPLIFICATION
PLAN 2020 - LA SLIP 240
NODES 34-35

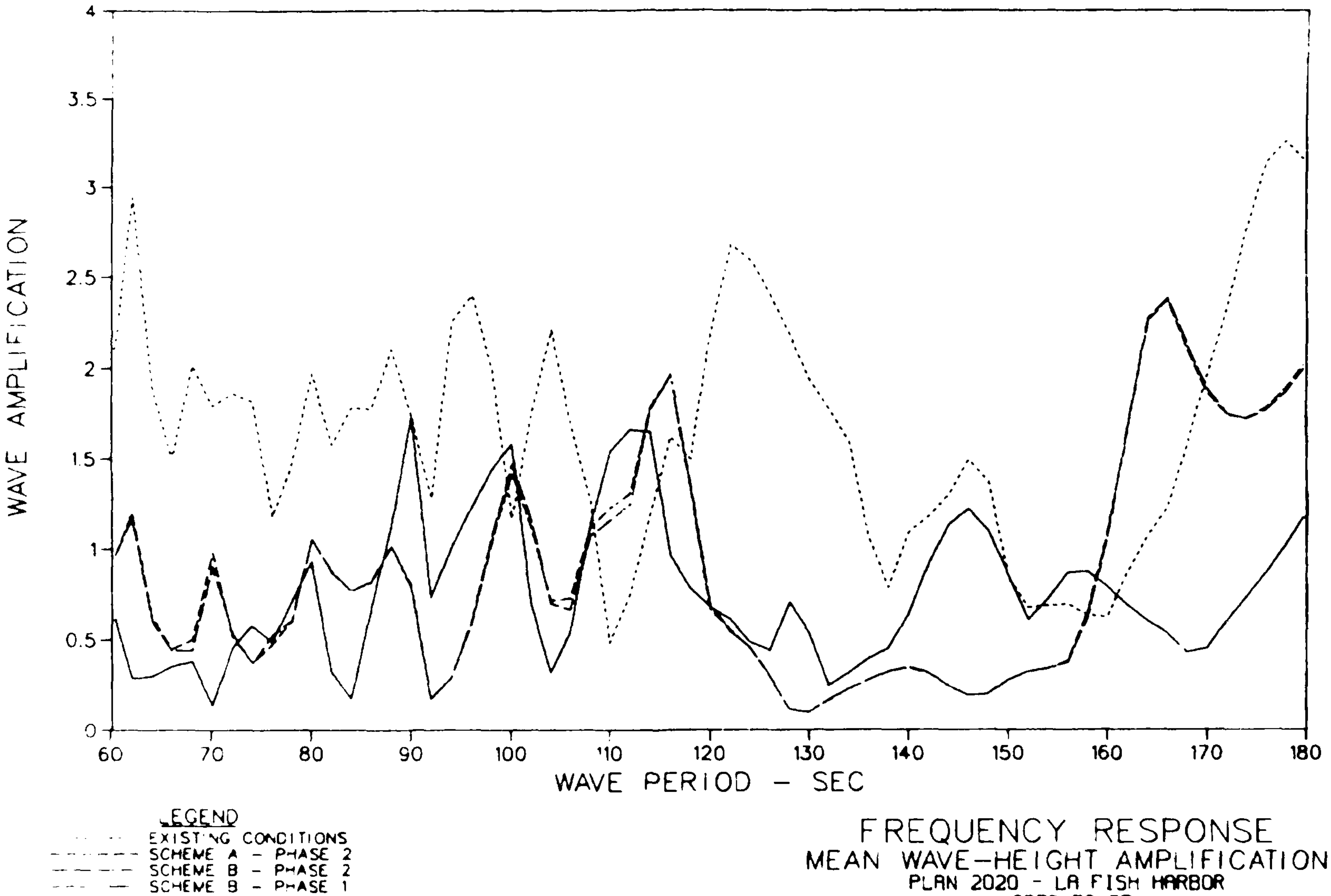

FREQUENCY RESPONSE
MEAN WAVE-HEIGHT AMPLIFICATION
PLAN 2020 - LA FISH HARBOR
NODES 36-37

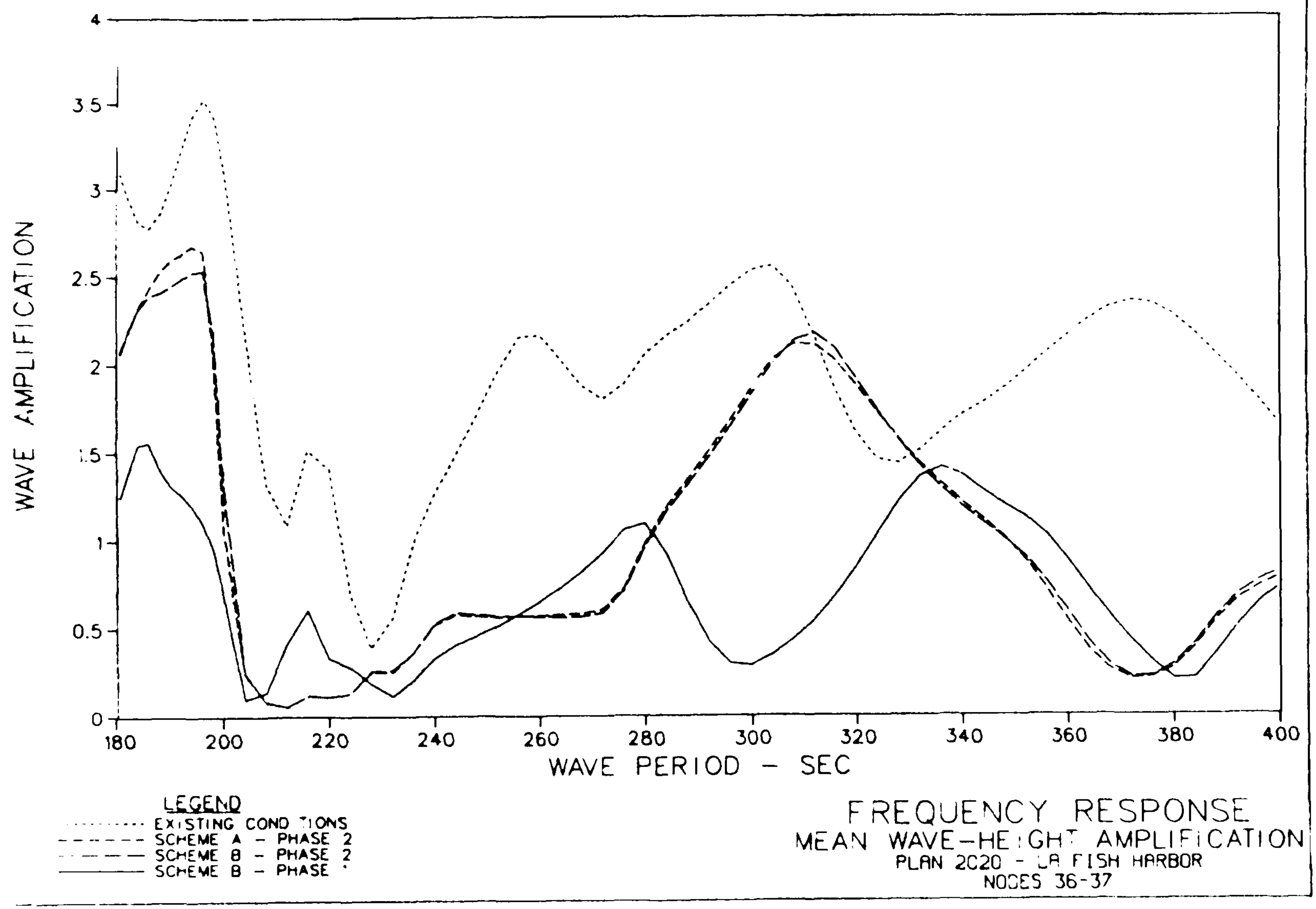

WAVE AMPLIFICATION
WAVE PERIOD - SEC
LEGEND
EXISTING COND TIONS
SCHEME A - PHASE 2
SCHEME B - PHASE 2
SCHEME B - PHASE
FREQUENCY RESPONSE
MEAN WAVE-HEIGHT AMPLIFICATION
PLAN 2020 - LA FISH HARBOR
NODES 36-37

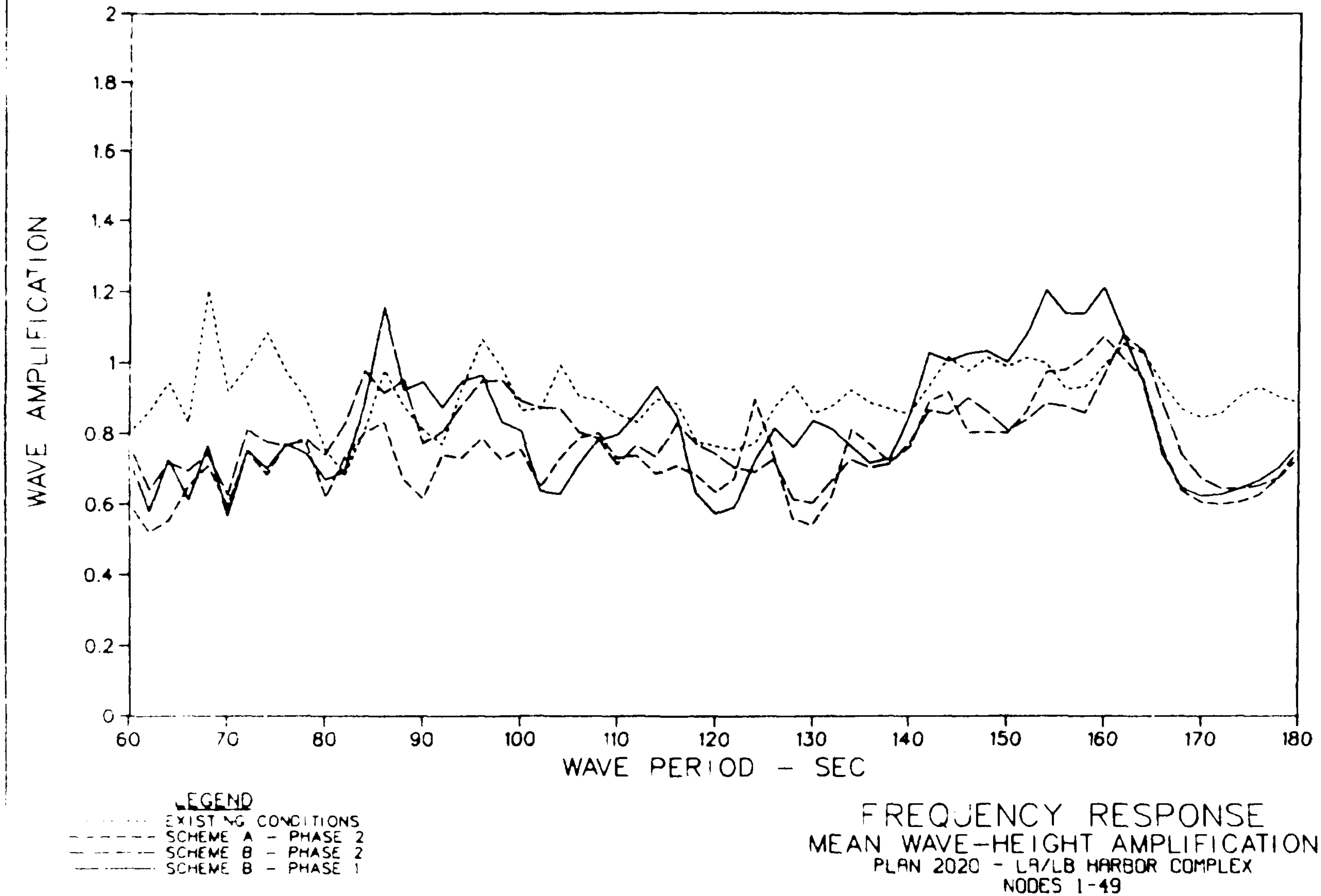

FREQUENCY RESPONSE
MEAN WAVE-HEIGHT AMPLIFICATION
PLAN 2020 - LA/LB HARBOR COMPLEX
NODES 1-49

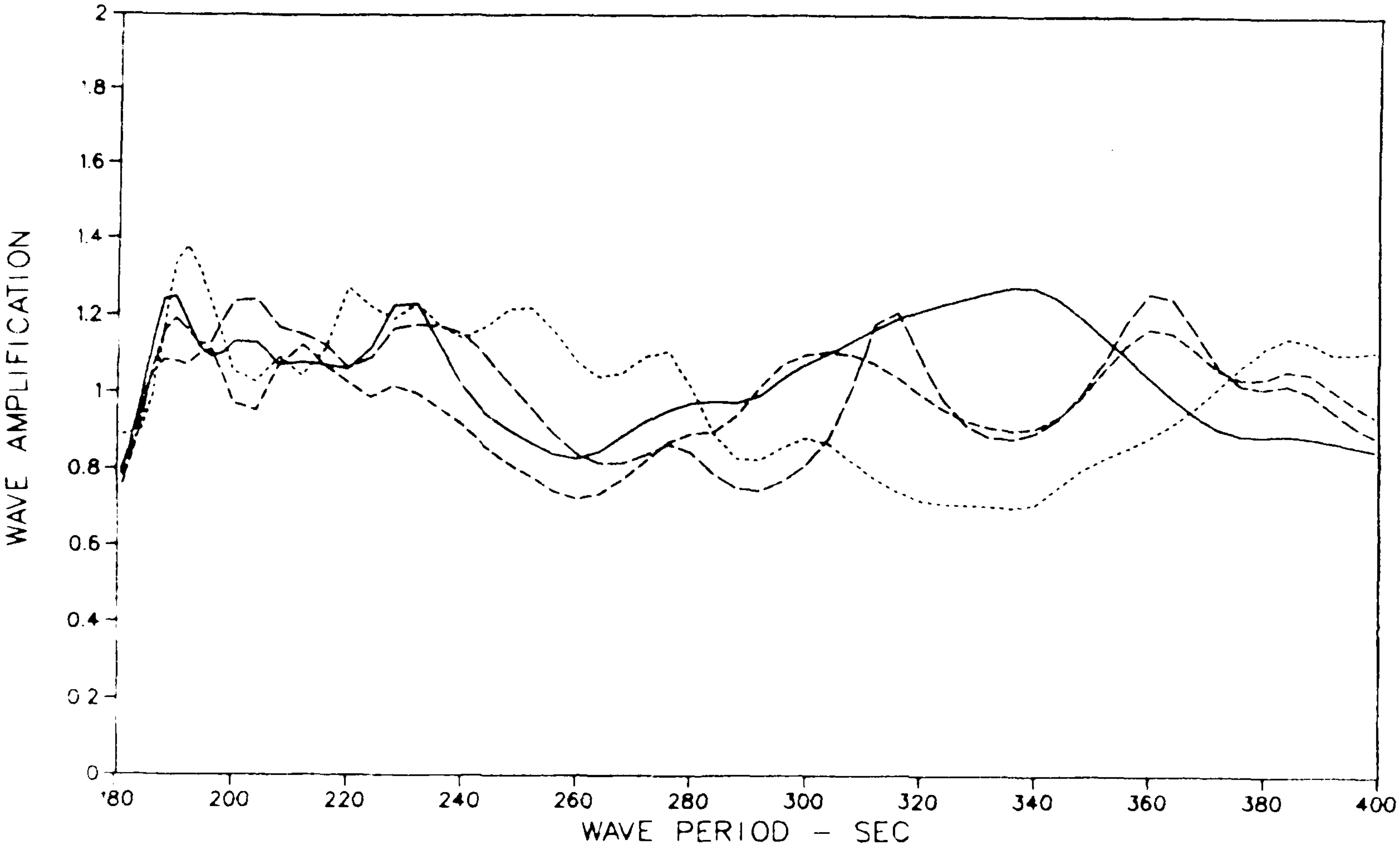

LEGEND
EXISTING CONDITIONS
SCHEME A - PHASE 2
SCHEME B - PHASE 2
SCHEME B - PHASE 1

FREQUENCY RESPONSE
MEAN WAVE-HEIGHT AMPLIFICATION
PLAN 2020 - LA/LB HARBOR COMPLEX
NODES 1-49

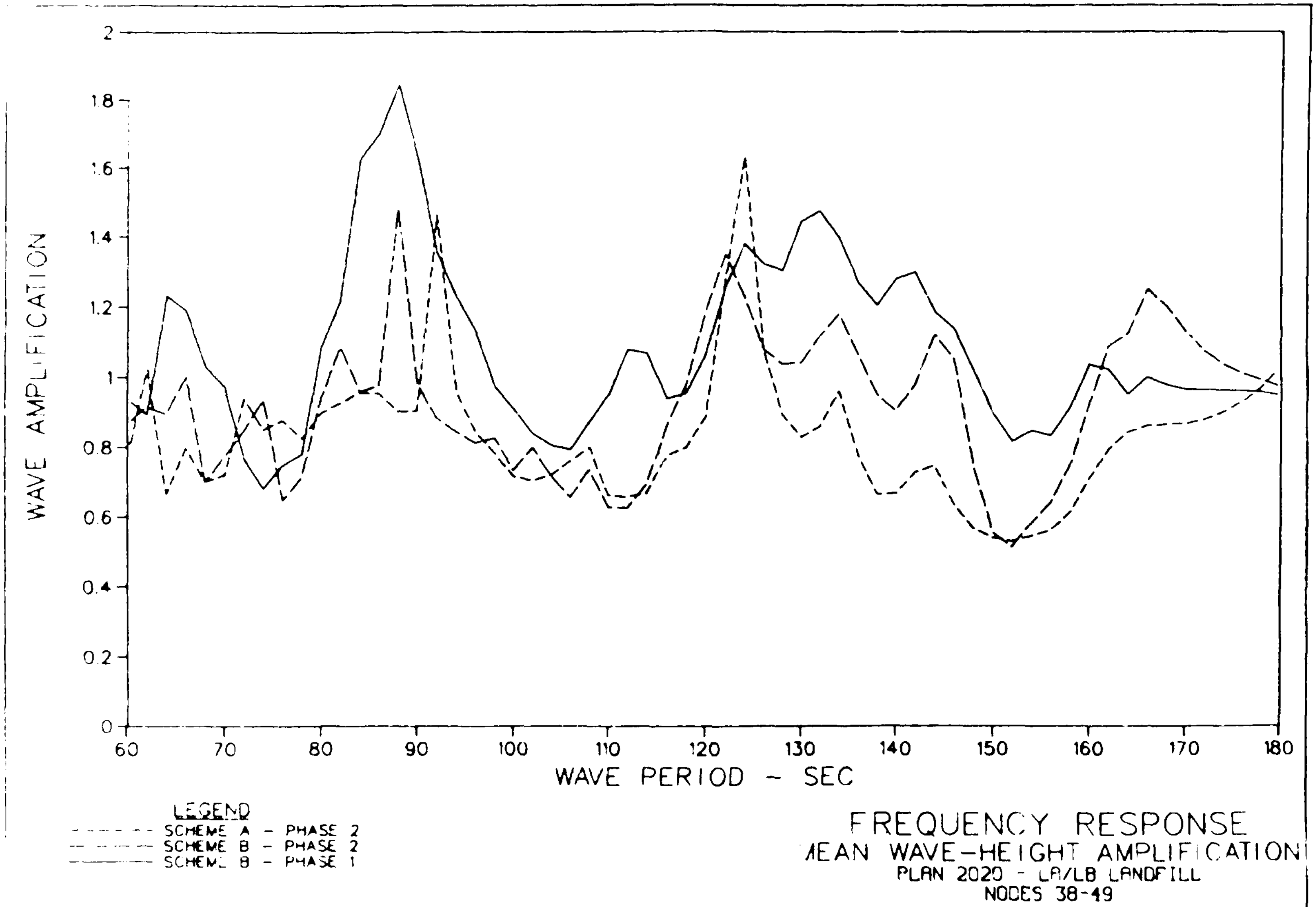

WAVE AMPLIFICATION
2
1.8
1.6
1.4
1.2
1
0.8
0.6
0.4
0.2
0
60
70
80
90
100
110
120
130
140
150
160
170
180
WAVE PERIOD - SEC
LEGEND
SCHEME A - PHASE 2
SCHEME B - PHASE 2
SCHEME B - PHASE 1
FREQUENCY RESPONSE
MEAN WAVE-HEIGHT AMPLIFICATION
PLAN 2020 - LA/LB LANDFILL
NODES 38-49

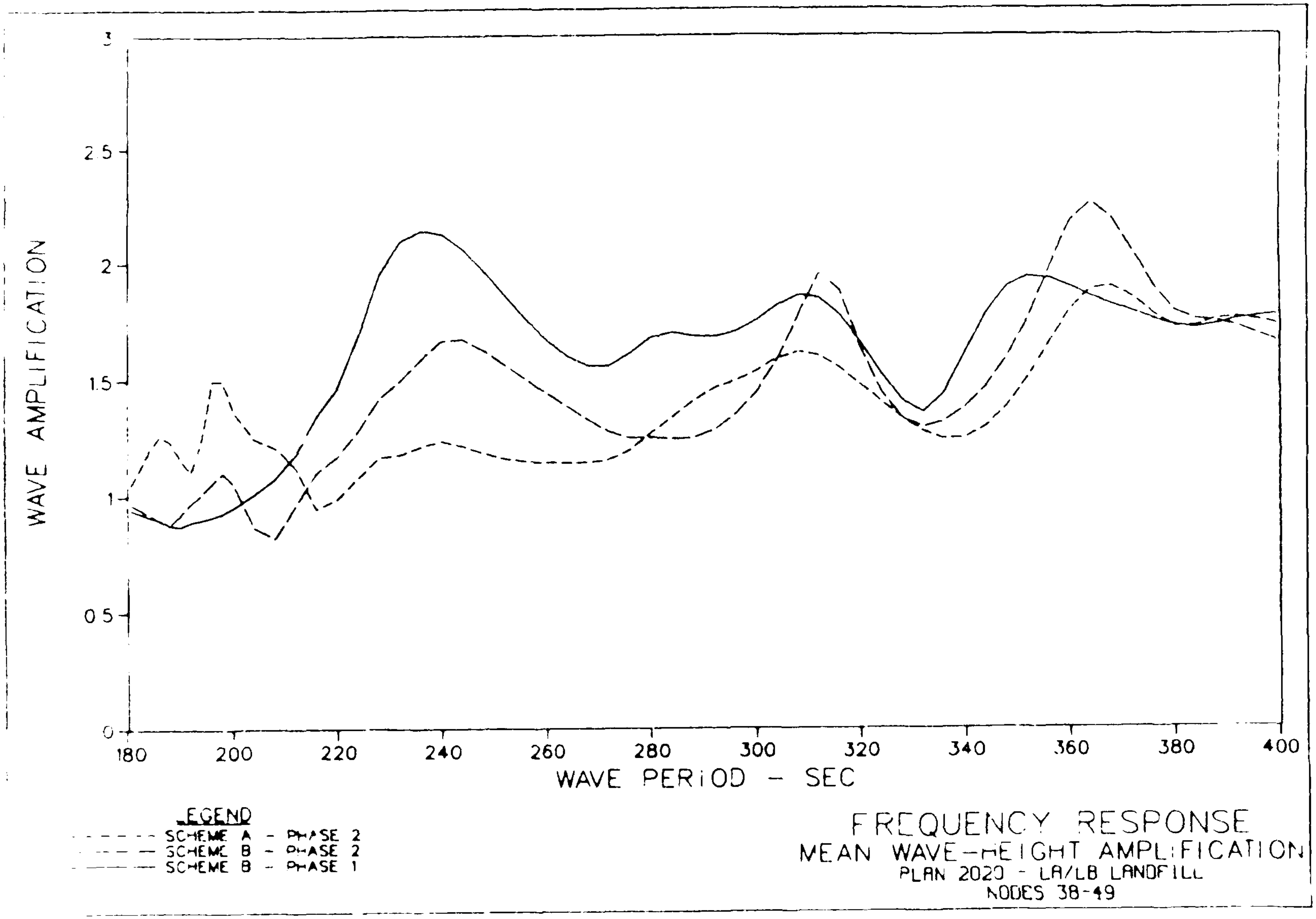

WAVE AMPLIFICATION
0
0.5
1
1.5
2
2.5
3
180
200
220
240
260
280
300
320
340
360
380
400
WAVE PERIOD - SEC
LEGEND
SCHEME A - PHASE 2
SCHEME B - PHASE 2
SCHEME B - PHASE 1
FREQUENCY RESPONSE
MEAN WAVE-HEIGHT AMPLIFICATION
PLAN 2020 - LA/LB LANDFILL
NODES 38-49

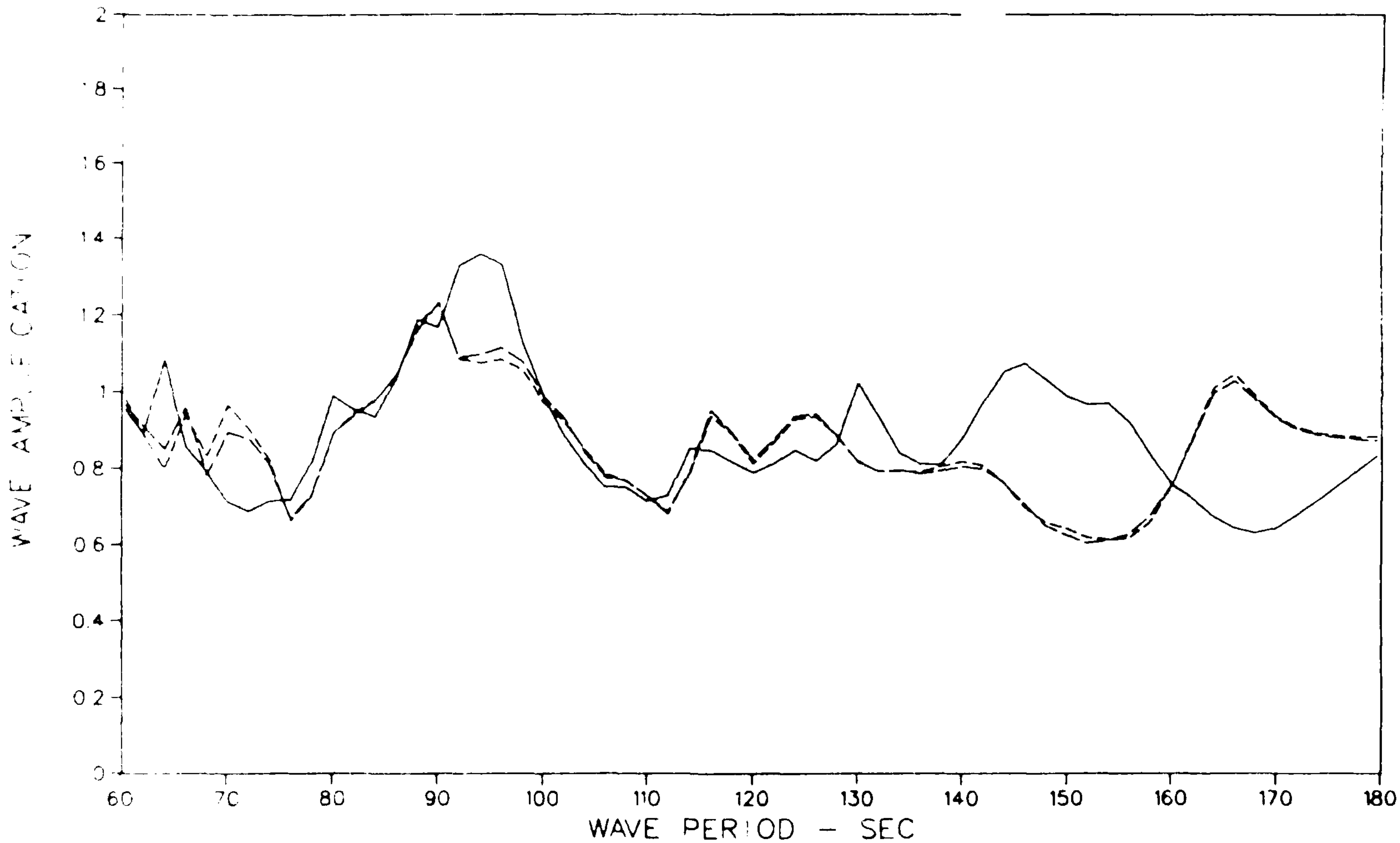

LEGEND
SCHEME A - PHASE 2
SCHEME B - PHASE 2
SCHEME B - PHASE 1

FREQUENCY RESPONSE
MEAN WAVE-HEIGHT AMPLIFICATION
PLAN 2020 - LA LANDFILL
NODES 38-44

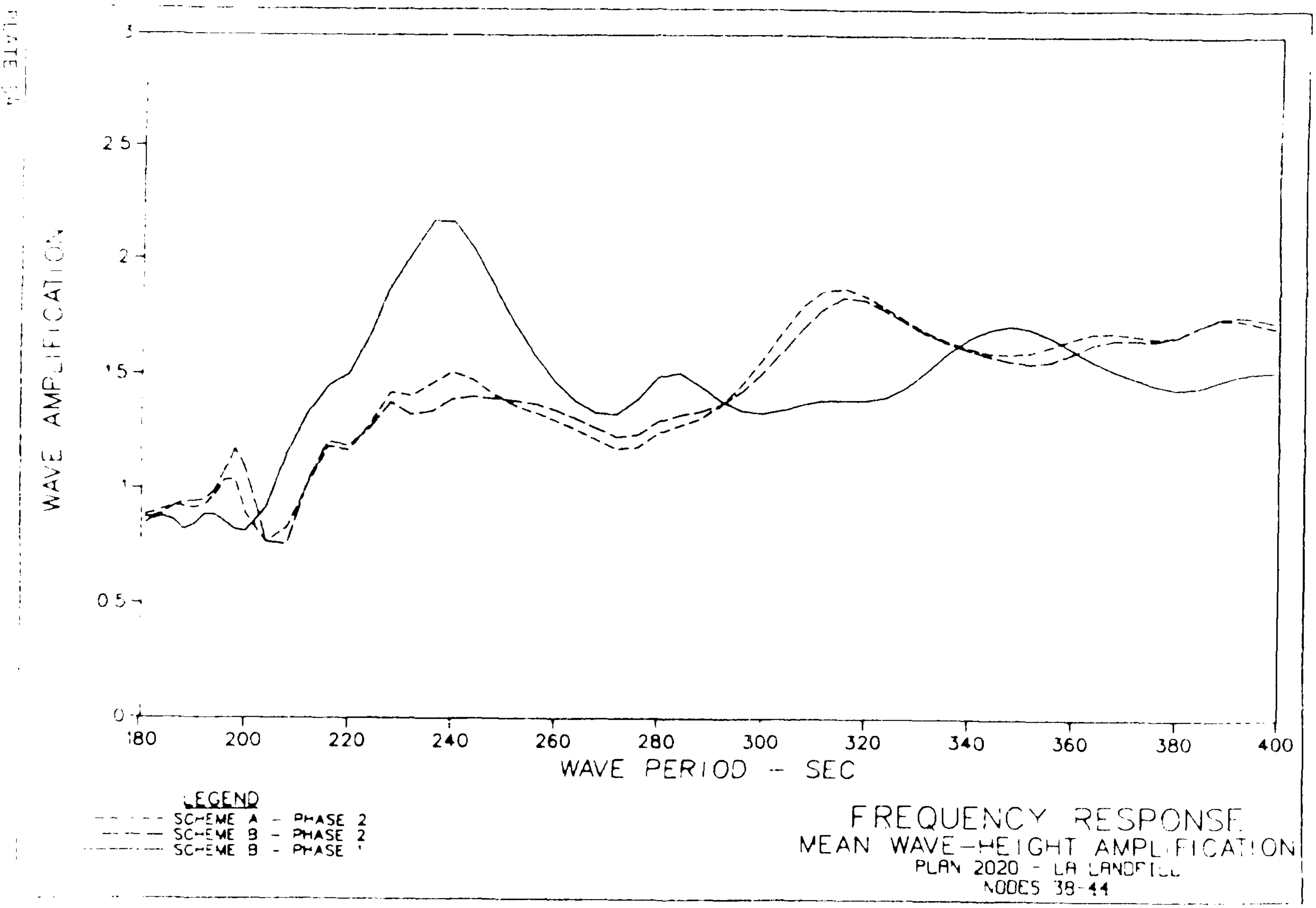
WAVE AMPLIFICATION
3
2.5
2
1.5
1
0.5
0
180
200
220
240
260
280
300
320
340
360
380
400
WAVE PERIOD - SEC
LEGEND
SCHEME A - PHASE 2
SCHEME B - PHASE 2
SCHEME B - PHASE 1
FREQUENCY RESPONSE
MEAN WAVE-HEIGHT AMPLIFICATION
PLAN 2020 - LA LANDFILL
NODES 38-44

PLATE 54

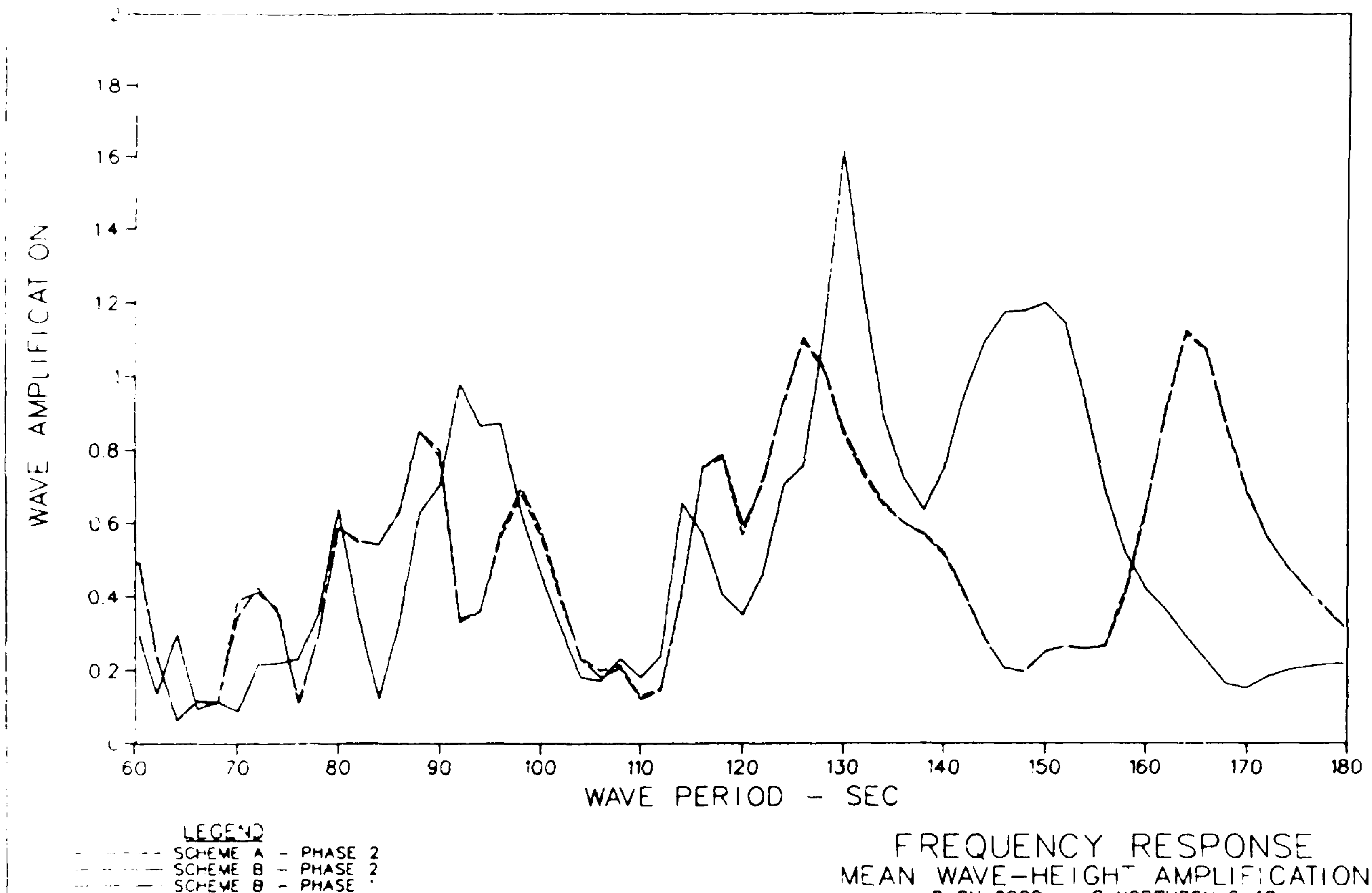

FREQUENCY RESPONSE
MEAN WAVE-HEIGHT AMPLIFICATION
PLAN 2020 - LA NORTHERN SLIP
NODES 38-40

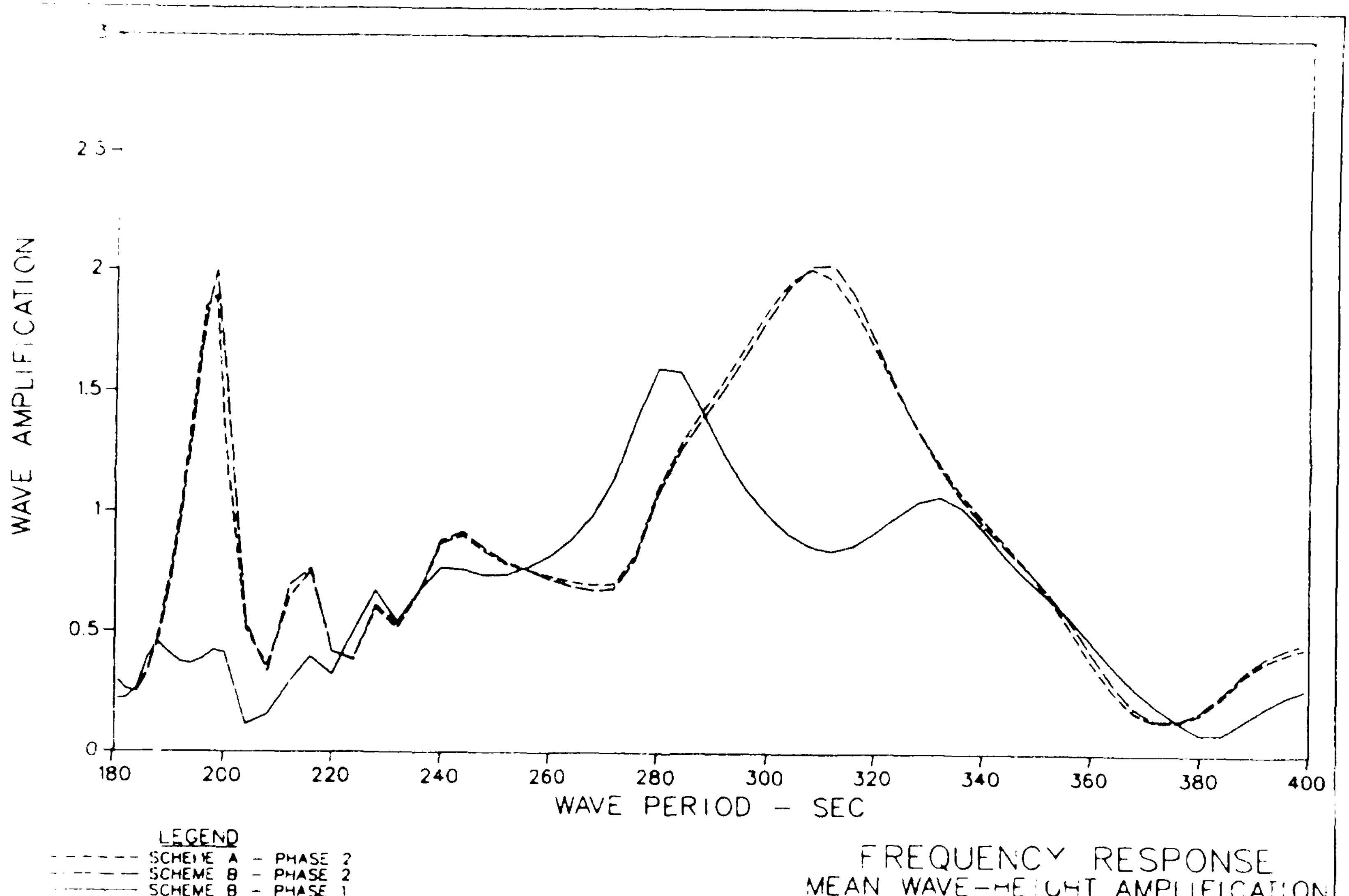

FREQUENCY RESPONSE
MEAN WAVE-HEIGHT AMPLIFICATION
PLAN 202C - LA NORTHERN SLIP
NODES 38-40

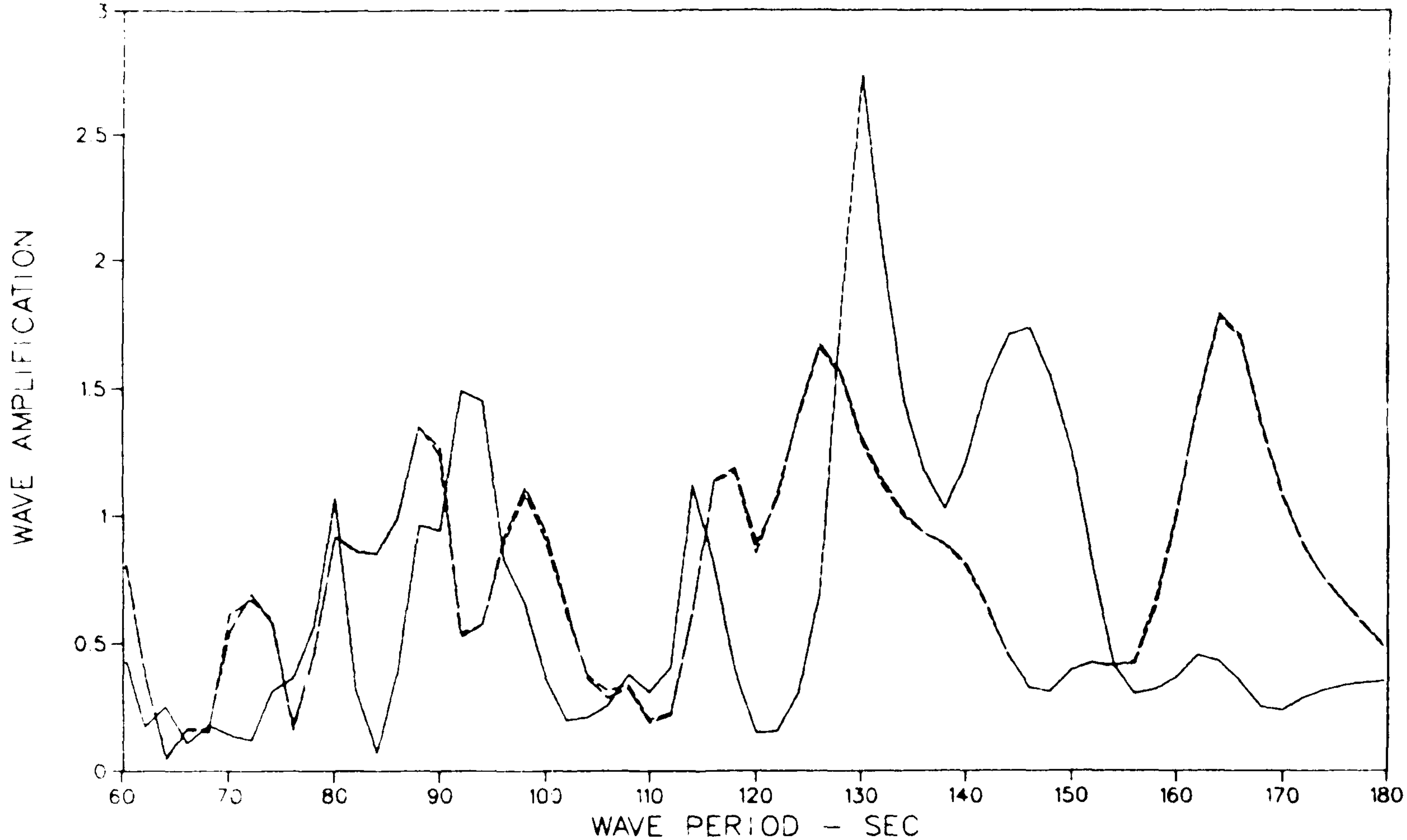

LEGEND
SCHEME A - PHASE 2
SCHEME B - PHASE 2
SCHEME B - PHASE 1

FREQUENCY RESPONSE
MEAN WAVE-HEIGHT AMPLIFICATION
PLAN 2020 - LA NORTHERN SLIP(END)
NODES 38-39

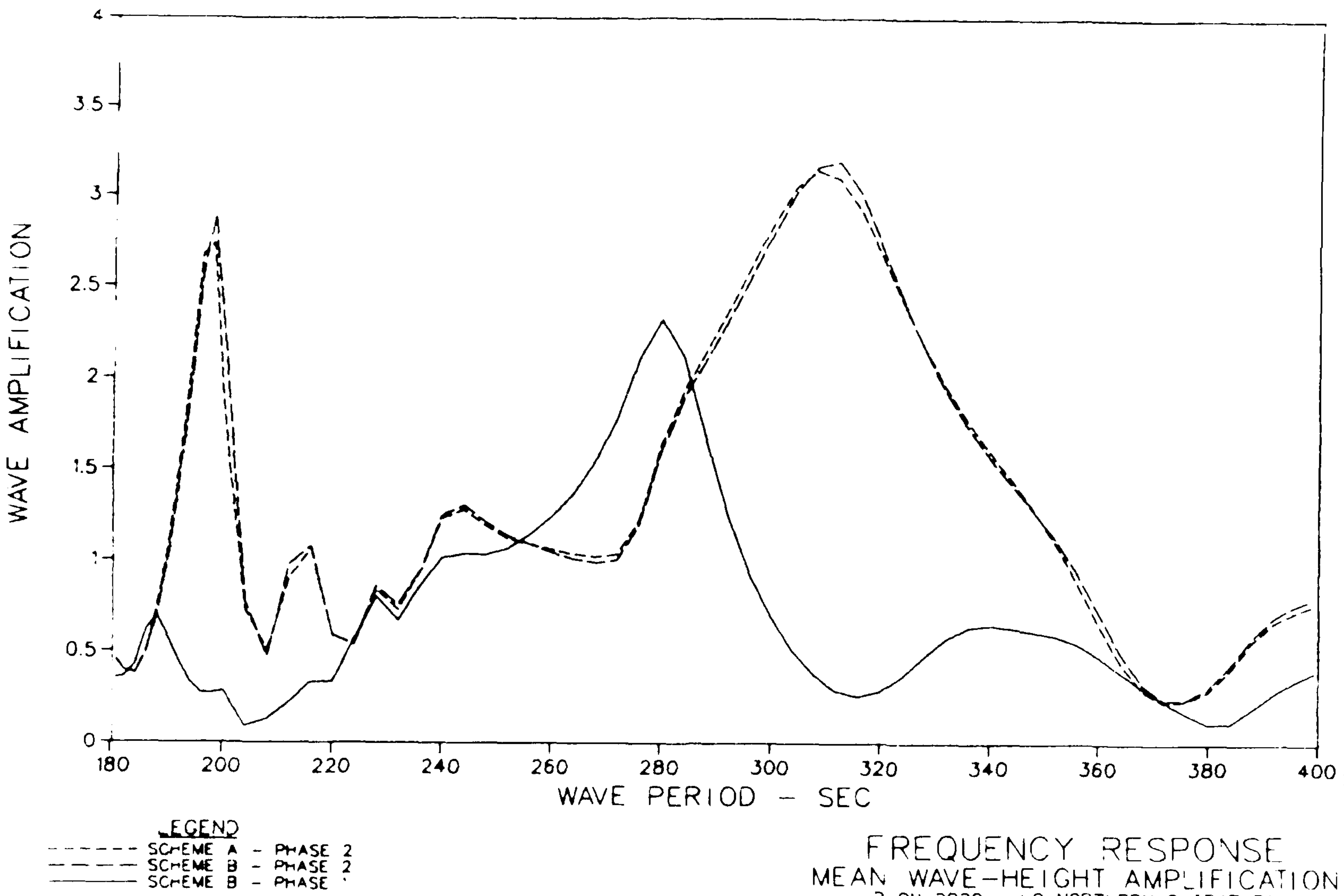

FREQUENCY RESPONSE
MEAN WAVE-HEIGHT AMPLIFICATION
PLAN 2020 - LA NORTHERN SLIP(END)
NODES 38-39

PLATE 58

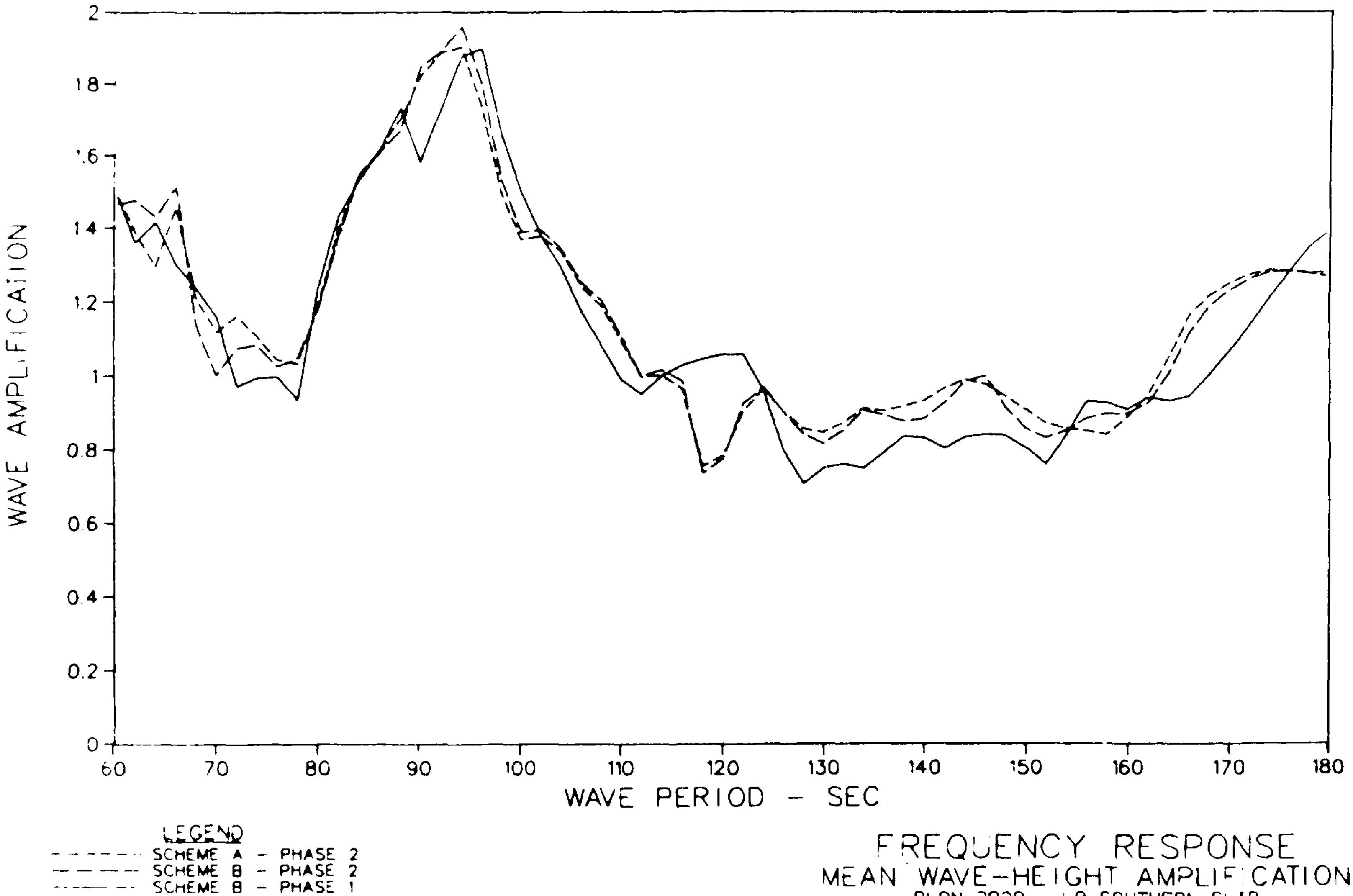

FREQUENCY RESPONSE
MEAN WAVE-HEIGHT AMPLIFICATION
PLAN 2020 - LA SOUTHERN SLIP
NODES 41-44

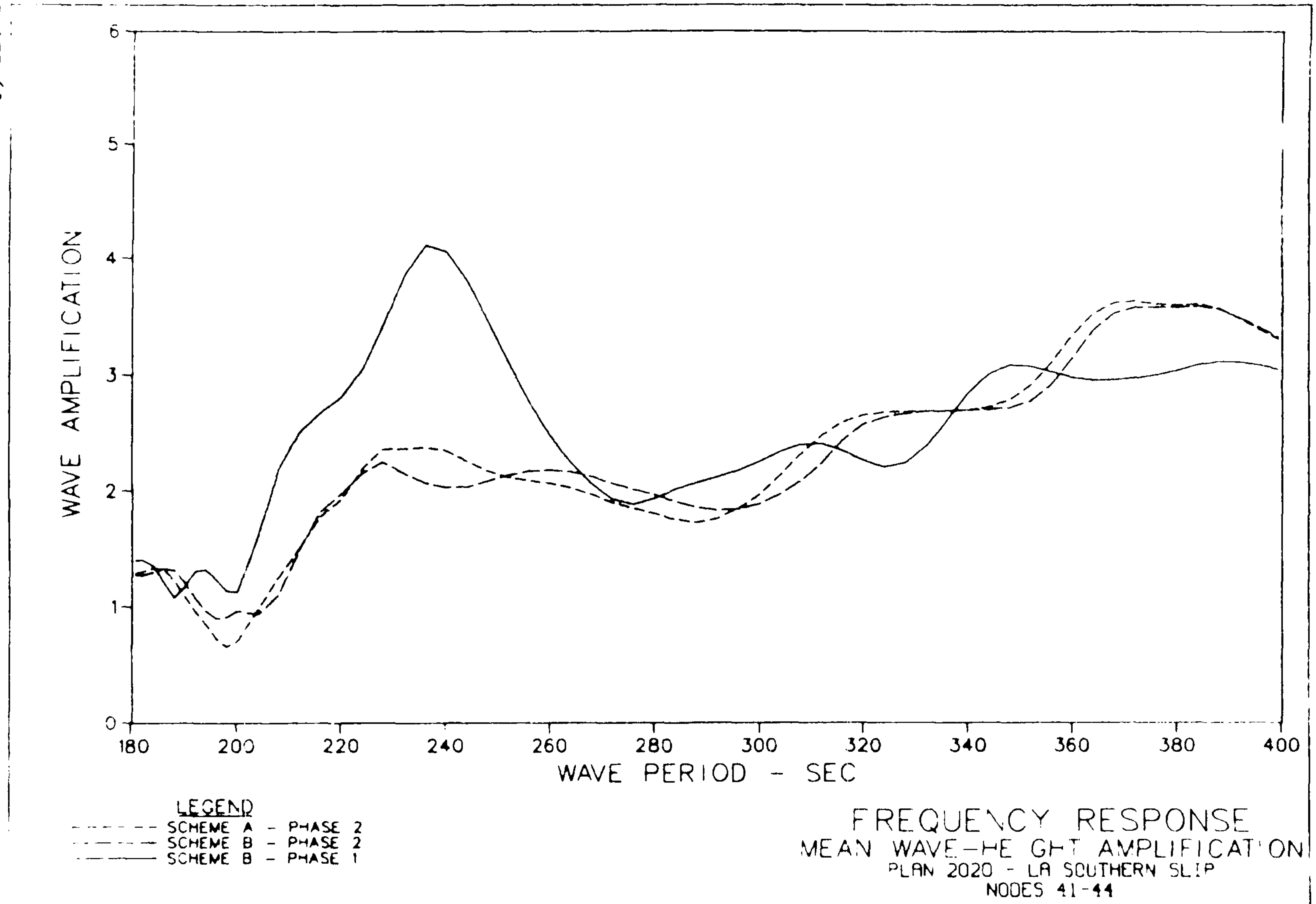
WAVE AMPLIFICATION
0
1
2
3
4
5
6
180
200
220
240
260
280
300
320
340
360
380
400
WAVE PERIOD - SEC
LEGEND
SCHEME A - PHASE 2
SCHEME B - PHASE 2
SCHEME B - PHASE 1
FREQUENCY RESPONSE
MEAN WAVE-HEIGHT AMPLIFICATION
PLAN 2020 - LA SOUTHERN SLIP
NODES 41-44

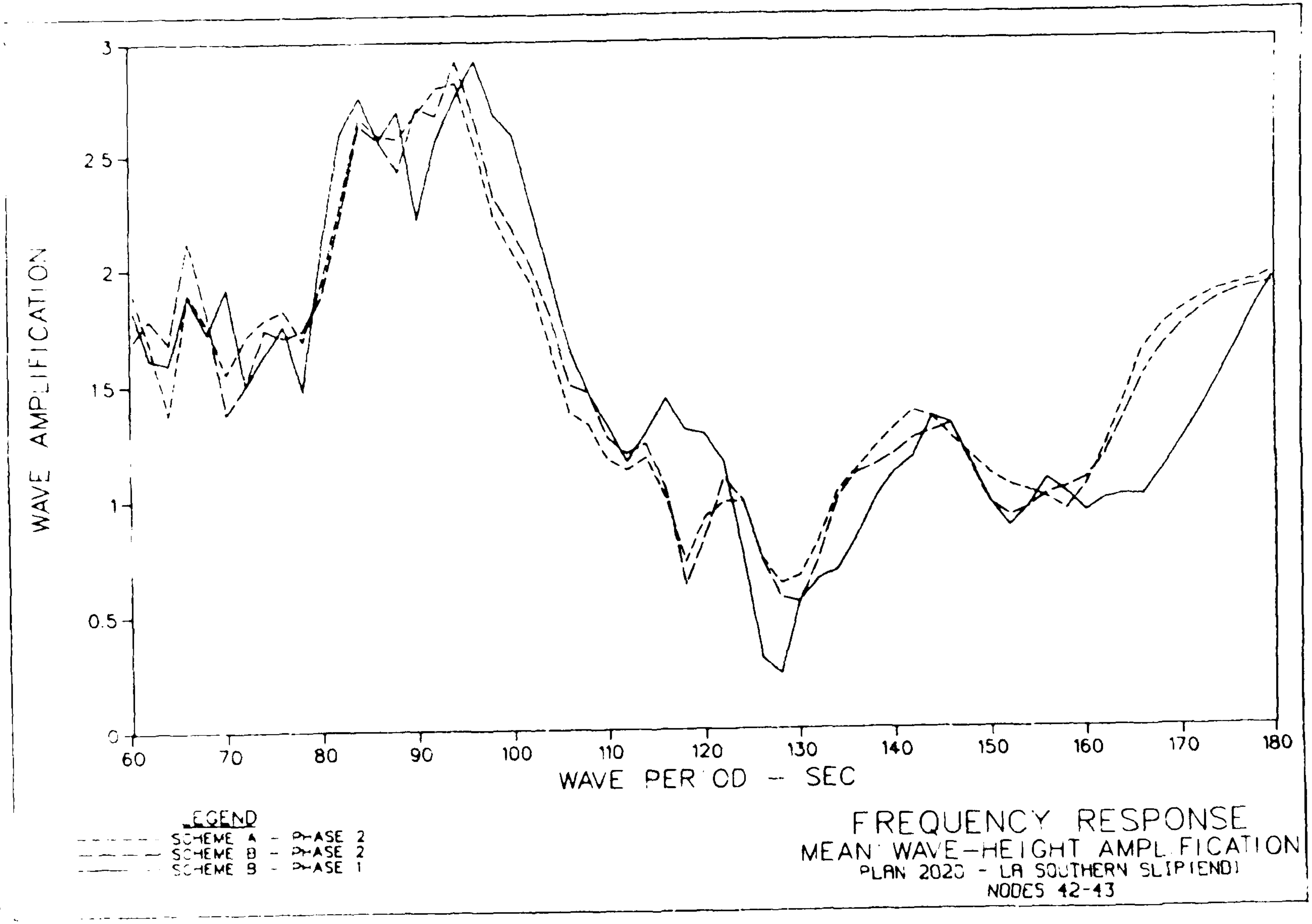
3
2.5
2
1.5
1
0.5
0
WAVE AMPLIFICATION
60
70
80
90
100
110
120
130
140
150
160
170
180
WAVE PERIOD - SEC
LEGEND
SCHEME A - PHASE 2
SCHEME B - PHASE 2
SCHEME B - PHASE 1
FREQUENCY RESPONSE
MEAN WAVE-HEIGHT AMPLIFICATION
PLAN 2020 - LA SOUTHERN SLIP(END)
NODES 42-43

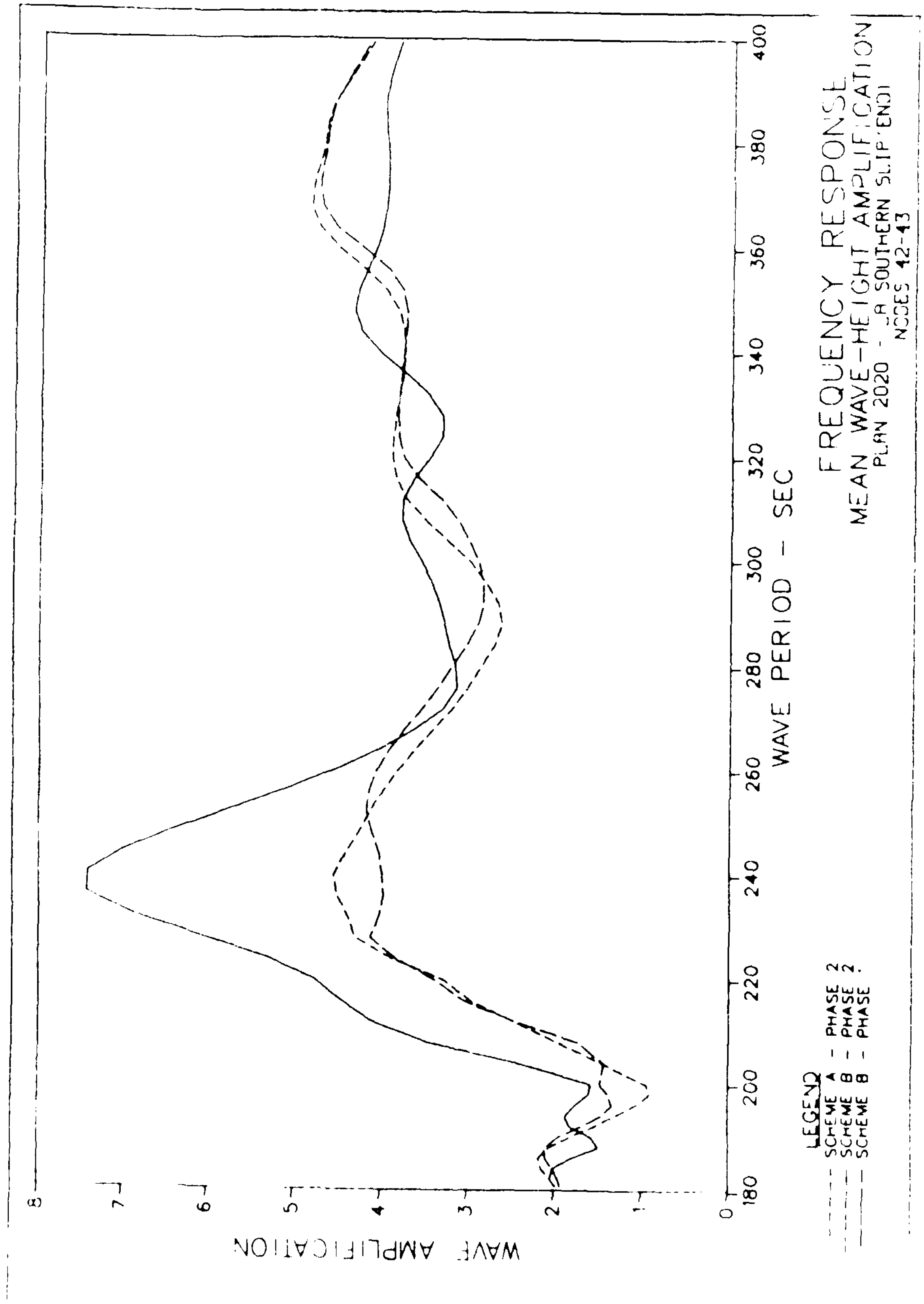
FREQUENCY RESPONSE
MEAN WAVE-HEIGHT AMPLIFICATION
PLAN 2020 - A SOUTHERN SLIP END)
NODES 42-43
WAVE PERIOD - SEC
WAVE AMPLIFICATION
LEGEND
SCHEME A - PHASE 2
SCHEME B - PHASE 2
SCHEME B - PHASE 1
180
200
220
240
260
280
300
320
340
360
380
400
0
1
2
3
4
5
6
7
8

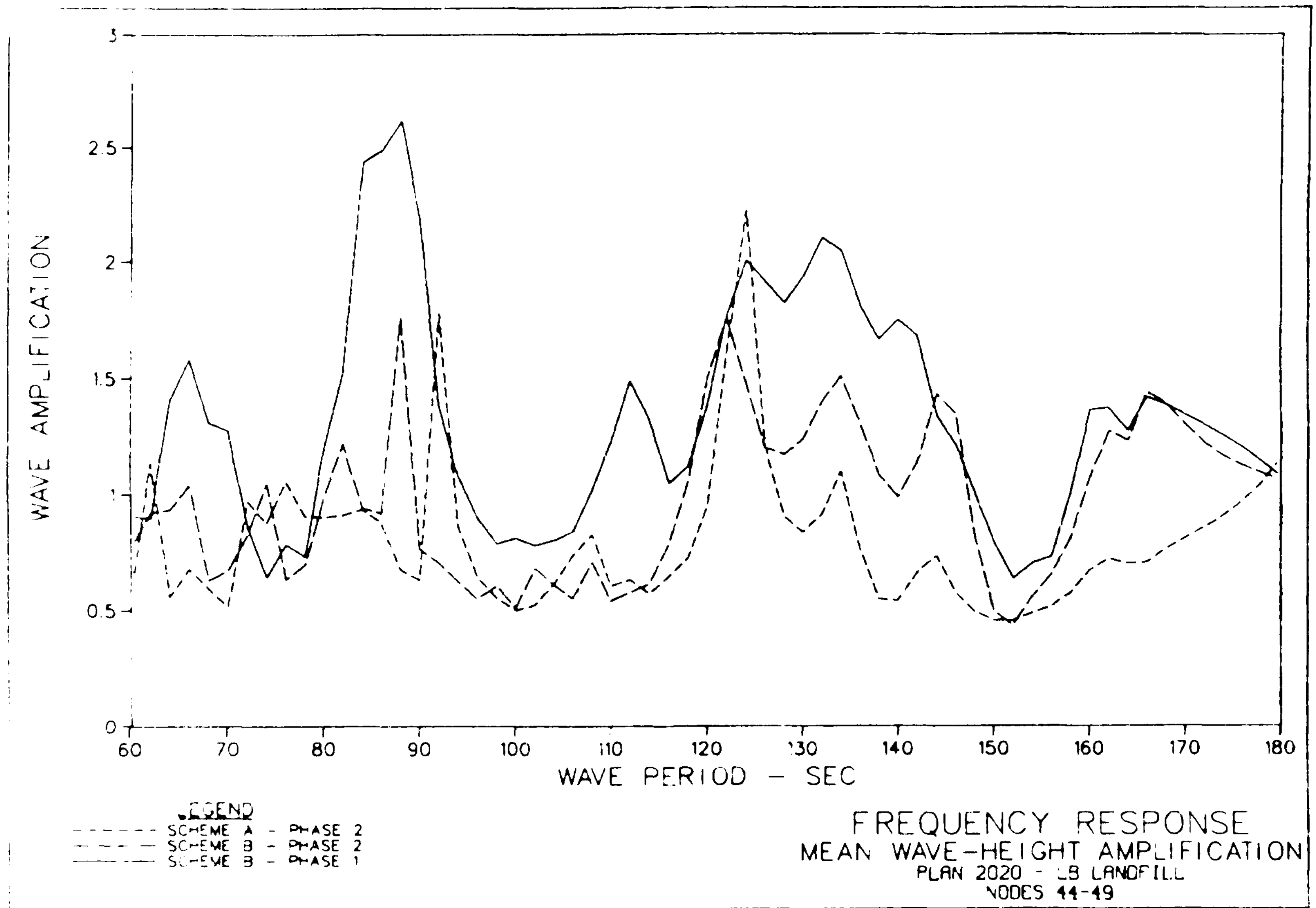

WAVE AMPLIFICATION
WAVE PERIOD - SEC
LEGEND
SCHEME A - PHASE 2
SCHEME B - PHASE 2
SCHEME B - PHASE 1
FREQUENCY RESPONSE
MEAN WAVE-HEIGHT AMPLIFICATION
PLAN 2020 - LB LANDFILL
NODES 44-49

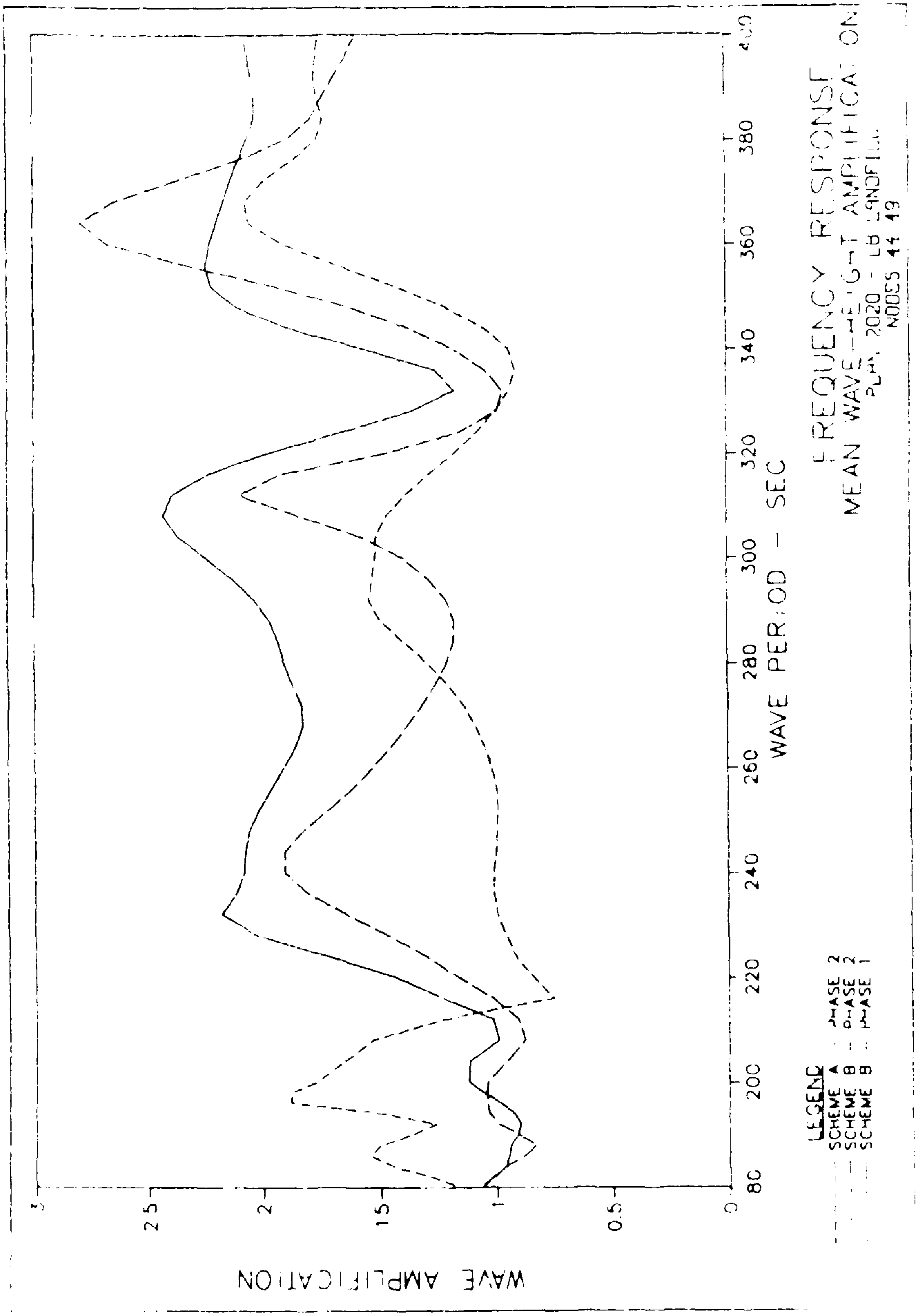
FREQUENCY RESPONSE
MEAN WAVE-HEIGHT AMPLIFICATION
PLAN 2020 - LB LANDFILL
NODES 44 49
LEGEND
SCHEME A : PHASE 2
SCHEME B : PHASE 2
SCHEME B : PHASE 1
WAVE PERIOD - SEC
WAVE AMPLIFICATION
0
0.5
1
1.5
2
2.5
3
180
200
220
240
260
280
300
320
340
360
380
400

PLATE 64

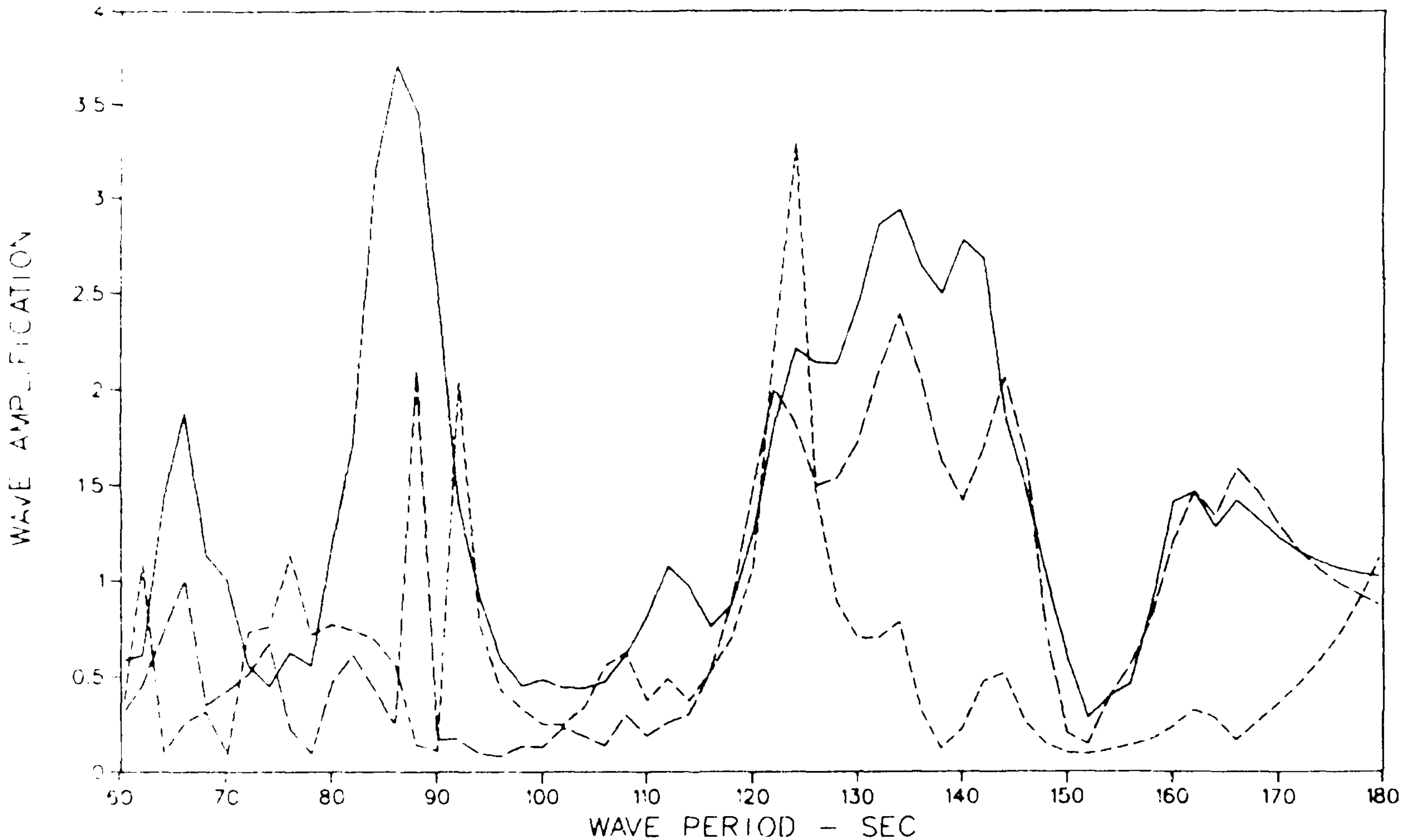

LEGEND
SCHEME A - PHASE 2
SCHEME B - PHASE 2
SCHEME B - PHASE 1

FREQUENCY RESPONSE
MEAN WAVE-HEIGHT AMPLIFICATION
PLAN 2020 - LB LANDFILL SLIP
NODES 45-48

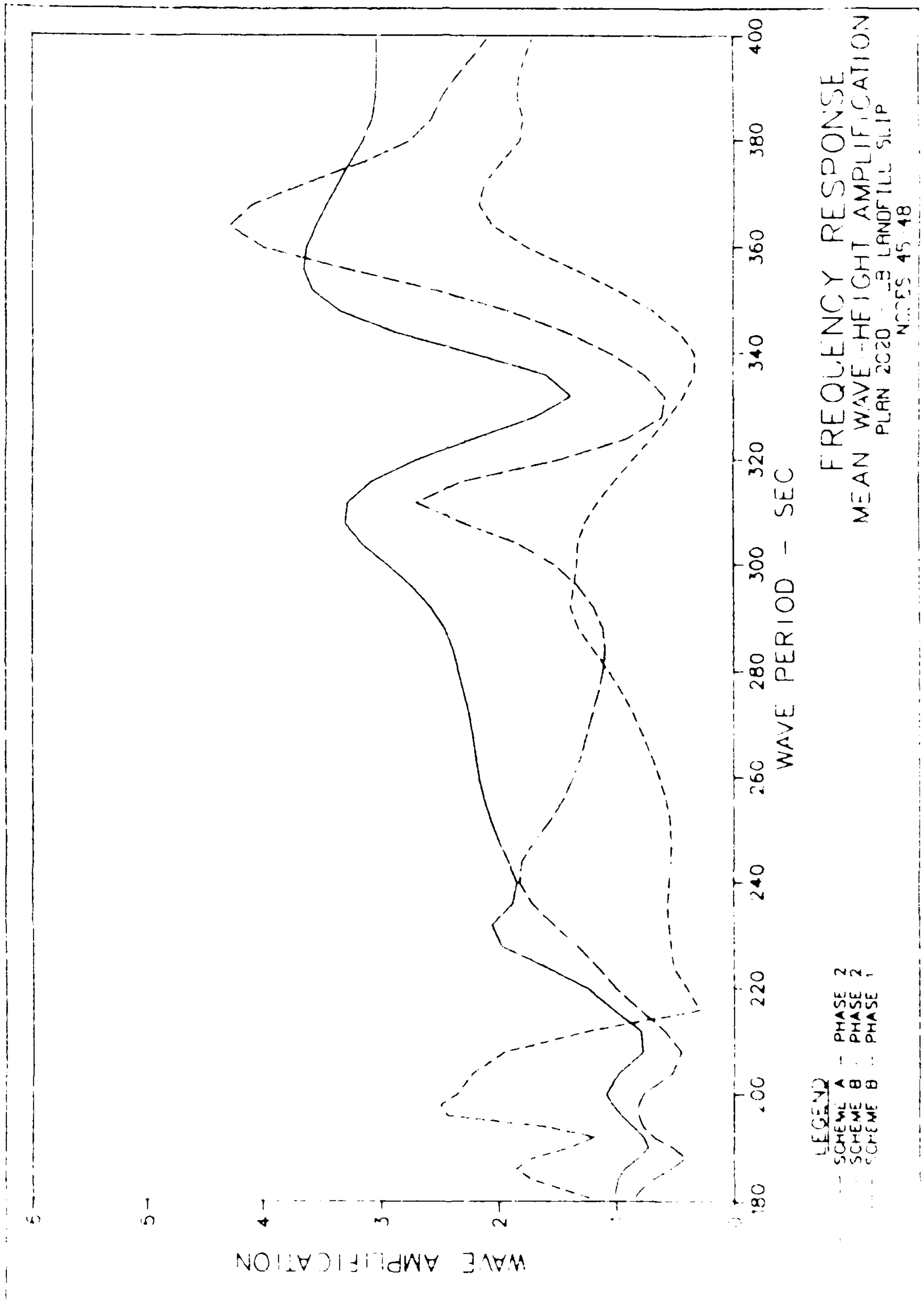

FREQUENCY RESPONSE
MEAN WAVE-HEIGHT AMPLIFICATION
WAVE PERIOD - SEC
WAVE AMPLIFICATION
LEGEND
SCHEME A - PHASE 2
SCHEME B - PHASE 2
SCHEME B - PHASE 1
180
200
220
240
260
280
300
320
340
360
380
400
1
2
3
4
5
6

PLATE 66

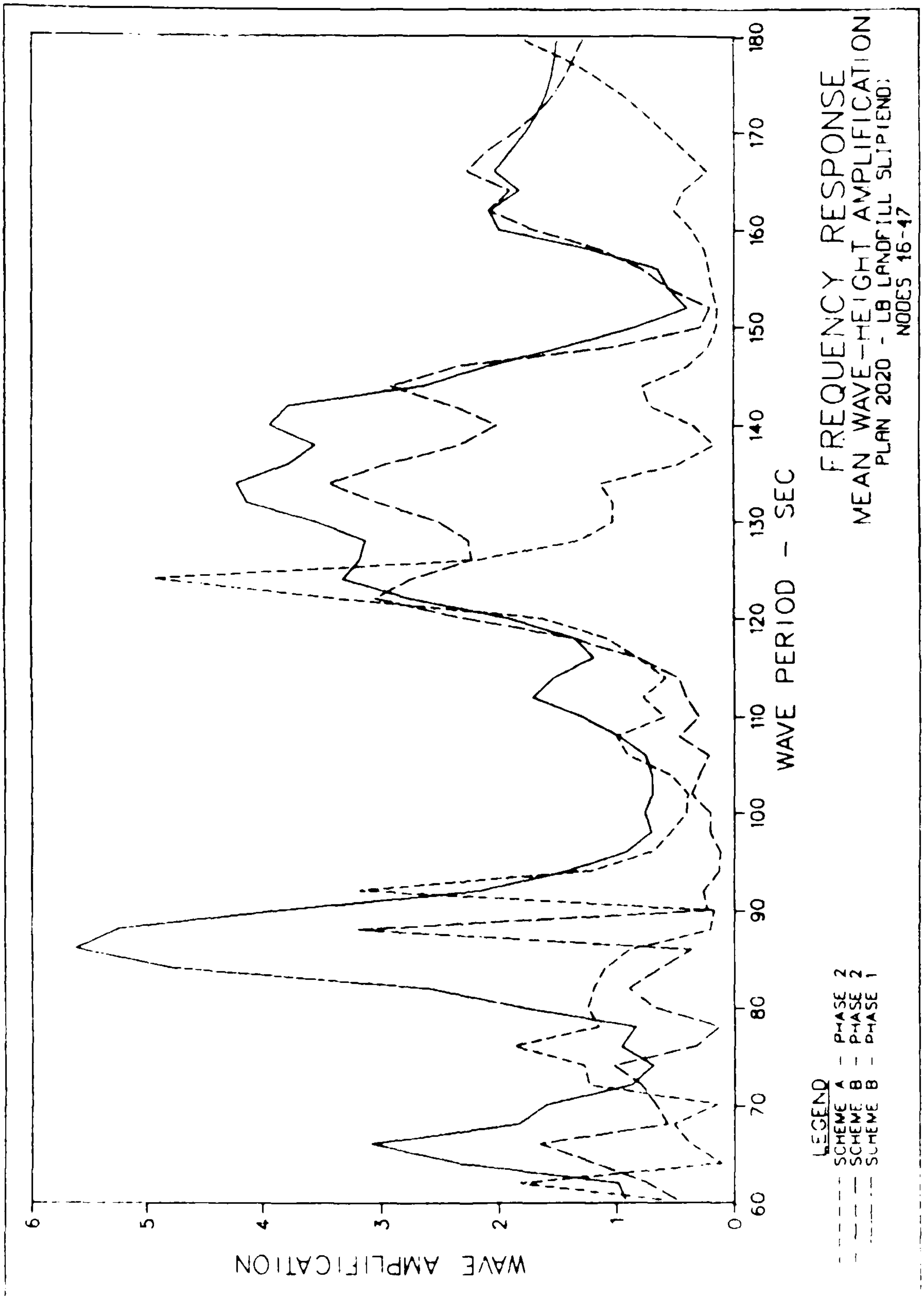
FREQUENCY RESPONSE
MEAN WAVE-HEIGHT AMPLIFICATION
PLAN 2020 - LB LANDFILL SLIP(END)
NODES 16-47
WAVE PERIOD - SEC
WAVE AMPLIFICATION
LEGEND
SCHEME A - PHASE 2
SCHEME B - PHASE 2
SCHEME B - PHASE 1
60
70
80
90
100
110
120
130
140
150
160
170
180
0
1
2
3
4
5
6

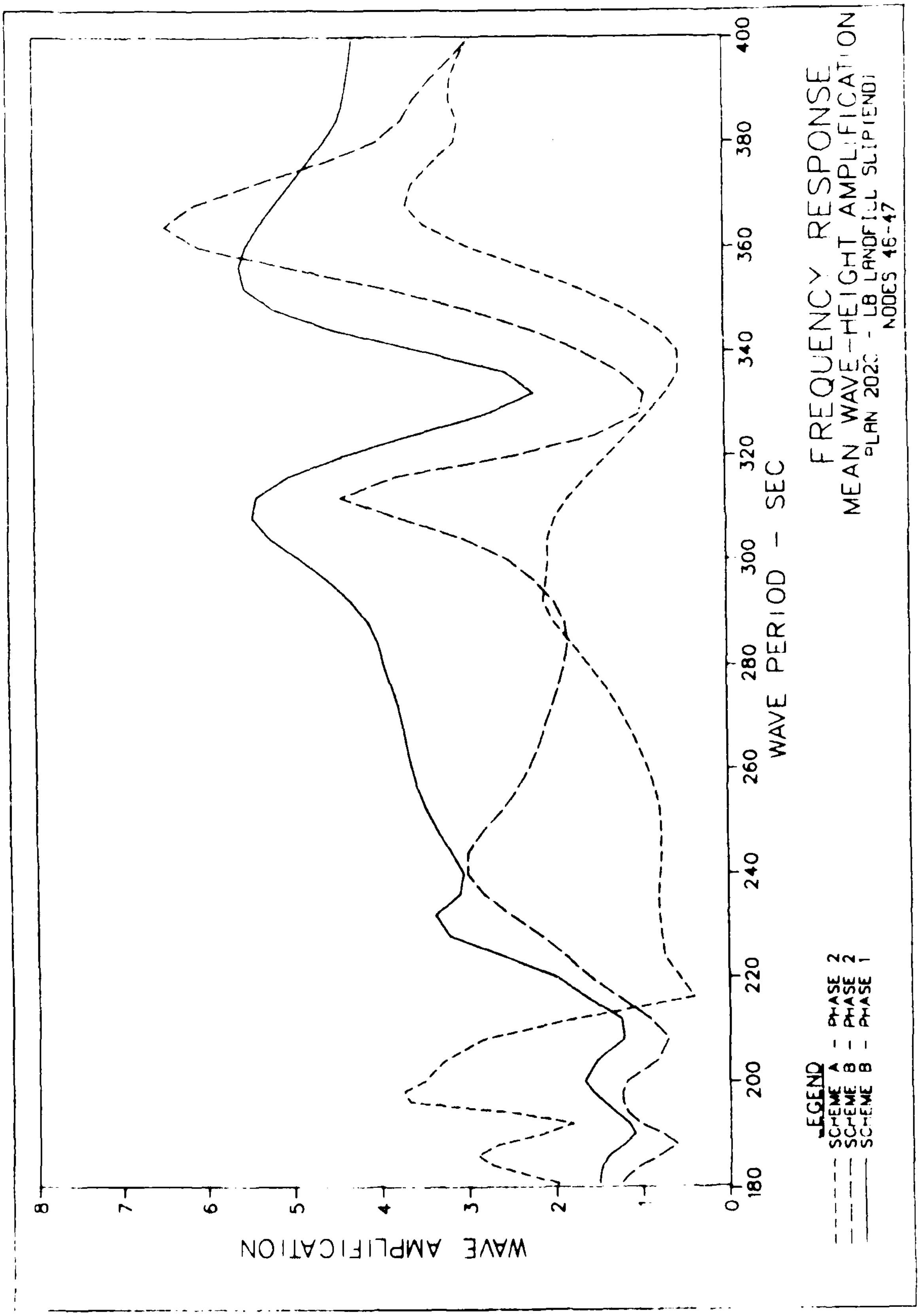
FREQUENCY RESPONSE
MEAN WAVE-HEIGHT AMPLIFICATION
PLAN 202 - LB LANDFILL SLIP(END)
NODES 46-47
WAVE PERIOD - SEC
180
200
220
240
260
280
300
320
340
360
380
400
WAVE AMPLIFICATION
0
1
2
3
4
5
6
7
8
LEGEND
SCHEME A - PHASE 2
SCHEME B - PHASE 2
SCHEME B - PHASE 1

PLATE 68